Dendritic Excitability and Protein Kinase C Activity Regulate Purkinje Neuron Dendrite Degeneration in Cerebellar Ataxia

by

Ravi Chopra

A dissertation submitted in partial fulfillment
of the requirements for the degree of
Doctor of Philosophy
(Neuroscience)
in the University of Michigan
2017

Doctoral Committee:

Assistant Professor Vikram G. Shakkottai (Chair)
Assistant Professor Asim Beg
Associate Professor Geoffrey Murphy
Professor Henry Paulson
Professor Edward Stuenkel

chopravi@med.umich.edu

ORCID iD: 0000-0001-5940-6097

2017

Acknowledgements

I would first like to thank my dissertation mentor, Dr. Vikram Shakkottai. His mentorship has been invaluable to my development as both a physician and a scientist, and he has become a role model for me as I improve my own knowledge, skill, and scientific imagination. I thank my dissertation committee members Dr. Asim Beg, Dr. Geoffrey Murphy, Dr. Henry Paulson, and Dr. Edward Stuenkel for supporting me through their effort and advice in committee meetings and beyond. I thank both current and former Shakkottai lab members that have directly contributed to this dissertation: Aaron Wasserman, David Bushart, and James Dell'Orco. I also thank current and former lab Shakkottai members who have worked with me and supported me throughout the years: John Cooper, Annie Zalon, Alexi Vasbinder, and Allison Sylvia. I thank Biswarathan Ramani, Dr. Samuel Pappas, Dr. Maria do Carmo Costa, Dr. Alison Althaus, Dr. Shannon Moore, and Xi Du for technical training and advice. I thank Dr. Lori Isom, Dr. Kelli Sullivan, Dr. Michael Sutton, Dr. Peter Todd, Dr. Robert Thompson, Dr. Michael Uhler, and Dr. Audrey Seasholtz for supporting my scientific and professional development. I thank Dr. William Dauer for helpful conversations over various aspects of the thesis. I thank the many staff of the Medical Scientist Training Program and the Neuroscience Graduate Program for their support over the many years. Other collaborators, contributors, and sources of funding are acknowledged throughout the dissertation.

Table of Contents

List of Figures

List of Tables

Abstract

Spinocerebellar ataxias (SCAs) are hereditary neurodegenerative disorders that are united by their autosomal dominant inheritance and their common clinical feature: cerebellar ataxia. Cerebellar ataxia is a disorder of impaired motor coordination, and in many SCAs the cause of degraded motor coordination is understood to be degeneration of cerebellar Purkinje neurons. The degeneration of Purkinje neurons in many SCAs is thought to progress from degeneration of the elaborate Purkinje neuron dendrite arbor to eventual cell death. Although it is likely that the early dendrite degeneration contributes substantially to motor impairment, the cellular processes which drive dendrite degeneration remain very poorly understood.

It is known that synaptic inputs and intrinsic excitability shape Purkinje neuron dendrites during development, and several studies in different SCA models have suggested that altered synaptic input or action potential firing contributes to Purkinje neuron degeneration. Not yet explored in any of the SCA models is whether the physiology of the Purkinje neuron dendritic shaft are altered. In a mouse model of spinocerebellar ataxia type 1 (SCA1), we tested the hypothesis that SCA1 Purkinje neurons would show an increase in intrinsic dendritic excitability that promotes dendrite degeneration. Our studies identified an increase in intrinsic dendritic excitability throughout the course of dendritic degeneration, and we showed that this increased dendritic excitability was associated with changes in expression of several channels that regulate dendritic excitability. Subsequently, we demonstrated that normalizing dendritic excitability

exerts a dendro-protective effect in SCA1 Purkinje neurons, supporting the hypothesis that increased intrinsic dendritic excitability drives SCA1 Purkinje neuron dendrite degeneration.

In our attempts to uncover the pathway(s) by which increased dendritic excitability drives SCA1 Purkinje neuron dendrite degeneration, we uncovered a large increase in phosphorylation of protein kinase C (PKC) enzyme targets in SCA1 mice and SCA1 patient tissue. PKC activity is an important regulator of Purkinje neuron dendritic structure, and we hypothesized that increased PKC activity downstream of increased excitability promotes dendritic degeneration. Surprisingly, suppression of PKC activity in SCA1 mice resulted in accelerated dendritic degeneration, suggesting that the increased PKC activation is dendro-protective. A similar dendro-protective effect was observed in a model of a different cerebellar ataxia, Spinocerebellar ataxia type 2 (SCA2). Studies from the SCA1 mice suggest that PKC enzymes may be exerting their dendro-protective effect by counteracting (although incompletely) increases in dendritic excitability, further supporting the role that dendritic excitability plays as a driver of Purkinje neuron dendritic degeneration.

This thesis establishes both intrinsic dendritic excitability and PKC activity as important regulators of Purkinje neuron dendrite degeneration in SCA1 and beyond. The results provide clinically-relevant therapeutic targets, and also provide a novel conceptual framework for understanding Purkinje neuron dendrite remodeling in health and disease. Together, these findings establish that Purkinje neuron dendrite degeneration is in fact a regulated process, with dendrite excitability and PKC activity specifically identified as two key regulators of that process.

Chapter 1

Introduction

1.1 Purkinje neuron dendritic degeneration: a poorly-understood neuropathologic feature of cerebellar ataxia

1.1.1 Cerebellar ataxia: an overview

Cerebellar ataxia is a neurologic syndrome characterized by degraded motor coordination, unsteady gait, and slurred speech. Ataxia is a clinical entity rather than a discrete disease, and there are a large number of causes of ataxia, including ischemic, toxic, metabolic, paraneoplastic, or genetic etiologies. In many cases, the underlying cause of a patient's ataxia cannot be addressed with existing therapies, meaning that management is symptomatic and supportive. Limited understanding of the diverse disease processes that produce ataxia have hampered the development of effective therapies for either discrete indications or more widespread applications.

Among the many causes of ataxia, there is a large and very diverse subset of progressive neurodegenerative diseases that affect the cerebellum and its associated pathways. The concurrent observation of cerebellar neurodegeneration and impaired motor coordination in these conditions is consistent with the cerebellum's undisputed importance in the performance of smooth and goal-directed movements[1]. Although most cases of neurodegenerative ataxia are sporadic, there are a subset of cases that can be attributed to genetic causes, and within that a smaller subset of monogenic diseases showing autosomal dominant inheritance[2]. These

autosomal dominant cerebellar ataxias, referred to as spinocerebellar ataxias (SCAs), are estimated to have a prevalence as a group of about 3 cases per 100,000[3].

The SCAs are a clinically and genetically heterogeneous group of progressive neurodegenerative diseases, typically presenting in the third, fourth, or fifth decade of life. SCAs are named and numbered (SCA1, SCA2, etc.) according to the order in which the pathogenic gene for that specific SCA was identified. While ataxia is a cardinal feature of the SCAs, many SCAs present with additional symptoms in association with neurodegeneration outside the cerebellar circuit[2]. It is nevertheless widely understood that for most of the SCAs, the ataxia is principally attributable to cerebellar pathology.

1.1.2 Purkinje neuron dendrite degeneration in cerebellar ataxia

Autopsy studies of cerebellar microcircuitry in many SCAs have revealed significant involvement of cerebellar Purkinje neurons[4-7], for some SCAs occurring to the exclusion of any other neurons in the central nervous system[6]. The pattern of Purkinje neuron pathology is similar to that which has been observed in other neurodegenerative diseases: significant Purkinje neuron loss, with surviving Purkinje neurons showing dramatic simplification of their dendritic arbor and pathological axonal swelling[4, 5, 8]. While these studies suggested a progressive cellular degenerative process which begins with neuritic degeneration and ends with cell loss, they did not by themselves identify the time course or relative importance of Purkinje neuron loss in terms of its effect on patients' motor performance. With the development of the first SCA mouse model, a transgenic model of spinocerebellar ataxia type 1 (SCA1), researchers identified symptom onset well before detectable cell loss[9]. Similarly, a knock-in SCA1 model[10] and transgenic models of spinocerebellar ataxias type 2, 6, and 7 (SCA2, SCA6, and SCA7) also found that ataxia precedes cell loss[11-13], with the study of the SCA2 transgenic model

demonstrating that motor impairment was fully penetrant by the age at which cell loss was first detected[11], suggesting that cell loss by itself makes no significant contribution to symptoms. These findings suggested that early histopathologic changes in Purkinje neurons might be particularly important for understanding motor impairment.

An important caveat for interpreting these data should be drawn from the Huntington disease (HD) mouse model literature. While HD in humans is an adult-onset neurodegenerative disease arising from CAG tract expansion in a single allele of the HTT gene, several types of HD mouse models have been developed where symptoms are observed within the short (~2 year) lifespan of the mouse, namely transgenic models expressing the N-terminal fragment of CAG-expanded HTT[14, 15], transgenic models expressing full-length CAG-expanded HTT[16, 17], and models where a CAG tract expansion has been knocked into the endogenous CAG tract of mouse *Htt*[18, 19]. Each model diverges from the human case in an effort to produce symptoms within the mouse's lifespan, with the transgenic models expressing under strong promoters while the knock-in models have CAG tract expansions much longer than what is observed in humans. For the different models, there is a broad range in how well cell death correlates with the onset of motor symptoms, with some models showing symptoms without detectable cell death[20] while other models show substantial cell loss by the time symptoms are first detected[18]. Although it remains consistently true in mouse models of any SCA that symptoms are observed before cell death regardless of model design (i.e. the knock-in[10] vs. transgenic[9] models of SCA1 or the Purkinje cell-specific transgenic[11] vs. BAC transgenic[21] models of SCA2), the spectrum of neuropathology-to-symptom relationships observed in HD mouse models and the fact that this spectrum depends heavily on model design raises important questions about the validity of mouse models in studying human adult-onset neurodegenerative diseases.

Despite the caveats, mice represent the only available models for studying SCA Purkinje neuron pathology in Purkinje neurons demonstrating primate-like properties and residing within a human-like cellular context. Within the SCA mouse model literature, one factor has emerged as being consistently correlated with motor impairment: degeneration of Purkinje neuron dendrites. In models of SCA1[9, 10], SCA2[11], and SCA6[12], dendritic degeneration is temporally-correlated with the onset of rota-rod deficits, although the strength of the correlation may depend on the method by which dendrite degeneration is measured. Studies using subjective assessment of dendrite structure in SCA1 transgenic mice[9] or measurement of dendrite capacitance in SCA1 knock-in mice[10] detected dendrite degeneration which coincides with motor impairment, suggesting that at least in these models there is a tight correlation between the onset of dendrite degeneration and motor impairment. In the studies of the SCA2 and SCA6 transgenic models the thickness of the molecular layer (the layer of the cerebellar cortex where Purkinje neuron dendrites reside) was used as a measure of dendrite structure, and these studies showed that molecular layer thinning weeks after symptom onset. It is worth noting that the SCA1 knock-in mouse has reduced Purkinje neuron dendrite capacitance but never has a detectable change in molecular layer thickness, suggesting that molecular layer thickness is a relatively crude measure of dendrite surface area. This is further supported by our own work (see section 3.3.1), which shows that dendrite capacitance it substantially reduced in the transgenic model of SCA1 before at a time point where there is no detectable reduction in molecular layer thickness.

The apparent correlation between dendrite degeneration and symptom onset in these SCA models raises the possibility that dendritic degeneration might account for symptomatic impairment. This conclusion is supported by several lines of evidence. The first is a finding in a study of *lurcher* aggregation chimera mice, which are formed by combining an embryo from the

lurcher mouse and a wild-type embryo to produce a mouse with a mixed population of neurons, some of which express the *lurcher* mutation while others do not. The *lurcher* mouse is a spontaneous mutant in the C57/BL6 background strain of mice that develops rapid ataxia with Purkinje neuron degeneration. The mutation was identified as being in *Grid2*[22], a gene encoding the GluRδ2 glutamate receptor subunit that is highly expressed in Purkinje neurons. Lurcher Purkinje neurons undergo rapid cell-autonomous neurodegeneration and death[23], such that chimeric mice lose a subset of their Purkinje neurons while the remaining Purkinje neurons are unaffected. Rota-rod performance is normal in *lurcher* chimeras unless they have fewer than surviving 15,000 Purkinje neurons[24], which is less than 10% of total Purkinje neurons based on stereological estimates in C57/BL6 mice[25]. It is worth noting that relatively subtle changes in the dendritic morphology of wild-type Purkinje neurons in *lurcher* chimeras have been described[26]. Nevertheless, these data demonstrate that there is significant Purkinje neuron reserve with the mouse cerebellum, such that the comparably modest cell loss in SCA mouse models is not sufficient to explain ataxia.

SCA1 is caused by an expanded glutamine-encoding CAG tract in the ATXN1 gene. As in other degenerative cerebellar ataxias, progressive Purkinje neuron dendritic degeneration precedes cell death, a feature modeled in a transgenic mouse model of SCA1 expressing a human ATXN1 cDNA with 82 glutamine-encoding CAG repeats ("ATXN1[82Q]")[9, 27]. Phosphorylation of ATAXIN-1 (the protein product from ATXN1) at a particular serine (Ser776) regulates its interaction with other proteins and influences diseases pathogenesis[28], such that mice expressing polyglutamine-expanded ATAXIN-1 with an S776A mutation ("ATXN1[82Q]-A776") show limited Purkinje neuron pathology[29] while mice expressing non-expanded ATXN1 with a phosphomimetic S776D mutation show significant neuropathology ("ATXN1[30Q]-

D776")[30]. The ATXN1[30Q]-D776 mouse shows profound ataxia comparable to the ATXN1[82Q] mouse, but ATXN1[30Q]-D776 Purkinje neuron pathology does not progress beyond dendritic degeneration to cell loss, suggesting that cell loss is not necessary for motor impairment in SCA1 mice. It is worth noting that none of these studies definitively demonstrates that dendritic degeneration is the cause for ataxia in these mice. Nevertheless, these studies demonstrate that Purkinje neuron dendritic degeneration is a much stronger structural correlate of motor impairment than cell loss, and they motivate exploration of the mechanisms behind Purkinje neuron dendritic degeneration in cerebellar ataxia.

Despite the experimental evidence suggesting that dendritic degeneration might be a clinically meaningful phase in Purkinje neuron degeneration, it remains very poorly understood. This is in large part due to the fact that dendritic pathology is seldom studied as an independent phenomenon. Several studies that have looked at dendritic pathology in different models of ataxia have demonstrated that dendritic pathology is associated with sequestration within the cell body of mitochondria[31] or proteins[32] that are normally localized to the dendrite, suggesting a model where dendritic degeneration arises because a cell fails to supply the dendritic arbor with necessary metabolic components. Another study of an ataxia model identified misfolded protein aggregates in neuronal dendrites, raising the possibility that local proteotoxic stress might contribute to dendritic pathology[33]. Based on these data, one might infer the observed structural changes reflect a dendritic arbor overwhelmed by a toxic challenge.

While these studies provide one framework for understanding dendritic pathology in the SCAs, the lack of rescue studies targeting metabolism or protein quality control specifically in the dendritic compartment makes it difficult to assess whether the proposed mechanism is in fact responsible for structural changes in dendrites. I take seriously a different hypothesis: that

Purkinje neuron dendritic degeneration is in fact a regulated process of atrophic remodeling, mediated by pathways that regulate dendritic structure in wild-type Purkinje neurons. This hypothesis has been put forth for other disease states[34-36], although it has not been explored specifically in ataxia. Below I will provide a broad overview about what is known regarding the pathways that regulate dendritic structure in developing and mature neurons, with a specific focus on Purkinje neurons.

1.2 Purkinje neuron dendrite structure: an overview

1.2.1 General principles of dendrite structure in the brain

A substantial literature exists exploring the structure of neuronal dendrites. From this, a few broad principles can be generalized. The first is that neuronal dendrite shape regulation can be divided roughly into two phases: development and maintenance, with large-scale structural decisions being made during a developmental critical period, after which dendrites enter a maintenance phase where dendrite arbor structure is relatively stable[37-39] while spines continue to be added, removed, or undergo structural changes[40-42]. The second is that regulators of dendritic structure operate within a nested hierarchy, with the earliest and in many cases most comprehensive shape decisions being determined through cell-autonomous transcriptional programs[43-46], while later and smaller-scale decisions regarding dendritic shape and organization are achieved through interactions between the neuron and extrinsic signals[47-49]. The third is that neuronal activity, including both neurotransmission[50-53] and intrinsic excitability[46, 54, 55], can influence developing dendrites, with a host of activity-dependent intracellular signaling cascades operating downstream to regulate dendritic structure[56-58].

Although there are many qualifiers to the principles described above, those that are most germaine to this thesis involve the idea of dendritic structure being stable in adult neurons. While it is true that long-term *in vivo* imaging of select neurons has confirmed critical periods for dendrite structural flexibility[37] and demonstrated that dendritic structure is stable over a period of months in adult mice in some neuronal subtypes[59, 60], molecules such as delta-catenin[61] and the Pten tumor suppressor[62] have been identified as being regulators of dendrite stability in adult neurons. What these findings suggest is that while dendrite structure is relatively stable in adult neurons, it is not that adult neurons have lost the capacity for dendritic remodeling, but that it remains latent and is instead constrained by active regulatory processes. Given the dramatic impact that neuronal activity has in shaping dendritic structure during development[53, 63], one might expect that there are circumstances where alterations in activity have been demonstrated to impact adult neurons' dendritic structure. In fact, studies of learning in the motor-sensory forelimb cortex have suggested that certain forms of intensive training in adult rats are accompanied by circuit-specific changes in dendritic architecture of cortical pyramidal neurons[64, 65]. Similarly, studies of adult rodents exposed to systemic amphetamine or cocaine have repeatedly shown that these drugs promote dendritic outgrowth in the prefrontal cortex and nucleus accumbens[66-68], and for medium spiny neurons of the nucleus accumbens shell the process is prevented when *c-fos* expression is prevented[69], a finding that mechanistically links structural changes in those neurons to drug-induced changes in their activity.

These findings complicate the idea that dendritic structure is stable in adult neurons. I propose that these data suggest that dendrite arbor structure remains flexible into adulthood (as is well-described in spines), but that the threshold for activity-dependent changes in structure is significantly higher such that "typical" activity seldom perturbs dendrite structure. If this were

the case, one would predict that pathologic states where neuronal activity is altered might trigger dendritic structural remodeling, particularly in neuronal subtypes where dendritic structure is heavily determined by activity. In fact, studies of Purkinje neuron dendrite development suggest that Purkinje neurons might represent one such neuronal population.

1.2.2 Purkinje neuron dendritic architecture: a product of activity

In Purkinje neuron dendrite development, it appears that dendritic structure is governed by the principles outlined above, but with the final dendritic architecture depending almost entirely on extrinsic signals and neuronal activity (see below). Purkinje neurons acquire their mature dendritic phenotype through a multi-stage process that begins after migration is completed. Starting as bipolar cells, Purkinje neurons develop a stellate phenotype with multiple neuritic protrusions, most of which retract to give rise to one or perhaps two apical dendrites[70, 71]. From there, the dendritic tree grows substantially, such that mouse Purkinje neurons achieve their mature, monoplanar dendritic structure by P20[72].

The earliest stages of Purkinje neuron dendritic differentiation depend heavily on intrinsic programs. This was demonstrated using cerebellar slice cultures where specific genes were overexpressed or silenced in only a subset of cells using lentiviral transfection, and the impact of both overexpression and knockdown on dendrite development could be assessed. One such study revealed that the nuclear receptor RORα controls the retraction of neurites during the stellate phase and that it also drives the progression of the subsequent outgrowth of the apical dendrite[73]. A study using the same strategy also revealed that SCLIP, a protein of the microtubule-interacting stathmin family, was necessary for any neuritic outgrowth and also supported subsequent outgrowth of the apical dendrite[74]. Although these early events in Purkinje neuron dendritic differentiation remain poorly understood, the lentiviral slice culture strategy

employed in these studies is likely to identify additional intrinsic regulators of early Purkinje neuron dendritic specification.

Past these early stages, Purkinje neuron dendrite development depends on extrinsic signals. Several diffusible ligand systems have been identified as being important for Purkinje neuron dendritic outgrowth (notably Reelin[75], thyroid hormone[76], and BDNF[77]) and patterning (Slit/Robo[78]). Similarly, contact-mediated ligand-receptor systems have been identified as important for Purkinje neuron dendrite outgrowth (cadherins[79]) and patterning (proto-cadherins[80] and the adhesion-GPCR BAI3[81]).

In addition to these dendrite guidance cues, Purkinje neuron activity has been demonstrated to be critical for the establishment of mature Purkinje neuron dendrite structure. Input from cerebellar granule cells is essential, as cerebellar granule cell loss *in vivo* causes a halting of Purkinje neuron apical dendrite development[82] and Purkinje neurons are only able to grow mature dendrites *in vitro* when co-cultured with granule cells[83]. It seems that synaptic transmission from granule cells onto Purkinje neurons is particularly important[84], although a role for intrinsic excitability cannot be excluded[85]. It is also well-established that a variety of activity-dependent signaling molecules play an important role in regulating Purkinje neuron dendrite structure (discussed in section 1.3.4). These data suggest that the robust and characteristic dendritic arbor observed in adult Purkinje neurons is largely a product of synaptic inputs, electrophysiologic activity, and downstream signaling, provided that more fundamental dendrite specification pathways remain intact. This suggests that Purkinje neuron dendrites might be particularly susceptible to perturbations in electrophysiologic activity.

In fact, several spontaneous mouse mutants exist where mutations in ion channel genes produce profound effects on Purkinje neuron dendritic development. The *lurcher* mutation is a

gain-of-function mutation in the GluRδ2 glutamate receptor subunit that produces a channel with constitutive inward current[22] and results in cell-autonomous Purkinje neuron dendrite atrophy[86]. The *moonwalker* mutation is a gain-of-function mutation in the transient receptor potential cation channel, type C3 (TRPC3) that results in increased responsiveness to mGluR stimulation, and *moonwalker* mice similarly display Purkinje neuron dendrite stunting[87] with early changes in Purkinje neuron spiking[88]. These studies suggest that changes in Purkinje neuron activity are capable of producing profound changes in dendritic structure.

It is worth noting that the observed changes in these models appear to be developmental, and do not by themselves suggest that adult Purkinje neuron dendrites would undergo dramatic activity-dependent structural remodeling, as is being proposed in SCA models. Nevertheless, the literature outlining dendritic remodeling in response to intensive training or psychoactive drugs (see section 1.2.1) suggests that dendritic remodeling can occur in adult neurons when there is late-onset aberrant activity. We propose that such a mechanism may be involved in dendritic remodeling in ataxia, consistent with the age of symptom onset in patients and mouse models. There is a growing literature pointing to adult-onset changes in Purkinje neuron activity as being a common feature of ataxia correlated with both neuropathology and symptom progression, and several studies demonstrate mechanistically that changes in activity actually drive the degenerative process.

1.3 Alterations in Purkinje neuron electrophysiology and their potential role in dendrite degeneration in models of spinocerebellar ataxias

Altered neuronal activity has been observed in many SCA models, such that changes in neuronal activity could play a role in dendritic remodeling. For any neuron, the activity of that

neuron is dictated by three interlinked processes: the synaptic inputs and their properties, the intrinsic spiking characteristics, and the electrical characteristics of the neuron's dendrite. Each of these processes will be discussed separately below, with a specific focus on Purkinje neurons and the ways in which these processes are affected in models of spinocerebellar ataxia. At the end of this section I will provide an overview of what is known about signaling systems downstream of excitability that mediate dendritic remodeling, with a specific focus on those systems that might be involved in Purkinje neuron dendritic remodeling in ataxia.

1.3.1 Purkinje neuron spiking in models of spinocerebellar ataxias

Purkinje neurons are tonic repetitively firing cells whose firing frequency changes during repetitive movement[89]. It is important to note that bistability characterized by "up" states of repetitive firing and "down" states of quiescence have been observed *in vivo* in anesthetized mice[90], although these are likely a byproduct of the anesthesia[91]. Purkinje neurons exert their effect on movement through their GABAergic projections to neurons of the deep cerebellar nuclei, which represent the sole outputs of the cerebellum (with the exception of direct projections from the cerebellar flocculonodular lobe onto the vestibular nuclei). Individual Purkinje neurons encode information in their firing frequency[92] and converge on individual nuclear neurons with inputs that facilitate nuclear neuron recognition of synchronous spikes from multiple Purkinje neuron afferents[93].

The repetitive action potential firing of Purkinje neurons is autonomous, such that acutely dissociated Purkinje neurons (which maintain the axon initial segments[94] from which action potentials are known to initiate in Purkinje neurons[95]) spike at ~60 Hz in the absence of synaptic input or injected current[96]. Purkinje neurons' autonomous action potential firing, referred to as pacemaking, depends on a precise sequence of currents, with each firing cycle involving 1)

initial depolarizing inward current mediated by the voltage-gated sodium channels $Na_V1.6$[97] and $Na_V1.1$[98], 2) repolarizing outward current mediated by K_V3 channels[99], 3) after-hyperpolarization mediated by the large- and small-conductance calcium-activated potassium channels (BK[100] and SK2[101, 102], respectively) coupled to P/Q-type voltage-gated calcium channels[103], and 4) resurgent inward sodium current through $Na_V1.6$[97] that depolarizes the neuron towards threshold for the next spike. The autonomous spiking produced by the orchestrated function of these channels is essential for appropriate participation of Purkinje neurons in the cerebellar system, such that the absence of any of these channels will result in irregular or absent Purkinje neuron firing and significant ataxia[98, 104-107].

The impact that dysfunctional Purkinje neuron spiking has on motor performance suggests that among the many genetic causes of ataxia, one might identify a number of disorders caused by mutations in ion channels that participate in pacemaking. In fact, there are a number of SCAs and other degenerative ataxias that are caused by mutations in Purkinje neuron pacemaking channels, including SCA13[108], SCA19/22[109, 110], episodic ataxias type 1[111] and 2[112], and Dravet syndrome[113]. Additionally, studies in mouse models of SCAs not caused by primary mutations in ion channel genes have revealed dysfunctional pacemaking correlates with the onset of motor symptoms and neurodegeneration[11, 114-119]. Many of these studies showed that symptoms of ataxia in SCAs that were not primary channelopathies could be improved by improving Purkinje neuron spiking[114-116, 118-120].

In SCAs caused by ion channel mutations, it is not necessarily clear that Purkinje neuron dendritic degeneration observed in these patients is a product of altered Purkinje neuron spiking. Although SCA13 and SCA19/22 mutations are known to impair function of the mutant channel gene product ($K_V3.3$ and $K_V4.3$, respectively)[121, 122], mice lacking functional *kcnc3* (the gene

mutated in SCA13) do not show obvious signs of Purkinje neuron dendritic degeneration[108], and Purkinje neuron pathology has not been described in mice lacking functional *kcnd3* (the gene mutated in SCA19/22)[123]. Knock-in models do not exist, making it difficult to assess how the mutations produce neurodegeneration.

Importantly, several studies in spinocerebellar ataxia type 1 (SCA1) have demonstrated that therapeutic strategies which target Purkinje neuron spiking can prevent dendritic degeneration. SCA1 is caused by expansion of the CAG tract within ATXN1[30], a gene whose protein product is thought to play important roles in regulating transcription[124] and RNA splicing[125]. Although not a primary channelopathy, studies in the ATXN1[82Q] transgenic mouse model of SCA1 have revealed reduced firing frequency, depolarization block, and altered input-output functions in response to injected current[114, 116]. These studies also found that when agents found to improve these spiking abnormalities *in vitro* were administered *in vivo*, Purkinje neuron dendritic surface area was preserved relative to vehicle-treated controls. These data were the first to implicate spiking abnormalities in the neuropathology observed in degenerative cerebellar ataxia. Importantly, they validate the principle that Purkinje neuron dendrites can undergo remodeling in response to significant perturbations in intrinsic excitability during adulthood.

1.3.2 Alterations in synaptic inputs onto Purkinje neurons in spinocerebellar ataxia models

Purkinje neurons reside within the cerebellar cortex in a characteristic monolayer, sitting superficial to the granule cell layer and extending their elaborate dendrites towards the pial surface through the molecular layer. Each Purkinje neuron receive two types of glutamatergic inputs: 1) tens to hundreds of thousands of parallel fiber synapses[126] originating from cerebellar granule cells, which are themselves targets of mossy fiber inputs to the cerebellum, and 2) a

single climbing fiber originating from principal neurons in the inferior olive. In addition these glutamatergic inputs, there are two subclasses of GABAergic interneurons in the molecular layer which synapse onto Purkinje neurons and themselves receive both parallel fiber and climbing fiber input[127]. Finally, Bergmann glia have cell bodies near the Purkinje neuron layer and extend radial processes expressing glutamate transporters and glutamine synthetase that allow them to modulate parallel fiber input[128].

The principle glutamatergic inputs onto Purkinje neurons produce very distinct effects on spiking. Parallel fiber inputs are thought to adjust Purkinje neuron spiking in a linear fashion, with recruitment of more parallel fibers resulting in higher Purkinje neuron firing frequencies[129]. The single climbing fiber onto each Purkinje neuron has many individual synaptic contacts onto that Purkinje neurons' soma and proximal dendrite[130], such that climbing fiber activation interrupts pacemaking and produces a high-frequency burst of spikes[131]. The role of the complex spike remains somewhat unclear, although it is important for several forms of Purkinje neuron plasticity[132] and can also modulate spiking, possibly through its inputs on molecular layer interneurons[133].

As discussed in section 1.2.2, establishment of mature Purkinje neuron dendritic architecture requires synaptic input (specifically from granule cells). This suggests that changes in the synaptic inputs onto Purkinje neurons might participate in dendritic remodeling observed in SCA models. In fact, alterations in synaptic function have been described in many SCA models.

In SCA models where transgene expression is limited to Purkinje neurons using the *Pcp2 (L7)* promoter, changes at the synapse have been identified which are most likely attributable to cell-autonomous changes in the Purkinje neuron. In the ATXN1[82Q] model of SCA1, reduced

climbing fiber responsiveness is observed *in vivo* at the onset of symptoms and reduced parallel fiber responsiveness is observed in advanced disease[134], while *in vitro* studies of climbing fiber or parallel fiber-induced AMPA currents reveal no difference[135] or reduced parallel fiber-induced AMPA current[114]. Altered metabotropic glutamate receptor signaling has also been reported in this model of SCA1, and the studies of parallel fiber-induced mGluR1 responses suggest a reduced amplitude[135] with slower decay[136]. In the ATXN2[127Q] transgenic model of SCA2, changes in expression of glutamate receptor subunits has been observed shortly after the onset of symptoms[11].

In addition, studies of SCA models have suggested changes on the pre-synaptic side of Purkinje neuron inputs, with Bergmann glia emerging as a potentially important participant in Purkinje neuron pathology. In studies of SCA7, an SCA7 model where transgene expression was restricted to Bergmann glia showed significant Purkinje neuron pathology[137], while an SCA7 model where the transgene was expressed in all neurons and then conditionally deleted in Bergmann glia showed behavioral improvement but no rescue of Purkinje neuron pathology[13]. Although these data conflict somewhat, both studies suggest that the role for Bergmann glia in Purkinje neuron pathology involves reduced expression of the glutamate transporter GLAST. Studies in a model of spinocerebellar ataxia type 5 (SCA5) similarly identify an important role for Bergmann glia GLAST expression, as they found that deletion of GLAST in an SCA5 model accelerated Purkinje neuron pathology[138].

1.3.3 Alterations in dendritic excitability and their potential role in spinocerebellar ataxia dendrite degeneration

Sitting physically and mechanistically between the synapse and the spike is the dendrite. Dendrites are not simply electrical conduits connecting the synapse to the axon initial segment;

instead, an abundant literature from many neuronal subtypes demonstrates that dendrites are full of ion channels that play an important and regulated role in neuronal information processing. The ways in which dendritic ion channels and structure regulate membrane depolarization and signal propagation along the dendritic shaft will be referred to as intrinsic dendritic excitability, in an effort to distinguish these properties from membrane potential characteristics depending directly on the function of ionotropic receptors in the synapse. Using this terminology, more faithful propagation of depolarization along the dendritic shaft would be a condition of increased dendritic excitability, while a degradation of depolarization spread along the dendritic shaft would be a condition of decreased dendritic excitability. It is important to note that there is significant cross-talk between the synapse, dendritic shaft, and cell body[139].

Propagation of depolarization along dendritic segments is described by the cable equation, which models the dendritic shaft as a pipe whose walls have an electrical capacitance and resistance to current flow and which also has a resistance to current flow along the length of the pipe. Although there are several forms of the cable equation, I will discuss the steady-state form of the equation for an infinite cable, in order to outline some general principles of signal propagation along a dendrite-like cable:

Equation 1.1 $$V_x = V_0 e^{-\frac{x}{\lambda}}$$

Here V_x is the membrane potential at a distance x along the dendritic cable from where depolarization V_0 is imposed. In this equation λ represents the length constant, which is a constant dictated by the physical properties of the dendritic cable using an equation described below:

Equation 1.2 $$\lambda = \sqrt{\frac{R_m}{R_i}}$$

The R_m is the membrane resistance to current flow across the wall of the cable, while R_a is the internal resistance to current flow down the axis of the cable. R_m and R_a in a cylindrical neuronal dendrite are described by the equation below:

$Equation\ 1.3 \qquad R_m = \frac{R_M}{\pi l d}$ $\qquad\qquad$ $Equation\ 1.4 \qquad R_i = \frac{R_I}{\pi r^2}$

R_m will be determined by the surface area of available membrane (πld) and the resistance per unit area (R_M), which is a function of the number and type of channels open, which will itself be determined by parameters that regulate the function of those channels (membrane potential, ligand concentration, etc.). R_i will be determined by the cross-sectional area of the dendrite (πr^2) and the resistivity of the dendritic cytoplasm (R_I), which is a measure of how readily electric current will travel through the cytoplasm.

From equation 1.1, it is clear that with increasing distance the measured voltage will attenuate. In addition, the other equations demonstrate that two features significantly impact signal propagation through the dendritic arbor: dendrite arbor shape and ion channel behavior. Ion channel behavior is collectively summed up in R_M above, but in general more open channels will result in a lower R_M and ultimately less depolarization at position x in equation 1.1, a property referred to as dendritic shunting. Changes in dendrite shape will vary depending on the specific change, but for a single cable a reduction in axial surface area will increase the axial resistance and reduce the measured depolarization at position x in equation 1.1.

The importance of dendritic structure and dendritic ion channel function for signal propagation through the dendritic arbor has been extensively studied, and different neuronal subtypes have employed the principles outlined above to confer unique computational properties. There is also substantial evidence that neurons change the properties of the dendritic cable to produce various forms of plasticity, including changing dendritic ion channel trafficking[140] or

function[139] and creating changes in spine neck structure[141]. For the remainder of this section, I will focus on what is known about Purkinje neuron dendritic signal integration, ending with the evidence suggesting that changes in Purkinje neuron dendritic excitability might be a feature of spinocerebellar ataxias.

In some neuronal subtypes, somatic action potentials back-propagate into the dendritic arbor and play an important role in regulating dendritic signal processing[142] and synaptic plasticity[143]. Purkinje neuron show comparatively poor backpropagation of action potentials into the dendritic arbor[95], likely due to the relative absence of functional dendritic voltage-gated sodium channels[144] and their highly-branched dendritic morphology. As such, Purkinje neuron dendrites are best thought of as receiving and shaping synaptic inputs that ultimately exerts its impact on somatic spiking. Modeling studies have suggested that this occurs through a mechanism where synaptic conductances in the Purkinje neuron dendrite exert a partial "voltage clamp" on dendritic membrane potential that then influences somatic spike frequency and irregularity[145], and *in vivo* studies have supported this model and demonstrated that dendritic membrane potential influences somatic spiking in response to a linear integration of excitatory granule cell inputs and inhibitory interneuron inputs[146].

Purkinje neurons are similar to some other types of neurons in that they show locally-generated dendritic spikes, which for Purkinje neurons are mediated by voltage-gated calcium channels[147] . Much like an action potential, dendritic calcium spikes are voltage-dependent events that likely involve a positive feedback loop of channel recruitment after dendritic membrane potential has reached a certain threshold. Dendritic calcium spikes have been found to be an important mechanism by which Purkinje neuron dendrites can shape synaptic input to influence action potential output[148]. Dendritic calcium spikes are seen in response to strong

parallel fiber stimulation, and they produce supralinear integration of parallel fiber input in somatic spiking immediately after the spike and then producing a temporary slowing of spiking rate[149]. Climbing fiber stimulation also produces dendritic calcium spikes, a process which is itself influenced by mGluR-dependent changes in dendritic A-type potassium currents[150], and the dendritic calcium spikes triggered during a complex spike appear to influence transitions in action potential firing measured from the soma between silent down-states and spiking up-states[148] that have been described under specific anesthetic conditions *in vivo*[90]. The presence or absence of a dendritic calcium spike during a somatic complex spike has also been demonstrated to determine whether somatic spike undergoes a pause following the complex spike itself[148]. These studies all highlight the ways in which dendritic calcium spikes influence Purkinje neuron dendritic integration.

Beyond the voltage-gated calcium channels which produce dendritic calcium spikes, Purkinje neuron dendrites express a host of potassium channels that regulate generation of those calcium spikes and more broadly participate in dendritic shunting. K_V3 and K_V4 channels appear to be the predominant voltage-gated potassium channel in Purkinje neuron dendrites[150, 151], and both types of K_V channels dampen action potential backpropagation and shape dendritic calcium spikes during the complex spike[151, 152]. BK[116] and SK2[153] are both abundant in the dendritic tree of Purkinje neurons, and both have been shown to regulate coupling between the dendritic and somatic compartments[101, 154]. Other potassium channels are expressed in Purkinje neuron dendrites, such as subthreshold-activated potassium channels[155] and two-pore potassium channels[156], although their role in Purkinje neuron dendrite shunting is not well-studied.
The dendritic shaft, as discussed during the introduction to section 1.3, represents a third "compartment" whose activity could influence dendritic structure. In fact, a study in *Drosophila*

C4da sensory neurons revealed that large-scale dendritic remodeling during the fly's metamorphic transition into adulthood is triggered by regulated changes in dendritic excitability, rather than changes in spiking or synaptically-driven events[157]. In considering potential causes of Purkinje neuron dendrite remodeling in spinocerebellar ataxias, I will be focusing in this thesis on the potential role that altered dendritic excitability might play.

Unlike spiking or synaptic activity, dendritic excitability has not been explored in any SCA models. Nevertheless, it is likely that changes in dendritic excitability are present in multiple forms of spinocerebellar ataxia. SCA13 is caused by mutations in the $K_V3.3$ channel and SCA19/22 is caused by mutations in $K_V4.3$ channel, both of which are important in Purkinje neuron dendrites. Additionally, BK and SK2 dysfunction has been implicated in SCA1[116], SCA2[115], and EA2[158], and these channels mediate important dendritic shunting conductances in addition to their role in somatic spiking. Perhaps most importantly, both studies in SCA1 mice where therapies designed to normalize action potential firing were able to preserve dendrite structure were using drugs that target potassium channels important to both the soma and the dendrite. These studies raise the possibility that the effect of these drugs on dendritic excitability might partly explain the preservation of dendrite structure.

Changes in dendritic excitability have been explored in several neurodegenerative diseases affecting non-Purkinje neuron populations. Studies in rodent models of Alzheimer disease have revealed increased dendritic excitability (as measured by an increase in dendritic backpropagating action potential amplitude) in CA1 pyramidal neurons, and both have implicated these changes in dendritic excitability as contributors to symptomatic impairment[159, 160]. Interestingly, one study focused on changes in dendritic potassium channel trafficking[159] while the other focused on the impact of altered dendritic structure[160], providing a nice

illustration of the multiple mechanisms by which dendritic excitability could be affected in neurodegenerative disease.

Changes in dendritic excitability have been implicated in the dendritic pathology of neuronal populations affected in Parkinson disease. When mice are treated with reserpine, profound striatal dopamine depletion and parkinsonism are induced[161], and this treatment was found to produce spine and dendrite degeneration in D_2-expressing medium spiny neurons (MSNs) but not D_1-expressing MSNs[162]. Study of the differences between D_1-expressing and D_2-expressing MSNs revealed that D_2-expressing MSNs show dopamine-induced suppression and acetylcholine-induced enhancement of backpropagating action potential propagation into the dendrite[163]. Backpropagating action potentials in dopaminergic neurons of the substantia nigra pars compacta produce dendritic calcium entry that triggers mitochondrial oxidant stress[164], which the authors view as a potential driver of Parkinson disease neurodegeneration in this population of neurons. Similar patterns of backpropagating action potential-induced calcium entry and oxidant stress have been observed in other neuronal populations that are affected in Parkinson disease, including neurons from the dorsal motor nucleus of the vagus[165] and noradrenergic neurons of the locus coeruleus[166]. Backpropagating action-potential-induced dendritic calcium entry through L-Type calcium channels has been suggested as a central risk factor of neurons which degenerate in Parkinson disease[167], placing dendritic excitability as potentially central to dendrite pathology in this disease.

1.3.4 Intracellular signaling systems operating downstream of altered Purkinje neuron excitability to mediate dendrite degeneration

Neuronal excitability exerts its influence on dendritic structure through a host of intracellular signaling systems. In this section I will provide a broad overview of these

regulators. I will end by discussing studies where changes in these activity-dependent regulators have been observed or linked to dendrite remodeling in ataxia.

As discussed in section 1.2.1, there are several activity-dependent transcriptional regulators which are known to be important for dendrite structure specification during development. These include NEUROD1[168], CREST[45], CREB[46], and chromatic remodeling complexes specific to terminally-differentiated neurons[169], with genetic ablation or pharmacologic suppression of these factors producing stunted dendrites in cerebellar granule neurons[168], cortical layer V pyramidal and hippocampal CA3 neurons[45], cultured cortical neurons[46], and cortical layer V pyramidal and cultured hippocampal neurons[169], respectively. Work in *Drosophila* suggests that transcriptional regulators of dendritic structure operate much like transcription factors that specify cell fate, such that a neuron's "dendritic specification" can be switched through exogenous expression of dendrite shape transcription factors from another neuronal population[43, 44]. The dramatic and rapid impact that changes in these transcriptional regulators have on dendritic structure is at odds with the slowly-progressive dendritic degeneration observed in ataxia, arguing against the involvement of these factors, although subtle changes in the function of these transcriptional regulators producing slowly-progressive remodeling cannot be ruled out. As such, the remainder of this section will focus on regulators of dendrite structure that produce smaller-scale changes by acting on the dendritic cytoskeleton.

Within neuronal dendrites, the core scaffold of the dendritic shaft is composed of a tightly-packed network of microtubules[170]. It is important to note that dendritic structure is not strictly microtubule-based, since the microtubule core within the dendritic shaft is surrounded by an outer matrix of filamentous actin (F-actin) from which spine F-actin extends[171] and the dendritic shaft also contains neurofilaments[172]. Studies of axon growth cone development have

suggested that establishment of neurites is initiated through F-actin polymerization, with maturation of the neurite occurring through subsequent microtubule invasion[173]. Furthermore, *in vitro* studies have shown that treatment with drugs that influence only actin polymerization can produce changes in the structure of mature dendrites[174, 175]. Finally, a study has suggested that alterations specific to neurofilaments can influence dendritic arborization[176]. Importantly, there is cross-talk between all three classes of cytoskeletal filaments. These findings have led to an understanding of dendrite structure as most dependent on microtubule and actin dynamics[177], with a likely (although less well-explored) contribution from neurofilaments, such that regulatory systems which impinge upon any of the three cytoskeletal systems are capable of producing remodeling of dendrites.

The activity-dependent regulators of the dendritic cytoskeleton are numerous. Because the establishment and maintenance of dendritic structure involves locally-determined decisions about polymerization vs. depolymerization and branching vs. outgrowth, it is difficult to generalize about how perturbations to a specific regulator might affect dendritic structure, particularly given findings where differences in the cell-type, method, and timing of perturbation have produced opposite results[56, 178]. Activity-dependent regulators of dendritic structure that act upon the cytoskeleton are outlined in Table 1.1. For the remainder of this section, I will be focusing on studies that have explored specific activity-dependent regulators of the dendritic cytoskeleton in Purkinje neurons, ending with discussion of studies where changes in these regulators have been identified in spinocerebellar ataxias.

Among the Rho-family GTPases, the clearest role has been identified for Rac1 in Purkinje neurons, although RhoA and Cdc42 are also expressed[179]. In a study where transgenic mice were generated expressing mutant constitutively-active Rac1 in Purkinje neurons, Purkinje

neurons showed fewer 3rd, 4th, 5th, and 6th order dendrites[56]. Furthermore, mice lacking the Rac1-GEF P-Rex2 show smaller Purkinje neuron dendrite arbors[180] while biolistic overexpression of the Rac1-GAP α1-chimaerin in slice cultures impairs Purkinje neuron dendrite outgrowth[57], consistent with the fact that Rac-GEFs promote Rac1 activation while Rac-GAPs oppose Rac1 activation. These data together suggest that active Rac1 limits the elaboration of Purkinje neuron dendrites.

A separate study identified CaMKII-mediated regulation of stathmin as a crucial participant in activity-dependent dendritic outgrowth following the stellate phase (see section 1.2.2). Stathmin is a microtubule destabilizing protein, and overexpression of stathmin in developing Purkinje neurons prevents the development of a mature dendritic arbor. This study demonstrated that neuronal activity stimulates CaMKII to phosphorylate stathmin, inactivating it and allowing for dendritic outgrowth[181]. This study connects Purkinje neurons' reliance on activity for dendritic outgrowth during development directly to the cytoskeleton.

Protein kinase C (PKC) isozyme activity has been demonstrated to be very important for mature Purkinje neuron dendrite structure, although the data are somewhat conflicting. Increased protein kinase C activity has been shown to impair dendritic outgrowth in developing Purkinje neurons from slice cultures[182] in a manner that depends on the function of voltage-gated calcium channels[183]. This would be consistent with the observation that mutations in the PKC substrate MARCKS that mimic PKC phosphorylation result in reduced dendritic complexity in cultured hippocampal neurons[184]. However, spinocerebellar ataxia type 14 (SCA14) is caused by mutations in *PRKCG*, the gene which encodes PKCγ, and the vast majority of SCA14-causing mutations in PKCγ produce an enzyme with reduced *in vivo* kinase activity[185], suggesting that the Purkinje neuron dendrite degeneration observed in SCA14[186] is mediated by reduced PKCγ

function. I propose that these data can be reconciled through a model where during development PKC activity promotes Purkinje neuron dendrite outgrowth but in mature Purkinje neurons PKC activity promotes dendrite stability. However, this model remains to be tested.

There is indirect evidence to suggest that activity-dependent regulators of the dendrite cytoskeleton may play a role in Purkinje neuron dendrite remodeling in spinocerebellar ataxias. In addition to the studies of SCA14 and PKC isozymes' role in dendritic remodeling, several studies in other forms of ataxia have hinted that there may be dysregulation of these systems. Studies in a SCA3 mouse have revealed that calpain family protease activity is an important modifier of Purkinje neuron dendrite degeneration[187], although this could also be attributable to calpain-mediated cleavage of the pathogenic protein product ataxin-3[188]. SCA5 is caused by mutations in *SPTNB2* (the gene encoding βIII-spectrin), and βIII-spectrin knockout mice show increased calpain activation in Purkinje neurons[189], a finding which follows the appearance of dendritic degeneration linked to reduced glutamate uptake[138]. Outside of the cerebellum, studies in a SCA1 mouse model have suggested a role for GSK-3β in hippocampal dendritic degeneration[190]. Although none of these studies makes a direct causal connection between neuronal activity, activity-dependent regulators, and Purkinje neuron dendrite remodeling, they do demonstrate that these systems are altered in multiple forms of ataxia, identifying potential pathways by which altered Purkinje neuron activity might drive dendritic remodeling in the SCAs.

1.4 Summary and aims of dissertation

Dendritic degeneration is a ubiquitous feature of neurodegenerative disease, and mouse model studies suggest that Purkinje neuron dendritic degeneration may be particularly important

to progressive ataxia in spinocerebellar ataxias (SCAs). Despite this, Purkinje neuron dendritic degeneration in spinocerebellar ataxias remains poorly understood. Changes in Purkinje neuron activity have been linked to Purkinje neuron degeneration, in keeping with the substantial role that activity plays in specifying mature Purkinje neuron dendrite structure, but any possible role for changes in dendritic excitability have not yet been explored. To address this, my dissertation sought to characterize any possible changes in the dendritic physiology of Purkinje neurons from the ATXN1[82Q] model of SCA1. In addition to characterizing those changes, I sought to explore potential activity-dependent signaling pathways that might operate downstream of altered dendritic excitability to mediate dendritic remodeling in SCA1 and other degenerative ataxias.

My thesis was motivated by two hypotheses: 1) ATXN1[82Q] Purkinje neurons show an increase in intrinsic dendritic excitability that drives dendrite degeneration, and 2) changes in activity-dependent regulators of dendrite structure contribute to dendrite degeneration observed in SCA1 and other forms of cerebellar ataxia. The first hypothesis was supported by the literature from ATXN1[82Q] mice which demonstrates reduced expression or function of potassium channels that should result in increased dendritic excitability and then also shows that reversing these changes is dendro-protective. The second hypothesis was supported by the substantial role that activity-dependent pathways play in Purkinje neuron dendrite development, and also by the fact that SCA14 is caused by mutations in PKCγ, an activity-dependent regulators of Purkinje neuron dendrite structure. These hypotheses fit together under a single hypothesis of dendritic degeneration, where I proposed that that increased dendritic excitability might be a major trigger for the hypothesized changes in activity-dependent regulators of

dendrite structure. A schematic representation of the hypothesis explored in this dissertation is outlined in Figure 1.1.

This dissertation explores this hypothesis by addressing three specific aims. The first aim is to assess whether there are abnormalities in ATXN1[82Q] Purkinje neuron dendritic physiology, to link observed abnormalities to changes in specific channels, and ultimately to assess whether there is a causal connection between altered dendritic physiology and dendritic remodeling. The second aim is to explore activity-dependent pathways that could act downstream of alterations in dendritic excitability to drive Purkinje neuron dendritic degeneration in SCA1. Work in this aim identified protein kinase C (PKC) isozyme activity as being an important modifier of Purkinje neuron dendritic degeneration, and suggested that the mechanism by which PKC activity regulates Purkinje neuron dendritic degeneration might also involve alterations in dendritic excitability. The findings from this second aim led to the third and final aim of this dissertation, which is to assess whether PKC activity might participate in the dendritic remodeling of Purkinje neurons in other forms of ataxia.

Pathway	Details	Primary target
Rho-family GTPases	The important Rho-family GTPases regulating dendrite structure are RhoA, Rac1, and Cdc42[191], although roles for other Rho-family GTPases have been demonstrated[192]. Activity is regulated by GAPs and GEFs, such that activity of these GAPs and GEFs can also influence dendrite structure[57, 193-195]. Rho-family GTPase targets regulating dendrites include Pak1[196] and N-WASP[197]	Actin
Protein Kinase C (PKC)	PKC isozymes[183, 198] regulate dendrite development and stability through substrates such as MARCKS[184] and Adducin[199]	Actin
Arp2/3	Arp2/3 is a multi-protein complex that can stimulate actin nucleation. PICK1, an inhibitor of Arp2/3, regulates NMDA-induced Arp2/3 function and is required for normal dendritic morphology[200]. Cobl has also been identified as an important	Actin
Cobl	Cobl is an actin-nucleating protein that operates independent of Arp2/3 to regulate dendrite structure[201]. Cobl appears to depend on calcium-bound calmodulin for activation in neurons[202]	Actin
Caspase-3	Caspase-3 activity can be stimulated locally by synaptic activity[203]. Rather than triggering cell death, local caspase 3 activation can trigger dendrite pruning[204], possibly through its activity on actin regulators or directly on neurofilaments	Actin and intermediate filaments
Calpain family proteases	Calpain proteases are calcium-responsive proteases that have been shown to regulate dendrite development[205] and stability[206] through their action on microtubules[207] or intermediate filaments[206]	Microtubules and intermediate filaments
Glycogen synthase kinase 3β (GSK-3β)	GSK-3β facilitates activity-dependent regulation of dendrite structure[58], possibly through its effect on the microtubule regulator CRMP2[208]	Microtubules
Microtubule-associated proteins (MAPs)	MAP1A[209] and MAP2[210] participate in activity-dependent dendrite elongation by binding to and stabilizing dendritic microtubule networks	Microtubules
Ras-family GTPases	Ras family GTPases can be activated by neuronal calcium entry[211] or membrane depolarization[212]. Local activation of MAPK downstream of Ras can stabilize nascent dendrites[213], potentially through the action of downstream JNK-1 on MAPs[214]	Microtubules
Stathmins	Stathmins are microtubule destabilizing enzymes that oppose dendrite outgrowth and are inhibited by activity-dependent phosphorylation[181].	Microtubules
Cypin	Cypin binds to tubulin heterodimers and promotes microtubule polymerization in dendrites[215]. Activity regulates cypin expression levels	Microtubules

The centrosome	A surprising role for the centrosome was identified in dendrite development. Typically thought of as being important for spindle formation during mitosis, it was discovered that cdc20-dependent signaling at the centrosome regulates dendrite outgrowth[216] and retraction[217], a process which is triggered by calcium entry through TRPC5[218]	Microtubules
Ca^{2+}/calmodulin-dependent kinases (CaMKs)	In addition to their well-established roles as activity-dependent regulators of dendritic structure through their impact on transcription[46, 219], they can also act through local phosphorylation of dendrite structure regulators, such as the small GTPase Rem2[220] or microtubule-binding proteins[221]	Actin and Microtubules

Table 1.1 Activity-dependent regulators of dendritic structure which act on cytoskeletal elements. Provided above is a list of activity-dependent pathways that operate by acting on dendritic cytoskeletal elements. It is worth noting that there is cross-talk between the pathways outlined above[198, 222, 223], and their separation into distinct pathways is intended for organizational clarity

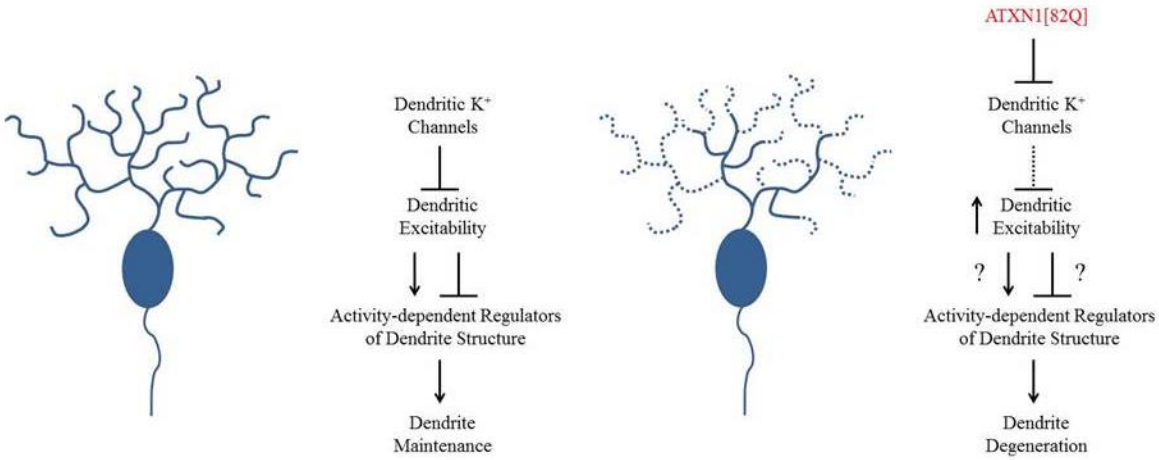

Figure 1.1 Hypothesis for the role that dendritic excitability and activity-dependent dendrite structure regulators play in Purkinje neuron dendrite degeneration in ataxia. Outlined above is the hypothesis explored in this dissertation. In healthy adult Purkinje neurons (left), dendritic excitability is regulated by a host of channels including potassium channels, such that dendritic excitability is consistent and activity-dependent regulators of dendrite structure do not show significant changes in their activity. This results in a stable dendritic arbor. In contrast, Purkinje neurons in ataxia (right) undergo dendritic degeneration. I hypothesize that this results from increased dendritic excitability and changes in activity-dependent regulators of dendritic structure that may operate within a single pathway.

Chapter 2

Materials and Methods

This chapter provides information on the materials and methods used in chapters 3, 4, and 5. Protocols are presented roughly in the order in which they will appear in later chapters. Most of this information is in a publication which is currently under review.

2.1 Animals and ethical use

All animal procedures were approved by the University of Michigan Committee on the Use and Care of Animals. The *ATXN1*[*82Q*] transgenic mice[27] overexpress mutant human ATXN1 with 82 CAG repeats selectively in cerebellar Purkinje neurons under the Purkinje neuron-specific murine *Pcp2 (L7*) promoter and were maintained on an FVB/NJ background (Jackson Labs, 001800). These mice were maintained homozygous for the transgene[116] except as indicated below. *ATXN1*[*82Q*] mice were used between two weeks old and fifteen weeks old. Age- and sex-matched wild-type FVB/NJ mice were used as controls for these studies. The ATXN2[127Q] transgenic mice[11] overexpress mutant human ATXN2 with 127 CAG repeats selectively in cerebellar Purkinje neurons under the *Pcp2 (L7)* promoter and were maintained on a mixed background. These mice were generated on a B6D2F1 hybrid background (Jackson Labs) and the line was maintained by crossing to this hybrid strain. Experiments using ATXN2[127Q] mice were done using hemizygous ATXN2[127Q] (tg/-) mice compared to wild-type ATXN2[127Q] (-/-) littermate controls. Mice used for these experiments were twelve weeks old. PKCi mice[224] express the pseudosubstrate PKC inhibitor (PKCi) peptide selectively

in Purkinje neurons under the *Pcp2 (L7)* promoter and were maintained on a C57B6J background (Jackson Labs). A balance of mice of both sexes were used in all studies.

In all experiments where ATXN1[82Q] bigenic mice were used, animals were always compared to litter-mate controls. Experimental mice originated from crosses between ATXN1[82Q] (tg/-) mice on an FVB/NJ background and PKCi (tg/-) mice on a C57B6J background, such that all experimental animals were F1 hybrids. The genotypes of mice used are specified as follows:

Wild-Type: ATXN1[82Q] (-/-); PKCi (-/-)

PKCi: ATXN1[82Q] (-/-); PKCi (tg/-)

ATXN1[82Q]: ATXN1[82Q] (tg/-); PKCi (-/-)

ATXN1[82Q] Bigenic: ATXN1[82Q] (tg/-); PKCi (tg/-)

All data presented from these experiments were from mice at twenty weeks of age.

In all experiments where ATXN2[127Q] bigenic mice were used, animals were always compared to litter-mate controls. Experimental mice originated from crosses between ATXN2[127Q] (tg/-) mice on a mixed background and PKCi (tg/-) mice on a C57B6J background, such that all experimental animals were on a mixed background. The genotypes of mice used are specified as follows:

Wild-Type: ATXN2[127Q] (-/-); PKCi (-/-)

PKCi: ATXN2[127Q] (-/-); PKCi (tg/-)

ATXN2[127Q]: ATXN2[127Q] (tg/-); PKCi (-/-)

ATXN2[127Q] Bigenic: ATXN2[127Q] (tg/-); PKCi (tg/-)

All data presented from these experiments were from mice at twenty-five weeks of age.

2.2 Genotyping

In all cases, DNA for genotyping was extracted from clipped mouse tails using a DNeasy Blood & Tissue Kit (Qiagen, Cat. no. 69504). DNA was stored at -20ºC until a PCR was run for genotyping. In all cases, products were run on a 1.5% agarose gel and visualized with ethidium bromide.

For genotyping of the ATXN1[82Q] transgene, two primer sets were used simultaneously. One primer set amplifies the transgene, producing an amplicon of size ~550 bp. The other primer set amplifies mouse genomic DNA from elsewhere in the genome, producing an amplicon of size ~220 bp and serving as a Taq and DNA control. Mice expressing the ATXN1[82Q] transgene would have both bands, while mice not expressing the transgene would only have a single band at ~220 bp. The PCR conditions for ATXN1[82Q] transgene genotyping are as follows: 1 cycle 94ºC for 5 minutes; 30 cycles of 94ºC for 1 minute, 60ºC for 1 minute, and 72ºC for 1 minute; 1 cycle of 72ºC for 8 minutes. Information on the primers is included in the table below:

Primer Name	Sequence	Description
Transgene Forward (5EX2B)	5' – AGGTTCACCGGACCAGGAAGG – 3'	Described previously[27], located within *Pcp2* exon 2
Transgene Reverse (Ruby)	5' – AATGAACTGGAAGGTGTGCGGC – 3'	Binds to ATXN1 cDNA, antisense to ~370 bp from start ATG
Genomic Forward (Gap60-1)	5' – AACTTTGGCATTGTGGAAGG – 3'	
Genomic Reverse (Gap60-2)	5' – ACACATTGGGGGTAGGAACA – 3'	

For genotyping of the ATXN2[127Q] transgene, one primer set was used. This primer set amplifies the transgene, and the primers span the intron between exon 6 and exon 7 of the human and mouse gene and bind to the cDNA contained within the transgene. This primer set produces an amplicon of size ~370 bp from the transgene, and is predicted to produce a mouse

genomic DNA amplicon of size ~68,000 bp (never seen). Mice expressing the ATXN2[127Q] transgene will have a single band at ~370 bp, while mice not expressing the transgene will have no band. The PCR conditions for ATXN1[82Q] transgene genotyping are as follows: 1 cycle 94ºC for 3 minutes; 40 cycles of 94ºC for 30 seconds, 57ºC for 30 seconds, and 68ºC for 45 seconds; 1 cycle of 68ºC for 5 minutes. Information on the primers is included in the table below:

Primer Name	Sequence	Description
Transgene Forward	5' - CGGGAAGCAAGGGCAAACCAGTTA – 3'	Within exon 6 of human ATXN2 refseq mRNA (NCBI ref no. NM_002973.3)
Transgene Reverse	5' – AGGAAGGAGATGGGCAAGGCGAT – 3'	Antisense to exon 7 of human ATXN2 refseq mRNA (NCBI ref no. NM_002973.3)

For genotyping of the PKCi transgene, two primer sets were used, each of which share the same reverse primer. One primer set has a forward primer sitting within the sequence for *Pcp2* and the reverse primer also sitting within the sequence for *Pcp2*. The other primer set has a distinct forward primer which sits at the 3' end of the PKCi peptide inhibitor sequence. Wild-type mice have a single amplicon of size 340 bp from the endogenous *Pcp2* locus. Mice expressing the transgene theoretically should have three bands, one from the endogenous *Pcp2* locus (340 bp), one which amplifies the transgene using *Pcp2* primers but contains the PKCi sequence (~400 bp), and one which uses a forward primer within the PKCi sequence and the reverse primer for *Pcp2* (~250 bp). In practice, the 340 bp band is not seen, thus mice expressing the PKCi transgene appear to have two bands while wild-type mice only have one. The PCR conditions for PKCi transgene genotyping are as follows: 1 cycle 94ºC for 5 minutes;

30 cycles of 94ºC for 1 minute, 57ºC for 1 minute, and 72ºC for 1 minute and 30 seconds; 1 cycle of 72ºC for 10 minutes. Information on the primers is included in the table below:

Primer Name	Sequence	Description
Pcp2 Forward (L7 Primer 1)	5' – CACTTCTGACTTGCACTTTCCTTGG – 3'	Amplifies *Pcp2* locus
PKCi Forward (L7 PKC Primer)	5' – CTGAGGCAGAAGAACGTGTAAG – 3'	This primer is the last 22 bp of the sense sequence for PKCi[224]
Reverse (L7 Primer 2)	5' – TTCTTCAAGCTGCCCAGCAGAGCTC – 3'	Binds *Pcp2* locus, is used as reverse primer for both forward primers

2.3 *Ex-vivo* electrophysiology

2.3.1 Solutions

Artificial CSF (aCSF) contained the following (in mM): 125 NaCl, 3.5 KCl, 26 $NaHCO_3$, 1.25 NaH_2PO_4, 2 $CaCl_2$, 1 $MgCl_2$, and 10 glucose. For all recordings except for measurements of dendritic capacitance, pipettes were filled with internal recording solution containing the following (in mM): 119 K Gluconate, 2 Na gluconate, 6 NaCl, 2 $MgCl_2$, 0.9 EGTA, 10 HEPES, 14 Tris-phosphocreatine, 4 MgATP, 0.3 tris-GTP, pH 7.3, osmolarity 290 mOsm (somatic recordings) or 285 mOsm (dendritic recordings). For measurements of dendritic capacitance, pipettes were filled with internal recording solution containing the following (in mM): 140 CsCl, 2 $MgCl_2$, 1 $CaCl_2$, 10 EGTA, 10 HEPES, 4 Na_2ATP, pH 7.3, osmolarity 287 mOsm. In dendritic capacitance experiments where post-hoc visualization of neurons was performed, biocytin (Cat. No. B4261, Sigma-Aldrich) was added to CsCl internal recording solution to a final concentration of 3.03 mg/mL.

2.3.2 Preparation of brain slices for electrophysiological recordings

Mice were anesthetized by isofluorane inhalation, decapitated, and the brains were submerged in pre-warmed (33°C) aCSF. Slices were prepared in aCSF held at 32.5-34°C on a VT1200 vibratome (Leica). Slices were prepared to a thickness of 300 µm for somatic recordings and a thickness of 250 µm for dendritic whole-cell recordings. Once slices were obtained, they were incubated in continuously carbogen (95% 0_2/5% CO_2)-bubbled aCSF for 45 minutes at 33°C. Slices were subsequently stored in continuously carbon-bubbled aCSF at room temperature until use. For recordings, slices were placed in a recording chamber and continuously perfused with carbogen-bubbled ACSF at 33°C with a flow rate of 2–3 mls/min, excepting compartment-specific capacitance measurements which were performed at room temperature (24-25°C).

2.3.3 Patch-clamp recordings

Purkinje neurons were identified for patch-clamp recordings in parasagittal cerebellar slices using a 40x water-immersion objective and Eclipse FN1 upright microscope (Nikon) with infrared differential interference contrast (IR-DIC) optics that were visualized using NIS Elements image analysis software (Nikon). Borosilicate glass patch pipettes were pulled with resistances of 3–5 MΩ for somatic recordings or 7-10 MΩ for dendritic whole-cell recordings. Recordings were made 1-5 hours after slice preparation in a recording chamber that was continuously perfused with carbogen-bubbled ACSF at 33°C at a flow rate of 2–3 mls/min. Data were acquired using an Axon CV-7B headstage amplifier, Axon Multiclamp 700B amplifier, Digidata 1440A interface, and pClamp-10 software (MDS Analytical Technologies). In all cases, acquired data were digitized at 100 kHz. Voltage data were acquired in current-clamp mode with bridge balance compensation and filtered at 2 kHz. Cells were rejected if the series resistance changed by >20% during the course of recording. Whole-cell somatic recordings were

rejected if the series resistance rose above 15 MΩ, with the majority of recordings have a series resistance of <10 MΩ. Whole-cell dendritic recordings were rejected if the series resistance fell outside a range of 15-30 MΩ. The liquid gap junction potential for all voltage measurements was calculated to be 10 mV[116]. All voltages are corrected for gap junction potential.

Acquisition of data for compartment-specific capacitance measurements was performed in the presence of 50 µM picrotoxin at room temperature (24-25°C). Capacitative transients were obtained in voltage-clamp mode using 1 second steps to -70 mV from a holding potential of -80 mV. Recordings were excluded if the measured input resistance was <100 MΩ.

Recordings to determine the current threshold for eliciting dendritic calcium spikes were performed as described previously, but in aCSF containing 1 µM tetrodotoxin (Tocris Bioscience). In experiments where baclofen was used, baclofen (Cat. no. B5399, Sigma-Aldrich) was used at a concentration of 2 µM.

2.3.4 Analysis of cell capacitance

Determination of dendritic capacitance was performed using a well-established method for analysis of an equivalent circuit representing the Purkinje neuron[225]. Input resistance was corrected offline, and the decay of the capacitative transient was fit using a two-exponential decay function described below:

$$I(t) = A_1 e^{-\frac{t}{\tau_1}} + A_2 e^{-\frac{t}{\tau_2}}$$

The constants from each cell's decay function can then be used to obtain four parameters: C_1 (representing the capacitance of the soma and main proximal dendrites), C_2 (representing the capacitance of the distal dendritic arbor), R_1 (representing the pipette access resistance), and R_2 (representing the composite resistance of dendritic segments separating the distal dendritic arbor

from the main proximal dendritic segments). This is done as follows (equations described previously[225]):

$$C_1 = \frac{\tau_1 (A_1 + A_2)^2}{A_1 \Delta V}$$

$$C_2 = \frac{A_2 \tau_2}{\Delta V}$$

$$R_1 = \frac{\Delta V}{A_1 + A_2}$$

$$R_2 = \frac{\Delta V}{A_2} - \frac{\Delta V}{A_1 + A_2}$$

In our measurement of dendritic capacitance in figure 1A, C_2 was used to represent dendritic capacitance.

In other experiments where whole-cell capacitance was measured, data were derived from experiments performed using K-gluconate-based internal and analyzed as described previously[116]. Briefly, capacitative transients were obtained in voltage-clamp mode using 1 second steps to -70 mV from a holding potential of -80 mV. The whole-cell capacitance was calculated as the area underneath the capacitative transient following correction for input resistance.

2.3.5 Analysis of dendritic calcium spike threshold

Analysis of dendritic calcium spike threshold was performed in the whole-cell configuration in current clamp mode. All spontaneous spiking was blocked with 1 µM tetrodotoxin, and +50 pA 1 second current steps were imposed. The current level of the first sweep where calcium spikes were elicited was reported. In neurons which did not firing calcium spikes even up to a maximum of +3.5 pA, the current threshold for the neuron was reported at +3.5 pA.

At five weeks of age, the majority of ATXN1[82Q] Purkinje neurons have undergone depolarization block, and their membrane potential can be restored using 1 μM tetrodotoxin and 100 μM $CdCl_2$[116]. We similarly observed non-firing cells in five week old ATXN1[82Q] Purkinje neurons. In non-firing ATXN1[82Q] Purkinje neurons, calcium spike measurements were performed, and subsequently the cells were exposed to 1 μM tetrodotoxin and 100 μM $CdCl_2$. Cells whose membrane potential began the recording at a membrane potential greater than -45 mV and fell to a membrane potential below -55 mV upon exposure to 1 μM tetrodotoxin and 100 μM $CdCl_2$ were deemed to be usable for subsequent analysis. Cells which were not firing and were more depolarized than -45 mV or did not respond to 1 μM tetrodotoxin and 100 μM $CdCl_2$ by hyperpolarization to below -55 mV were excluded.

Input resistance for each cell was calculated by generating an input-output curve for membrane potential vs. injected current. This input-output curve encompassed only membrane potential measurements between -80 mV and -75 mV in an effort to minimize the influence of dendritic excitability on measurement of input resistance. This method is consistent with previous studies using the calcium spike method to measure intrinsic dendritic excitability[152].

2.3.6 Analysis of dendritic whole-cell patch clamp recordings

Analysis of back-propagating action potential amplitude was performed by subtracting the peak and anti-peak of each spike across a single 10 second trace obtained during dendritic whole-cell patch clamp recording, with the mean of all such measurements reported as the back-propagating action potential amplitude for each cell. Somatic peak-to-trough action potential amplitude was determined by subtracting the peak and anti-peak of each spike across a single 10 second trace

obtained during somatic whole-cell patch clamp recordings, with the mean of all such measurements reported as the peak-to-trough action potential amplitude for each cell. Soma-to-patch distance was determined using still IR-DIC images captured during recording, and measurement was done using shortest-distance free-form line measurements which originate at the center of an ellipse that just encloses the soma and end at the position where the patch pipette is in contact with the dendritic membrane. Measurements were performed in NIS Elements (Nikon), and the experimenter was blind to the genotype of the visualized neuron during measurement.

2.3.7 Analysis of baseline firing properties

Analysis of baseline firing properties was performed using Clampfit 10.2 (MDS Analytical Technologies). Firing frequency and coefficient of variation (CV) calculations were performed using a single 10 second trace obtained ~3 minutes after formation of a stable seal. CV was calculated as follows:

$$CV = \frac{Standard\ Deviation\ of\ Interspike\ Interval}{Mean\ Interspike\ Interval}$$

Analysis of the after-hyperpolarization (AHP) was performed using a single 10 second trace obtained ~1 minute after break-in. To calculate the AHP for each neuron, the minima for each spike in the trace were determined using the antipeak function of Clampfit, and the mean of those minima was reported as the AHP for each neuron. To calculate the AHP CV for each neuron, the following calculation was performed:

$$AHP\ CV = \frac{Standard\ Deviation\ of\ AHP}{Mean\ AHP}$$

Input resistance for each cell was calculated by generating an input-output curve for membrane potential vs. injected current. This input-output curve encompassed only membrane potential measurements between -80 mV and -75 mV in an effort to minimize the influence of dendritic excitability on measurement of input resistance. This method is consistent with previous studies using the dendritic calcium spike method to measure intrinsic dendritic excitability[152].

2.4 Visualization and reconstruction of Purkinje neurons after recording

2.4.1 Visualization of biocytin-filled Purkinje neurons from capacitance recordings

Visualization of biocytin-filled Purkinje neurons was performed as described previously[226]. After recordings were complete, slices were immediately placed in 4% paraformaldehyde (Sigma-Aldrich) in phosphate-buffered saline (PBS) (pH 7.4) and refrigerated at 4ºC for at least 24 hours and no longer than 1 wk. For biocytin visualization, slices were rinsed with PBS, and the endogenous peroxidase activity was quenched by incubation for ~30 minutes with 0.1% hydrogen peroxide in 10% methanol and PBS. After an additional wash in PBS, slices were permeabilized with 2% Triton X-100 (Sigma-Aldrich) in PBS and then incubated at room temperature in avidin/biotinylated enzyme complex (Cat. no. 32020, ThermoFisher). After 1–2 days, slices were rinsed with PBS and then reacted with 3,3′-diaminobenzidine (Life Technologies Invitrogen). Slices were mounted and coverslipped.

Visualized neurons were imaged using an Axiophot microscope (Zeiss) with attached motorized XYZ stage (MBF Bioscience). Images stacks were acquired at 20X. After acquisition, image stacks were merged, and the merged image stacks were used for subsequent analysis.

2.4.2 NeuroLucida reconstructions of biocytin-filled neurons

Reconstructions were performed on merged image stacks in Neurolucida 11.02 (MBF Bioscience) using the neuron tracing module. Dendrites and somata were traced semi-manually with experimenter blind to sample genotype, and surface area measurements for individual dendritic segments were generated automatically using the surface area measurement function. For each neuron, composite dendritic surface area measurements for each neuron were obtained by taking the sum of all individual dendritic segment surface area measurements for that neuron. These composite measurements were used for subsequent analysis. For each neuron, a sholl analysis[227] was performed in Neurolucida using the sholl analysis tool and 10 μm concentric rings, with the number of dendrite crossings at each ring used for subsequent analysis.

2.5 RNA isolation, cDNA synthesis, and quantitative real-time PCR

Mice were euthanized following anesthesia with isoflurane, and cerebella were removed and flash-frozen in liquid nitrogen. Tissue was stored at −80°C until the time of processing. Total RNA from each harvested mouse cerebellum was extracted using Trizol Reagent (Invitrogen) and subsequently purified using the RNeasy mini kit (Qiagen) following the manufacturer's instructions. cDNA was synthesized from 1 μg of purified RNA using the iScript cDNA synthesis kit (Cat. no. 1708891, Bio-Rad). Quantitative real-time PCR assays were performed using the iQ SYBR Green Supermix (Cat. no. 1708880, Bio-Rad) in a MyiQ Single Color Real-Time PCR Detection System (Bio-Rad), with each reaction performed at a 20 μl sample volume in an iCycler iQ PCR 96-well Plate (Bio-Rad) sealed with Microseal optical sealing tape (Bio-Rad). The relative amount of transcript mRNA was determined using the comparative C_t method for quantitation[228] with *ActinB* mRNA serving as the reference gene. C_t values for each sample

were obtained in triplicate and averaged for statistical comparisons. The primers used for qRT-PCR are listed below:

Amplicon	Forward Primer (5' to 3')	Reverse Primer (5' to 3')
Kcnma1 (C-Terminus)	GGGCCAAGAAAAGAAATGGT	GATCAGGCTGCTTGTGGATT
Kcnma1 (N-Terminus)	AGCCAACGATAAGCTGTGGT	AATCTCAAGCCAAGCCAACT
Kcnn2	ACCCTAGTGGATCTGGCAAA	GGGTGACGATCCTTTTCTCA
Itpr1	CAGCACAAATTGAGATTGTCAGA	ATCCCGCTCTGTGGTGTAAT
Cacna1g	GTCGCTTTGGGTATCTTTGG	TACTCCAGCATCCCAGCAAT
Trpc3	GAGGTGAATGAAGGTGAACTGA	CGTCGCTTGGCTCTTATCTT
Kcnj3	TGTGGAAACCACAGGAATGA	TTGCATGGAACTGGGAGTAA
ActinB	CGGTTCCGATGCCCTGAGGCTCTT	CGTCACACTTCATGATGGAATTGA

2.6 Adeno-associated virus (AAV) transduction of Purkinje neuron

Adeno-associated virus injection was performed by David Bushart, another graduate student in the lab. Both AAV constructs used in this study (BK-AAV and GFP-AAV) have been described previously[116]. Stereotaxic administration of AAV2/5 or sham PBS injection was performed on 28 day old ATXN1[82Q] transgenic or wild-type mice placed under anesthesia using a mixture of O_2 and isoflurane (dosage 4% for induction, 1.5% maintenance). Mice received bilateral intracerebellar injections (2 sites/hemisphere) of virus. For each injection site, $\sim 5.0 \times 10^9$ viral genomes per injection site (3 μl total volume) or an equal volume of PBS was delivered to the medial or lateral cerebellar nucleus at an infusion rate of 0.5 μl/min using a 10 μl Hamilton syringe (BD Biosciences). The number of viral genomes delivered was within a range capable of producing widespread viral transduction with a minimal gliosis response[229]. One minute after the infusion was completed, the micropipette was retracted 0.3 mm and allowed to remain in place for 4 min before complete removal from the mouse brain. Anterior–posterior coordinates were calculated separately for medial and lateral injection into each cerebellar hemisphere. The coordinates for the medial injection were −6.4 mm anterior–posterior, ±1.3 mm medial-lateral, and 1.9 mm dorsal-ventral as measured from bregma. The coordinates for the lateral injection

were −6.0 mm anterior–posterior, ± 2.0 mm medial-lateral, and 2.2 mm dorsal-ventral as measured from bregma.

2.7 Rotarod phenotype analysis

Motor coordination was evaluated using a rotarod. The study was powered to detect a 25% improvement in motor performance, and estimated to require at least eight mice in each group. The groups were randomly allocated within cage and balanced with respect to sex, age, and number in each cohort, although some cohorts did not include animals treated with the combination of sham surgery and baclofen (Cat. no. B5399, Sigma-Aldrich). Approximately 1 week after virus injection or sham surgery, all mice were handled for four consecutive days. Once handling was complete, mice were trained for four consecutive days on the rotarod. The first 3 days were done on an accelerated protocol (4 to 40 rpm, at a rate of 0.12 rpm/s) and the last day was done at a constant speed of 24 rpm. Following the training period, mice were tested on the rotarod at a constant speed of 24 rpm on 5 consecutive days, with four trials per day. Latency score was recorded as the time taken before the animal either fell off the bar or if an animal made three full rotations on the rotating rod, to a maximum time of 300 s. During both training and testing, mice were given twice-daily intraperitoneal injections of either baclofen (10 mg/kg in PBS) or an equal volume of PBS vehicle. After acute motor performance testing was complete, one cohort of mice was maintained on either baclofen-containing (150 mg/L) or vehicle drinking water until 14 weeks of age, with baclofen-containing or vehicle drinking water bottles replaced every 72 hours. At 14 weeks of age, these mice were sacrificed and molecular layer thickness measurements were performed. The tester remained blinded to treatment

condition during experimentation. Performance on the rotarod was analyzed with a two-way repeated-measures ANOVA by trial with Holms-Sidak multiple comparison test.

2.8 Tissue immunohistochemistry

2.8.1 Paraformaldehyde-fixed mouse immunofluorescence

Mice were anesthetized with isoflurane and brains were removed, fixed in 1% paraformaldehyde for 1 h, immersed in 30% sucrose in PBS and sectioned on a CM1850 cryostat (Leica). 14 μm parasagittal sections were processed for immunohistochemistry.

For double immunofluorescence experiments, PKCα or PKCγ were labelled with mouse anti-PKCα (1:100, Cat. no. ab4124, Abcam) or mouse anti-PKCγ (1:500, Cat. no. ab71558, Abcam) and goat anti-mouse Alexa488-conjugated secondary antibody (1:200, Ref. no. A11001, Life Technologies Invitrogen), while Purkinje neurons were labeled with rabbit anti-calbindin (1:200, Cat. no. 13176, Cell Signaling) and goat anti-rabbit Alexa594-conjugated antibody (1:200, Ref. no. A11012, Life Technologies Invitrogen). Sections were imaged using a FV500 Olympus Confocal Microscope at 60X magnification and single-plane images were obtained. Image acquisition settings were kept consistent for all samples prepared with a specific set of antibodies to allow for comparison between genotypes. Sample preparation was performed and images were obtained with experimenter blind to genotype.

For molecular layer thickness measurements, sections were prepared by the same method described above. Purkinje neurons were labelled with mouse anti-calbindin (1:1000, Cat. no. C9848, Sigma-Aldrich) and goat anti-mouse Alexa488 conjugated secondary antibody (1:200, Ref. no. A11001, Life Technologies Invitrogen). Sections were imaged using an Axioskop 2 plus microscope (Zeiss) at either 10X or 20X magnification. Measurements were performed using

cellSens Standard image analysis software (Olympus). Sample preparation was performed and images were obtained with experimenter blind to genotype.

2.8.2 Molecular layer thickness measurements

Measurement of molecular layer thickness was performed as previously described[116]. A line was drawn to measure 100 µm from the depth of the primary fissure along the length of the fissure. From the end of this line, a line was drawn to measure the distance to the nearest Purkinje neuron cell body in the appropriate lobule. Measurements of molecular layer thickness were performed in two sections per animal, and reported molecular layer thickness for each animal is the mean of these two measurements. Molecular layer thickness measurement was performed with experimenter blind to genotype and/or treatment condition.

2.8.3 Purkinje neuron cell counts

Purkinje neuron cell counts reflect manual counts of the total number of neurons in lobule IV/V. Lobule IV/V was defined as having an anterior border formed by a line extending from the depth of the fissure between lobules III and IV and a posterior border formed by a line extending from the depth of the primary fissure between lobules V and lobule VI. Purkinje cell counts were counted for two sections per animal, and the reported Purkinje cell count for each animal is the mean of these two measurements. Purkinje cell counts were performed with experimenter blind to genotype.

2.8.4 Paraffin-fixed mouse immunohistochemistry

Mice were anesthetized with isoflurane and brains were removed and fixed in 1% paraformaldehyde in PBS. Subsequently, brains were embedded in paraffin. 4 μm parasagittal sections were prepared.

Slides were hydrated by performing xylene rinses followed by ethanol gradient incubation. Subsequently, 10 mM sodium citrate antigen retrieval was performed by microwave boiling for five minutes. Tissue was then processed for immunohistochemistry. PKC substrate phosphorylation was labelled with rabbit anti-Phospho-(Ser) PKC substrate antibody (1:200, Cat. no. 2261, Cell Signaling) and goat anti-rabbit Alexa488-conjugated secondary antibody (1:200, Ref. no. A11059, Life Technologies Invitrogen). Purkinje neurons were labelled with mouse anti-calbindin (1:1000, Cat. no. C9848, Sigma-Aldrich) and goat anti-mouse Alexa594-conjugated secondary antibody (1:200, Ref. no. A11005, Life Technologies Invitrogen). Sections were imaged using a FV500 Olympus Confocal Microscope at 60X magnification and single-plane images were obtained

2.8.5 Paraffin-fixed human autopsy tissue immunohistochemistry

For all immunohistochemistry using human autopsy tissue, 4 μm thick sections were prepared from paraffin-embedded human cerebellar tissue blocks. 11/12 SCA1 specimens were obtained from Arnulff Koeppen (Albany Medical College, Albany NY), 1/12 SCA1 specimens were obtained from the University of Michigan Brain Bank, and 7/7 age-matched healthy control specimens were obtained from the University of Michigan Brain Bank. Slides were hydrated by performing xylene rinses followed by ethanol gradient incubation. Subsequently, 10 mM sodium citrate antigen retrieval was performed by microwave boiling for five minutes. Tissue was then processed for immunohistochemistry. PKC substrate phosphorylation was labelled with rabbit

anti-Phospho-(Ser) PKC substrate antibody (1:200, Cat. no. 2261, Cell Signaling) and goat anti-rabbit Alexa488-conjugated secondary antibody (1:200, Ref. no. A11059, Life Technologies Invitrogen). Purkinje neurons were labelled with mouse anti-calbindin (1:1000, Cat. no. C9848, Sigma-Aldrich) and goat anti-mouse Alexa594-conjugated secondary antibody (1:200, Ref. no. A11005, Life Technologies Invitrogen). Sections were imaged using a FV500 Olympus Confocal Microscope at 60x magnification and single-plane images were obtained. Image acquisition settings were kept consistent for all samples to allow for comparison between patients and controls. Sample preparation was performed and images were obtained with experimenter blind to patient disease status.

For each patient and age-matched control, Purkinje neurons were identified as calbindin positive cells whose somata were located in the Purkinje neuron layer. 6 images of individual Purkinje neurons were obtained for each patient or control, although for some MSA patients there were few surviving Purkinje neurons and it was not possible to obtain 6 images, in which case no fewer than 4 images were obtained. To reduce bias, images were obtained in areas were Purkinje neurons showed strong calbindin signal. Images were obtained with experimenter blind to patient disease status.

2.8.6 Analysis of human autopsy tissue immunohistochemistry images

In SCA1 and age-matched healthy control tissue, measurements of average staining intensity for both phosphorylated PKC substrate staining and calbindin staining were performed in the soma and proximal dendrite. Measurements in each cell reflect the average intensity of a circular area encompassing either the soma or proximal dendrite. For MSA samples there were very few Purkinje neurons with visible dendrite, so MSA and AD tissue included only somatic

measurements, performed as described above. Measurements were performed with experimenter blind to sample disease status.

For each Purkinje neuron from a given individual, a phosphorylated PKC substrate-to-calbindin intensity ratio was calculated, and in all graphs each data point represents the mean of these ratios calculated from the 4-6 images obtained from a single patient. Error bars represent the standard error of the mean for those measurements within a given patient. Lines indicating the mean intensity ratio value across all patients of a group are also included. Statistics reflect a two-way ANOVA analysis that revealed a statistically significant effect of disease state on phosphorylated PKC substrate-to-calbindin ratio, with no effect of sample number and no interaction.

2.9 Western blotting

2.9.1 Preparation of whole cerebellar samples

Mice were euthanized following anesthesia with isoflurane, and cerebella were removed and flash-frozen in liquid nitrogen. Tissue was stored at −80°C until the time of processing.

Igepal homogenization buffer was prepared as follows: 50 mM Tris HCl, 150 mM NaCl, 5 mM EDTA, 1 mM EGTA, pH to 8.0, 1% Igepal CA-630 (Sigma-Aldrich). EDTA-free protease inhibitor tablets (Cat. no. 11873580001, Sigma-Aldrich) and PhosSTOP phosphatase inhibitor tablets (Cat. no. 4906845001, Sigma-Aldrich) were added to homogenization buffer immediately before use. Whole cerebellar samples were homogenized using a Potter-Helvejm tissue grinder (Corning). The supernatants (soluble protein fractions) were collected and total protein concentration was determined using the Pierce BCA protein assay kit (Prod. no. 23225,

ThermoFisher), at which point the supernatants were resuspended in Laemmli buffer. Samples were then utilized immediately for Western blots.

In all cases where ATXN1[82Q] and wild-type mice were compared, ATXN1[82Q] and wild-type mice were matched so that slices were prepared from matched mice on the same day with the same reagents, and all subsequent sample preparation and analysis was performed using matched samples. In experiments where ATXN2[127Q] mice were compared with littermate controls, all samples were prepared on the same day with the same reagents, and all subsequent sample preparation and analysis was performed using matched samples.

2.9.2 Preparation of organotypic slice culture samples

Sagittal brain slices (300 μm thickness) were prepared as previously reported[116]. 5-6 slices per brain were used in each set of cultures, divided evenly between control medium and experimental medium. After a quick wash in the corresponding medium, each slice was placed on a cell culture insert (0.4 μm pore size, 30 mm diameter; Millipore), which had been previously placed on a well (6-well plate) containing 1.2 ml of culture medium that had been pre-incubated at 37ºC in 95% O_2 / 5% CO_2. Control medium was prepared as follows: 50% minimal essential medium with Earle's salts, 25% horse serum, 25% Hank's balanced salts solution, 25 mM HEPES, 2 mM L-glutamine, 6.5 mg/ml glucose. EGTA-containing medium was prepared by starting with control medium, adding EGTA to a final concentration of 5 mM, and adjusting the pH to 7.4 with NaOH. Any slice-culture experiment involving treatment with a pharmacological agent was performed using experimental medium containing the pharmacological agent or control medium which contained an equivalent volume of vehicle.

After 24 h of incubation at 37°C in 95% O_2 / 5% CO_2, lysates were prepared from brain slices for immunoblotting. For immunoblotting protein lysate preparation, the cerebellum from each slice was macrodissected, and all cerebellar samples exposed to a given condition from each mouse were pooled and placed in ice cold Igepal homogenization buffer containing protease and phosphatase inhibitors (40 µL per slice), prepared as described above. Samples were immediately homogenized by pipette trituration followed by sonication in a 500 watt sonic dismembranator with Misonix 3" cup horn attachment (Cat. no. FB505110, QSonica). The supernatants (soluble protein fractions) were collected and total protein concentration was determined using the Pierce BCA protein assay kit (Prod. no. 23225, ThermoFisher), at which point the supernatants were resuspended in Laemmli buffer. Samples were then utilized immediately for Western blots.

In all cases where ATXN1[82Q] and wild-type mice were compared, ATXN1[82Q] and wild-type mice were matched so that slices were prepared from matched mice on the same day with the same reagents, and all subsequent sample preparation and analysis was performed using matched samples.

2.9.3 Electrophoresis and Western blotting

Total protein from whole cerebellar extracts or slice culture extracts (30 µg) were resolved in either 6%, 8%, or 10% sodium dodecyl sulphate-polyacrylamide gel electrophoresis (SDS-PAGE) gels, and corresponding polyvinyl difluoride membranes were incubated overnight at 4°C with primary antibodies: rabbit anti-Phospho-(Ser) PKC substrate antibody (1:1000, Cat. no. 2261, Cell Signaling), rabbit anti-Phospho-GSK-3β (Ser9) (1:1000, Cat. no. 9323, Cell Signaling), rabbit anti-GSK-3β (1:1000, Cat. no. 9315, Cell Signaling), mouse anti-Spectrin

alpha chain (nonerythroid) (1:1000, Cat. no. MAB1622, Clone no. AA6, EMD-Millipore), rabbit anti-PKCα (1:1000, Cat. no. ab4124, Abcam), rabbit anti-PKCγ (1:2000, Cat. no. ab71558, Abcam), rabbit anti-α-Tubulin (11H10) (1:5000, Cat. no. 2125, Cell Signaling). Bound primary antibodies were visualized by incubation with a peroxidase-conjugated goat anti-mouse IgG secondary (1:10000, Code no. 115-035-146, Jackson ImmunoResearch Laboratories) or goat anti-rabbit IgG secondary antibody (1:10000; Code no. 111-035-003, Jackson ImmunoResearch Laboratories) followed by treatment with the Western Lightning ECL-plus reagent (Prod. no. NEL121001EA, PerkinElmer) and exposure to autoradiography films.

2.9.4 Analysis of Western blot films

Developed films were scanned and densitometry analysis was performed in ImageJ. For analysis of phosphorylated PKC substrates, the intensity of the entire lane after phospho-(Ser) PKC substrate antibody blotting was normalized to the intensity of α-tubulin for each mouse. For analysis of αII-spectrin breakdown products (SBDPs) produced by the activity of calpain family proteases and caspase-3, intensity of the caspase-3-specific 120 kDa fragment was normalized to full-length αII-spectrin at 280 kDa and intensity of the calpain-specific 145 kDa fragment was normalized to full-length αII-spectrin at 280 kDa[230]. For analysis of all other proteins, intensity of the band of interest was normalized to the intensity of α-tubulin for each mouse.

2.10 Statistical analysis

Statistical tests are described in the figure legends for all data. Data are expressed as mean ± SEM unless otherwise specified. Sample numbers are included in each panel, with the number of cells (n) or number of animals (N) included where appropriate. Studies were powered and

analysis was performed assuming unequal variance between groups. Statistical significance for all Student's T-test analysis was defined as $P<0.05$. For one-way ANOVA with Holms-Sidak multiple comparison test, adjusted $P<0.05$ was considered statistically significant, and presented P values are adjusted P values. For two-way ANOVA, statistical significance was defined as $P<0.05$. For two-way ANOVA with Sidak multiple comparison test, adjusted $P<0.05$ was considered statistically significant, and presented P values are adjusted P values. For extra sum of squares F test, statistical significance was defined as a rejection of the null hypothesis that wild-type and ATXN1[82Q] data are better described by a single curve with $P<0.05$. For two-way repeated measures ANOVA without multiple comparisons, statistical significance was defined as $P<0.05$. For two-way repeated measures ANOVA with Holms-Sidak multiple comparison test, adjusted $P<0.05$ was considered statistically significant, and presented P values are adjusted P values. Data were analyzed using SigmaPlot (Systat Software), GraphPad Prism (GraphPad), and Excel (Microsoft).

2.11 Chemicals

Reagents and chemical were obtained from Sigma-Aldrich unless otherwise specified.

Chapter 3

The ATXN1[82Q] model of SCA1 shows increased Purkinje neuron intrinsic dendritic excitability that drives dendrite degeneration

3.1 Abstract

Degeneration of Purkinje neuron dendrites is a prominent histopathologic feature observed in autopsy tissue from human spinocerebellar ataxias (SCAs), and studies in SCA mouse model have demonstrated that Purkinje neuron dendrite degeneration correlates with the onset of motor impairment. While the evidence mediating dendrite degeneration in the SCAs remains poorly understood, studies of Purkinje neuron dendrite development and maintenance have demonstrated that mature dendritic structure is regulated heavily by synaptic and intrinsic activity. Changes in synaptic transmission and autonomous pacemaking have been studied in multiple SCA models, but intrinsic dendritic excitability has not been explored. To explore the role that changes in dendritic excitability might play in Purkinje neuron dendrite remodeling in the SCAs, we performed a characterization of dendritic physiology in Purkinje neurons from the ATXN1[82Q] model of SCA1, and assessed the role that those changes might have in dendritic remodeling. We demonstrate that ATXN1[82Q] Purkinje neurons show increased intrinsic dendritic excitability throughout the course of dendritic degeneration. Furthermore, we demonstrate that this increase in dendritic excitability is accompanied by changes in expression of a number of ion channels that are important for Purkinje neuron dendrite physiology. Finally, we demonstrate that a therapeutic strategy which normalizes ATXN1[82Q] Purkinje neuron

intrinsic dendritic excitability is able to improve motor performance and preserve dendrite structure *in vivo*. These findings identify changes in intrinsic dendritic excitability as a novel mechanism underlying Purkinje neuron dendrite degeneration in the SCAs, and adds to the literature from other neurodegenerative diseases implicating changes in dendritic physiology in dendritic pathology. Most of the work of this chapter has been included in a paper that is currently under review. Some of the data in figure 3.3.4 was included in a paper that has already been published[116].

3.2 Introduction

Spinocerebellar ataxia type 1 (SCA1) is one of the more common and well-studied forms of spinocerebellar ataxia[231]. SCA1 is caused by expansion of the repetitive CAG tract within the first coding exon (exon 8) of a single ATXN1 allele, such that healthy individuals have between 6 and 42 CAG repeats (with those greater than 21 repeats being interrupted by several CAT exons) while individuals with SCA1 have a pure CAG tract ranging from 39 to 82 CAG repeats[232]. The CAG exon encodes glutamine, and as such SCA1 is one of the so-called polyglutamine disorders. Because expansion of the CAG tract beyond disease threshold is only required in a single allele, SCA1 is inherited in an autosomal dominant fashion, and *de novo* mutations have not been described. Like other polyglutamine disorders, SCA1 shows earlier age of onset and accelerated progression in individuals with longer CAG repeats, although the correlation is imperfect and suggests the presence of additional genetic modifiers[233]. Also like other polyglutamine disorders, SCA1 shows instability of the CAG repeat tract, such that the length can vary with each intergenerational transmission event[232].

Clinically, SCA1 presents with loss of motor coordination and balance, slurred speech, swallowing difficulties, spasticity, and cognitive impairment[231]. These symptoms map well onto

the select brain regions where neurodegeneration is observed, with particularly prominent involvement of the cerebellar Purkinje neurons, neurons of the deep cerebellar nuclei, and pyramidal neurons of the motor cortex, as well as involvement of the basal forebrain, thalamus, and multiple brainstem nuclei[234]. The selective pattern of neurodegeneration is observed despite widespread expression of ATAXIN-1, the protein product produced from the ATXN1 gene[235].

The first animal model of SCA1 was the ATXN1[82Q] mouse, which was a transgenic model expressing full-length cDNA from an SCA1 patient (82 CAG repeats) specifically in Purkinje neurons under the control of the *Pcp2 (L7)* promoter[27]. When maintained homozygous for transgene expression on the FvB/NJ background, these mice develop rota-rod impairment at 5 weeks of age, and Purkinje neuron dendritic degeneration has been observed by immunohistochemistry at 6 weeks of age, with cell loss first apparent at 12 weeks but not achieving statistical significance until later[9]. This model has been found to have abnormalities in Purkinje neuron spiking that correlate with the onset of motor impairment and dendritic degeneration[114, 116]. This model has also been found to have a number of alterations in synaptic transmission from both parallel fibers and climbing fibers[134-136]. The intrinsic excitability of Purkinje neuron dendrites in this model has not been explored.

Here, we examine changes in the intrinsic excitability of Purkinje neuron dendrites in ATXN1[82Q] mice. We provide the first fine-grained analysis of the time course of dendritic remodeling in this model, using both electrophysiologic and morphologic measures. We then identify increased intrinsic dendritic excitability by two methods, and we demonstrate that the increase is correlated with the onset of dendritic degeneration. Subsequently, we use expression analysis to demonstrate changes in expression of multiple ion channels that are important for regulating intrinsic dendritic excitability. Then we show that improving the expression of large-

conductance calcium-activated potassium (BK) channel and pharmacologically activating subthreshold-activated potassium channels (subthreshold K) can normalize ATXN1[82Q] Purkinje neuron dendrite excitability, suggesting that reduced expression of these channels might account for observed changes in intrinsic dendritic excitability. Finally we assess the impact of normalizing intrinsic dendritic excitability on motor performance and dendrite degeneration *in vivo*. The work described here outlines a novel mechanism underlying Purkinje neuron dendrite remodeling in ataxia, and it adds to the body of literature exploring alterations in dendritic physiology in neurodegenerative disease. This provides a new conceptual framework for understanding dendritic remodeling in ataxia, and it also highlights novel therapeutic targets that could be pursued.

3.3 Results

In all experiments outlined below, ATXN1[82Q] mice are maintained homozygous for the ATXN1[82Q] transgene. Age- and sex-matched FvB/NJ mice were used as wild-type controls.

3.3.1 ATXN1[82Q] Purkinje neuron dendrite degeneration begins at 5 weeks of age

Previous studies have demonstrated that ATXN1[82Q] mice have a rota-rod phenotype at five weeks of age[9, 114]. Several studies in this mouse have used the thickness of the molecular layer (where Purkinje neuron dendrites reside) as an indicator of when dendrite degeneration begins, and these studies have identified molecular layer thinning as beginning no earlier than ten weeks of age[9, 114]. Qualitative observations of dendrite structure in calbindin-stained tissue found that evidence of dendrite degeneration could be seen as early as six weeks of age[9]. Visualization and reconstruction of single Purkinje neurons from this model showed dramatic dendrite degeneration by twelve weeks of age, suggesting that looking at a population of

individual Purkinje neurons' dendrites might provide a more sensitive measure for the time course of ATXN1[82Q] Purkinje neuron dendrite degeneration.

We assessed the capacitance of ATXN1[82Q] and wild-type Purkinje neurons in acute cerebellar slices at 2, 3.5, 5, and 15 weeks of age using a CsCl internal, which dramatically increases input resistance by blocking potassium channels and thereby improves the ability to clamp the extensive dendritic arbor. Using a well-established model based on an equivalent circuit model of a Purkinje neuron (see section 2.3.4), we separated the capacitative current into two capacitance values, one reflecting the capacitance of the distal dendritic arbor while the other reflects the capacitance of the proximal dendrite and soma. Using these measurements, we were able to establish that ATXN1[82Q] Purkinje neuron dendrite atrophy is first apparent at 5 weeks and progresses until it is nearly complete at 15 weeks (Figure 3.1A). Notably, developmental pruning of the Purkinje neuron dendrite in mature wild-type neurons can also be resolved with this technique, a process which has been described previously[72]. By contrast, at no age was the capacitance of the soma and proximal dendrite different between ATXN1[82Q] Purkinje neurons and wild-type Purkinje neurons . Based on the trajectory of dendrite capacitance in ATXN1[82Q] Purkinje neurons it appears that dendrite degeneration may begin before the dendritic arbor reaches its maximal surface area. The ATXN1[82Q] transgene begins to express at around P12, and it has been noted that later onset of transgene expression results in significantly less Purkinje neuron pathology[236], raising the possibility that this reflects developmental rather than neurodegenerative pathology associated with transgene expression. However, there is no clear evidence that SCA1 has a neurodevelopmental component in humans, calling into question the relevance of this observation to human disease.

Biocytin was included in the recording pipette when capacitance measurements were performed, allowing for post-hoc visualization of Purkinje neurons after recording (Figure 3.1C). Digital reconstructions of these neurons were created in NeuroLucida, and analysis of the dendrite surface area in reconstructions matched what was observed with capacitance measurements (Figure 3.1D), including the observation of developmental pruning in wild-type neurons. Sholl analysis performed on reconstructions revealed decreased dendritic complexity in ATXN1[82Q] Purkinje neurons at 5 weeks of age (Figure 3.1E) and 15 weeks of age (Figure 3.1F). All of these findings are consistent with Purkinje neuron dendrite degeneration beginning at 5 weeks of age, coinciding with the onset of motor symptoms[9, 114, 116].

3.3.2 Measurement of dendritic calcium spike threshold suggests increased intrinsic dendritic excitability in ATXN1[82Q] Purkinje neurons at 5 weeks of age, but not 15 weeks of age

In order to explore potential alterations in Purkinje neuron dendritic physiology that might relate to dendritic degeneration in ATXN1[82Q] mice, we performed experiments to look at the intrinsic excitability of the Purkinje neuron dendrite arbor. Using the terminology outlined in section 1.3.3, evidence of more dramatic spatial decay of depolarization along the dendrite shaft will be referred to as reduced intrinsic dendritic excitability. Conversely, evidence of more faithful propagation of depolarization along the dendritic shaft will be considered increased intrinsic dendritic excitability.

Previously, a study examined intrinsic dendritic excitability in the *Kcnc3* knockout mouse by blocking spiking with bath application of tetrodotoxin (TTX) and then injecting current into the soma in order to elicit a dendritic calcium spike[152]. A reduced level of injected current required to elicit a dendritic calcium spike was viewed as a reflection of increased intrinsic

dendritic excitability, in this case due to the absence of the $K_V3.3$ channel encoded by *Kcnc3*. The underlying assumption of this experiment is that the local membrane potential required to achieve the threshold of a dendritic calcium spike is unchanged; thus, the level of injected current required to elicit a spike would be a reflection of the extent to which depolarization produced by somatic current injection is spreading into the dendritic arbor, making it a valid measure of the intrinsic excitability of the dendritic arbor.

We performed similar studies in ATXN1[82Q] Purkinje neurons at 5 weeks of age (Figure 3.2A). Relative to wild-type Purkinje neurons, ATXN1[82Q] Purkinje neurons required significantly less injected current in order to elicit a dendritic calcium spike (Figure 3.2B). The input resistance of ATXN1[82Q] Purkinje neurons used in these experiments was modestly but not statistically significantly increased relative to wild-type Purkinje neurons (Figure 3.2C), suggesting that the reduced threshold was not simply a reflection of more somatic depolarization in response to current injection. These findings suggest that ATXN1[82Q] Purkinje neurons have increased intrinsic dendritic excitability at 5 weeks of age.

To assess whether increased dendritic excitability was a consistent feature of disease in ATXN1[82Q] Purkinje neurons, we performed the same experiment at 15 weeks of age (Figure 3.2D). Surprisingly, ATXN1[82Q] Purkinje neurons required significantly more injected current to elicit a dendritic calcium spike (Figure 3.2E), although 6/9 ATXN1[82Q] Purkinje neurons showing no calcium spikes even after +3.5 nA of injected current and were incorporated into analysis as firing a calcium spike at +3.5 nA (see section 2.3.5). Additionally, the input resistance of the neurons used in these experiments was significantly increased for ATXN1[82Q] Purkinje neurons relative to wild-type Purkinje neurons.

This finding was somewhat perplexing, as it suggested a dramatic reversal of the observation at 5 weeks. This finding raised several possibilities: 1) there is a paradoxical decrease in intrinsic dendritic excitability in ATXN1[82Q] Purkinje neurons at 15 weeks, or 2) there is an experimental confound that prevents this assay from effectively measuring intrinsic dendritic excitability in ATXN1[82Q] Purkinje neurons at 15 weeks of age. In order to explore this possibility further, I thought it would be best to utilize an additional technique to measure intrinsic dendritic excitability in ATXN1[82Q] Purkinje neurons.

3.3.3 Measurement of dendritic action potential backpropagation suggests increased intrinsic dendritic excitability in ATXN1[82Q] Purkinje neurons at 5 weeks and 15 weeks of age

As discussed in section 1.3.3, action potentials initiated at the axon initial segment also spread into the dendritic arbor, but in Purkinje neurons they attenuate strongly as they backpropagate into the dendrite[95]. This is thought to be a function of both the highly-branched structure of Purkinje neuron dendrites and dendritic potassium channels. Measurement of backpropagating action potential amplitude is another method for measure the intrinsic excitability of neuronal dendrites, and a study in Purkinje neurons has used this method to demonstrate that synaptic plasticity protocols also induce plastic changes in intrinsic dendritic excitability that are input-specific[237].

We performed direct whole-cell patch clamp dendritic recordings in Purkinje neurons at 5 weeks of age. Because Purkinje neurons spike spontaneously, the amplitude of the spontaneously-generated action potentials could be measured at the site of recording in the dendritic arbor (Figure 3.3A). In both wild-type and ATXN1[82Q] Purkinje neurons, the relationship between patch distance and peak-to-trough backpropagating action potential

amplitude was fit with a single-exponential decay function. The ATXN1[82Q] distance-to-amplitude function showed a statistically significant right shift (Figure 3.3.B), indicating that action potentials were attenuating less as they backpropagate into the dendritic arbor. This did not appear to be a function of the order of dendrite from which recordings were performed, as there was a similar proportion of 1^{st}, 2^{nd}, and 3^{rd} order dendrites sampled in wild-type and ATXN1[82Q] Purkinje neurons. Because the peak-to-trough amplitude of the action potential when measured at the soma does not differ between wild-type and ATXN1[82Q] Purkinje neurons (Figure 3.3C-D), this indicates that ATXN1[82Q] Purkinje neuron dendrites have increased intrinsic dendritic excitability at 5 weeks of age. This is consistent with what was observed with somatically-evoked dendritic calcium spikes (see section 3.3.2).

We also performed direct whole-cell patch clamp dendritic recordings in Purkinje neurons at 15 weeks of age (Figure 3.3E). At this age, we also found that ATXN1[82Q] Purkinje neurons showed increased intrinsic dendritic excitability, as indicated by a statistically significant right-shift in the relationship between recording location and peak-to-trough backpropagating action potential amplitude (Figure 3.3F). Also similar to 5 weeks of age, the peak-to-trough amplitude of the action potential when measured at the soma does not differ between wild-type and ATXN1[82Q] Purkinje neurons at 15 weeks, despite changes in the shape of the spike (Figure 3.3G-H). These findings suggest that ATXN1[82Q] Purkinje neuron dendrites have increased intrinsic dendritic excitability at 15 weeks, in contrast to what was observed with somatically-evoked dendritic calcium spikes (see section 3.3.2). The discrepancy between these two methods for measuring dendritic excitability remains unclear, although we will postulate possible reasons behind this discrepancy in the discussion section.

In summary, measurement of backpropagating action potentials showed less attenuation in the dendritic arbor of ATXN1[82Q] Purkinje neurons relative to wild-type Purkinje neurons at 5 weeks and 15 weeks of age. This finding is consistent with an increase in intrinsic dendritic excitability from the onset of dendritic degeneration through its entire course. This finding could be attributable to changes in dendritic structure, changes in dendritic channels, or both. We focused on changes in dendritic channels, and specifically looked at changes in expression of mRNA for ion channels that play an important role in Purkinje neuron dendrites.

3.3.4 ATXN1[82Q] cerebella show changes in mRNA expression for many ion channels that play important roles in dendritic physiology

Studies in both the ATXN1[82Q] transgenic and *Atxn1*^{154Q} knock-in model have demonstrated profound changes in expression of a number of mRNAs[238, 239], suggesting that disease pathogenesis might derive from changes in gene expression. It is particularly likely that mutant ATAXIN-1 exerts its effect by perturbing transcription, as it was found that the polyglutamine-expanded ATAXIN-1 forms functional complexes with the transcriptional repressor Capicua[124] and that the ATXN1[82Q] transgene produces no pathology in the mouse when its nuclear localization sequence is ablated[240]. Because of the proposed role that altered transcription plays in SCA1 pathology, we hypothesized that the observed increases in dendritic excitability might be due to changes in expression of mRNA for ion channels important in Purkinje neuron dendrites.

As discussed in section 1.3.3, calcium-activated potassium channels are important regulators of Purkinje neuron dendritic excitability, and their action reduces intrinsic dendritic excitability, resulting in reduced electrical coupling between the dendrite and the soma[101, 154], attenuation of backpropagating action potentials[237], and reduced dendritic calcium entry[149].

Although Purkinje neurons express small-[153], intermediate-[241], and large-conductance[242] calcium activated potassium channels, we focused on expression of the small-conductance calcium-activated potassium channel isoform 2 (SK2) and the large-conductance calcium activated potassium channel (BK), as a role for these channels in limiting Purkinje neuron dendritic excitability has been well-characterized[101, 149, 154, 237]. We found that expression of *Kcnma1*, the gene encoding the α subunit for BK, shows a progressive reduction in expression with 67.7% of wild-type expression at 5 weeks of age and 26.2% of wild-type expression at 15 weeks of age (Figure 3.4A). Surprisingly, expression of *Kcnn2*, the gene encoding SK2, showed increased expression at both 5 and 15 weeks (Figure 3.4B). These data demonstrate that there is dysregulated expression of calcium-activated potassium channels important for Purkinje neuron dendritic physiology, although the direction of those changes is not consistent.

Upstream of calcium-activated potassium channels are a number of potential dendritic calcium sources. Purkinje neurons have an unusually high endogenous calcium buffering capacity relative to other neurons[243] and show significant attenuation of backpropagating action potentials, such that Purkinje neurons show very modest dendritic cytosolic [Ca^{2+}] increases associated with backpropagating simple spikes[244, 245]. In contrast, Purkinje neurons show more substantial dendritic cytosolic [Ca^{2+}] increases in response to synaptic input, with parallel fiber input producing localized dendritic calcium transients in response to parallel fiber input and more widespread dendritic cytosolic [Ca^{2+}] increases in response to climbing fiber stimulation[246]. This synaptically-evoked calcium increase is largely attributable to glutamate binding to and activating mGluR1 receptors on Purkinje neurons[247-250]. This mGluR1-mediated cytosolic [Ca^{2+}] increase arises as follows: 1) glutamate binding to mGluR1 activates the Gq subclass of G proteins[251], 2) Gq proteins activate PLCβ, which cleaves phosphatidylinositol 4,5-bisphosphate

(PIP_2) to form diacylglycerol (DAG) and inositol 1,4,5-trisphosphate (IP_3), and 3) IP_3 binds to IP_3 receptors on the dendritic endoplasmic reticulum (ER) to trigger release of ER-receptor mediated stores, which contribute substantially to synaptically-driven mGluR1-mediated calcium release[252], with additional contributions from the transient receptor potential channel 3 (Trpc3) channel[253] and voltage-gated calcium channels[150] that are activated by an incompletely understood non-canonical G-protein mediated pathway[254]. These calcium sources have all been shown to be coupled to calcium-activated potassium channels in Purkinje neurons or other cell types[255, 256]; as such, cytosolic [Ca^{2+}] increases through these sources has the effect of activating calcium-activated potassium channels.

Because the IP_3 receptor, Trpc3, and voltage-gated calcium channels each serve as important calcium sources in the dendrite, and because those calcium sources are coupled to calcium-activated potassium channels, we were interested in assessing whether increased dendritic excitability could be linked to changes in any of these channels. As such, we examined the expression of *Itpr1* (Figure 3.4C), which encodes the major IP_3 receptor subtype expressed in Purkinje neurons[257], *Trpc3* (Figure 3.4 D), and *Cacna1g* (Figure 3.4E), which encodes the α subunit of the voltage-gated calcium channel Cav3.1. In all cases, mRNA levels are dramatically reduced at 5 weeks and 15 weeks, with no apparent progression between the two ages. It is important to note that reduced expression of *Itpr1* and *Trpc3* has been described previously as early as four weeks of age in this mouse[258], in agreement with our findings. These data suggests that multiple calcium sources for calcium-activated potassium channels show reduced expression, which could contribute to increased intrinsic dendritic excitability.

In addition to calcium-activated potassium channels, subthreshold-activated potassium channels (subthreshold K channels) play an important role in regulating dendritic excitability in

other neuronal subtypes, although a role has not been explored in Purkinje neurons[259]. Previous work in the ATXN1[82Q] mouse identified reduced expression of several subthreshold K channel genes by RNAseq and suggested a role for dysregulation of subthreshold potassium channels in ATXN1[82Q] Purkinje neuron dendrite degeneration[116]. This study found reduced expression of *Kncj3*, the gene encoding the G-protein-coupled inward rectifier potassium channel type 1 (GIRK1), and we attempted to recapitulate this finding with qRT-PCR. Surprisingly, we did not find any change in expression of *Kncj3* at 5 weeks or 15 weeks (Figure 3.4F). This experiment was repeated with many other primers for *Kcnj3* and a difference was never identified (data not shown).

3.3.5 Adeno-associated viral expression of BK in combination with baclofen normalizes dendritic calcium spike threshold in ATXN1[82Q] Purkinje neurons at 5 weeks of age

In order to assess the role that dendritic excitability might play in ATXN1[82Q] Purkinje neuron dendritic degeneration, we aimed to identify a strategy which could normalize dendritic excitability. We decided to employ a strategy which acted to normalize BK channel function and increase subthreshold K channel function, as both of these channels act to limit intrinsic dendritic excitability and our expression data demonstrated reduced expression of *Kcnma1*. We utilized an adeno-associated virus to drive expression of BK in Purkinje neurons (referred to as BK-AAV) in combination with the $GABA_B$ agonist baclofen, which strongly activates an inwardly-rectifying potassium current in Purkinje neurons[260].

Based on the data described in sections 3.3.2 and 3.3.3, evoking dendritic calcium spikes is an effective measure of intrinsic dendritic excitability at 5 weeks of age. Because dendritic degeneration also begins at 5 weeks of age, we decided to test the proposed treatment strategy and its effect on dendritic excitability using this method (Figure 3.5A). Purkinje neurons

transduced with BK-AAV or treated with 2μM baclofen each required more injected current to elicit a dendritic calcium spike, suggesting that normalizing BK expression or potentiating subthreshold K channels could each improve dendritic excitability (Figure 3.5B). Importantly, it was only the combination that was able to normalize the current required for eliciting dendritic calcium spikes in ATXN1[82Q] Purkinje neurons, and the observed rescue indicated a synergistic effect of concurrent BK-AAV transduction and baclofen treatment. None of the groups showed statistically significant differences in their input resistance during these experiments (Figure 3.5C), indicating that any observed changes in threshold reflect changes in the intrinsic excitability of Purkinje neuron dendrites.

3.3.6 Treatment with both BK-AAV and baclofen improves motor performance and preserves Purkinje neuron dendrite structure in ATXN1[82Q] mice

As demonstrated in section 3.3.5, ATXN1[82Q] Purkinje neurons transduced with BK-AAV and treated with baclofen showed a normalization of intrinsic dendritic excitability. Next we examined the consequences of normalizing dendritic excitability on motor impairment and dendritic degeneration. We analyzed the motor performance of four groups of animals: 1) ATXN1[82Q] mice injected with BK-AAV and simultaneously treated with baclofen; 2) ATXN1[82Q] mice that received baclofen and sham surgery; 3) ATXN1[82Q] mice that received vehicle and sham surgery; 4) wild-type control mice. Motor impairment was assessed by rotarod performance two weeks after initiation of therapy, a time point where BK-AAV treatment by itself produces no detectable improvement in motor performance[116]. Combined treatment with BK-AAV and baclofen significantly improved motor performance of ATXN1[82Q] mice (Figure 3.6A). These mice also showed preservation of the thickness of the cerebellar molecular layer (Figure 3.6B-C), demonstrating that this combined treatment also

significantly reduced dendritic degeneration. Mice treated with baclofen alone did not show significant improvement in either motor behavior or molecular layer thickness, and our previous work demonstrates that BK-AAV alone does not acutely improve motor performance or prevent thinning of the molecular layer in ATXN1[82Q] mice[116]. The fact that normalizing dendritic excitability protects ATXN1[82Q] Purkinje neuron dendrites suggests that increased intrinsic dendritic excitability drives dendritic degeneration in SCA1.

3.4 Discussion

Here we report that Purkinje neurons from the ATXN1[82Q] model of SCA1 show increased intrinsic dendritic excitability in association with dendritic degeneration, and we also demonstrate that a treatment strategy which normalizes intrinsic dendritic excitability can improve motor performance and preserve Purkinje neuron dendrite structure *in vivo*. Using electrophysiologic and single-cell morphologic reconstruction, we demonstrate that dendritic degeneration is first detectable in ATXN1[82Q] Purkinje neurons at 5 weeks of age and that the dendrite is markedly attenuated by 15 weeks of age. We show that ATXN1[82Q] Purkinje neurons require less current to induce dendritic calcium spikes at 5 weeks but not 15 weeks, and also show that ATXN1[82Q] Purkinje neurons show less backpropagating action potential attenuation in the dendritic arbor at 5 and 15 weeks of age. We show that in association with these changes in dendritic physiology there are changes in expression of many channels important for dendritic physiology in wild-type Purkinje neurons. Finally, we show that the BK-AAV and baclofen treatment normalizes intrinsic dendritic excitability and is able to improve motor performance and preserve ATXN1[82Q] Purkinje neuron dendrites *in vivo*. These data support the hypothesis that changes in dendritic excitability contribute to degenerative dendrite

remodeling in SCA1, and they also present a therapeutic strategy for symptomatic and neuroprotective therapy.

In section 3.3.2, we demonstrated that ATXN1[82Q] Purkinje neurons require less injected current than wild-type neurons to elicit a dendritic calcium spike at 5 weeks of age, but at 15 weeks of age the majority of ATXN1[82Q] Purkinje neurons never fired calcium spikes. In contrast, in section 3.3.3 we demonstrated that ATXN1[82Q] Purkinje neurons show less attenuation of backpropagating action potentials in the dendritic arbor at both 5 and 15 weeks of age. While both assays support the conclusion that ATXN1[82Q] Purkinje neurons have increased intrinsic dendritic excitability at 5 weeks of age, the calcium spike and dendritic recording experiments point to opposite conclusions at 15 weeks of age. I would argue that the dendritic recording experiment is a more reliable measure of intrinsic dendritic excitability, as we have measurement of both the input signal (the somatic action potential) and the measured output (the dendritic backpropagating action potential), in contrast to the dendritic calcium spike experiment where the measure of intrinsic dendritic excitability is more indirect. Furthermore, the fact that 6/9 ATXN1[82Q] Purkinje neurons would not fire a dendritic calcium spike even up to a peak current injection of +3.5 nA raises the possibility that those neurons are much less capable of firing calcium spikes in general, making the assay invalid at this time point. Without further study, it is difficult to understand the reasons for this paradoxical finding. Nevertheless, the dendritic calcium spike experiment and backpropagating action potential measurements provide independent measures of increased intrinsic dendritic excitability at 5 weeks of age, and backpropagating action potential measurements at 15 weeks of age confirm that ATXN1[82Q] Purkinje neuron intrinsic dendritic excitability is increased throughout the course of dendritic degeneration.

One larger question that remains outstanding from this study is to understand the molecular basis for increased intrinsic dendritic excitability in ATXN1[82Q] Purkinje neurons. The observation that *Kcnma1* expression is reduced and that BK-AAV treatment partially rescues the dendritic calcium spike threshold implicates reduced BK as being involved. However, changes in other channels must be involved, as BK-AAV treatment did not produce full rescue. One possibility is that reduced transcript levels for subthreshold K channels, identified previously[116] but not recapitulated here, accounts for the remaining increase in intrinsic dendritic excitability that can then be rescued with baclofen. The second possibility is that other as-of-yet unidentified channels acting in parallel with BK are affected, producing an impact on dendritic excitability, with baclofen acting on existing subthreshold K channels. I propose instead a third possibility: the reduction in *Cacna1g*, *Itpr1*, and *Trpc3* transcripts represents a second "hit" upstream of BK. In support of this hypothesis, it has been shown that ATXN1[82Q] Purkinje neurons show reduced mGluR1-dependent cytosolic [Ca^{2+}] increases at 5 weeks of age and treatment with baclofen can rescue this deficit[135], consistent with data showing potentiation of mGluR1 signaling by $GABA_B$[261]. Furthermore, our own study found a synergistic relationship between BK-AAV and baclofen on calcium spike threshold, which would be more consistent with two interventions operating on a single pathway than operating on parallel pathways. Within this framework, the increased dendritic excitability is a combination of 1) reduced BK expression, and 2) reduced cytosolic [Ca^{2+}] to activate BK. These three potential pathways for increased dendritic excitability and the targets engaged by our therapeutic strategy are outlined in Figure 3.7. Further study will be required to dissect the molecular underpinnings of increased intrinsic dendritic excitability, including identifying specific channel blockers than can occlude the effect of baclofen *in vitro* and *in vivo*.

As discussed in section 1.3, a number of studies have reported abnormalities of Purkinje neuron spiking in ataxia models, and several studies have identified neuroprotective interventions that normalize aberrant spiking. Other studies have focused on Purkinje neuron synaptic function in models of ataxia, and several have suggested that changes at synapses onto Purkinje neurons influence Purkinje neuron pathology. Notably, changes in dendritic excitability have not been explored. The current study suggests that changes in dendritic excitability are not merely a read-out of cell-wide neuronal dysfunction, but instead reflect a specific driver of neurodegeneration. In previous studies of ataxia, pharmacologic modulation of spiking resulted in neuroprotection[114-116]; however, the channels targeted in these studies also regulate dendritic excitability, raising the possibility that some or all of the neuroprotective effect could reflect excitability changes in the dendritic compartment. It is important to acknowledge that even in our current study, the effect of increasing BK and subthreshold K channel function was not restricted to the dendritic compartment. A definitive demonstration of the role for dendritic excitability in SCA1 Purkinje neuron dendrite degeneration would require intervening only in the excitability of the dendritic compartment while leaving synapses and somatic spiking unchanged. Although the tools do not currently exist to perform this experiment, improvements in the understanding of how ion channels are trafficked to specific compartments of the neuron may allow for development of channel constructs whose expression is restricted only to the dendritic arbor, allowing for such a targeted intervention[262].

The findings from this study are likely to have implications for other forms of cerebellar ataxia. As discussed previously, studies of Purkinje neuron spiking in many models of ataxia have revealed changes in the excitability of the soma, and in most cases the channels that are implicated are expressed and functionally important in Purkinje neuron dendrites. Additionally,

the human ataxias Spinocerebellar ataxia type 13 (SCA13) and Spinocerebellar ataxia type 19/22 (SCA19/22) are caused by function-impairing mutations in the genes encoding the potassium channels Kv3.3[122] and Kv4.3[121], respectively, and studies of these channels or their paralogs have demonstrated that they limit dendritic excitability[152, 263]. Focusing on intrinsic dendritic excitability in Purkinje neurons from models of these other ataxias may yield important insights, and these ataxias may similarly respond to agents that target dendritic excitability.

Alterations in intrinsic dendritic excitability may extend to other neurodegenerative diseases. The studies of neuronal populations affected in Parkinson disease[162-164, 264] and CA1 pyramidal neurons in Alzheimer disease mouse models[159, 160] point to increased intrinsic dendritic excitability as a potentially common feature of neurodegenerative disease. To the best of our knowledge, our study is the first to identify changes in the excitability of the dendritic compartment and to link those changes to neuropathology in a rodent model of neurodegenerative disease. Our study also identifies a strategy for normalizing dendritic excitability that has motor performance benefits as well as neuroprotective benefits. These data present an exciting possibility: that targeting dendritic excitability is an attractive therapeutic strategy to both improve neurologic symptoms and produce long-term benefits by slowing disease progression in ataxias and other neurodegenerative diseases.

3.5 Acknowledgements

I thank members of the Shakkottai laboratory for helpful comments. I thank David Bushart for performing the AAV virus injections, James Dell'Orco for technical assistance performing whole-cell somatic recordings of spikes in 5 and 15 week old ATXN1[82Q] Purkinje neurons, and Aaron Wasserman for technical assistance performing qRT-PCR, molecular layer thickness measurements, and phenotype analysis. I thank Brian Martin, Dr. Stanley Watson, and

Dr. Huda Akil for their support in performing Neurolucida reconstructions of biocytin-filled Purkinje neurons. This work was supported by the National Institutes of Health [R01NS085054 to V.G.S., T32GM007863 to R.C.].

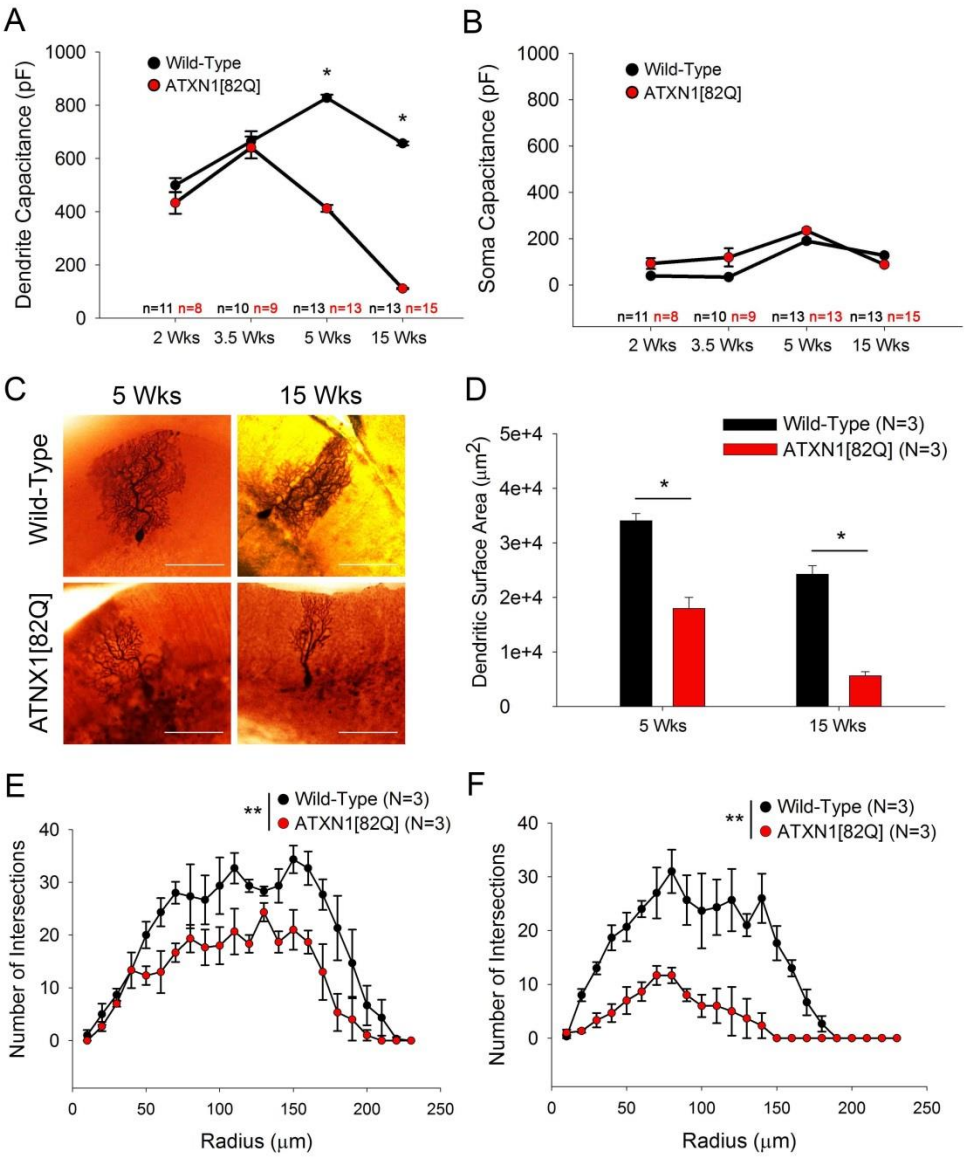

Figure 3.1 Characterization of Purkinje neuron dendritic degeneration in ATXN1[82Q] Purkinje neurons. **(A)** Dendritic capacitance measurements reveal ATXN1[82Q] Purkinje neuron dendritic degeneration starting at five weeks of age. **(B)** Somatic and proximal dendrite capacitance measurements reveal no significant differences in somatic and proximal dendrite surface area. **(C)** Visualized neurons Representative biocytin-filled Purkinje neurons used for dendritic capacitance measurements and for Neurolucida reconstruction and surface area measurement. **(D)** Measurement of dendritic surface area in reconstructed Purkinje neurons match surface area measurements using capacitance. **(E)** Sholl analysis at 5 weeks of age reveals reduced dendritic complexity in ATXN1[82Q] Purkinje neurons. **(F)** Sholl analysis at 15 weeks of age reveals reduced dendritic complexity in ATXN1[82Q] Purkinje neurons. Throughout, data are mean ± SEM. ** = P<0.01; *** = P<0.001. Statistical significance derived by two-way ANOVA with Sidak's multiple comparison test with statistically significant differences after multiple comparisons indicated (**A**, **B**, **D**) or two-way repeated-measures ANOVA (**E**, **F**).

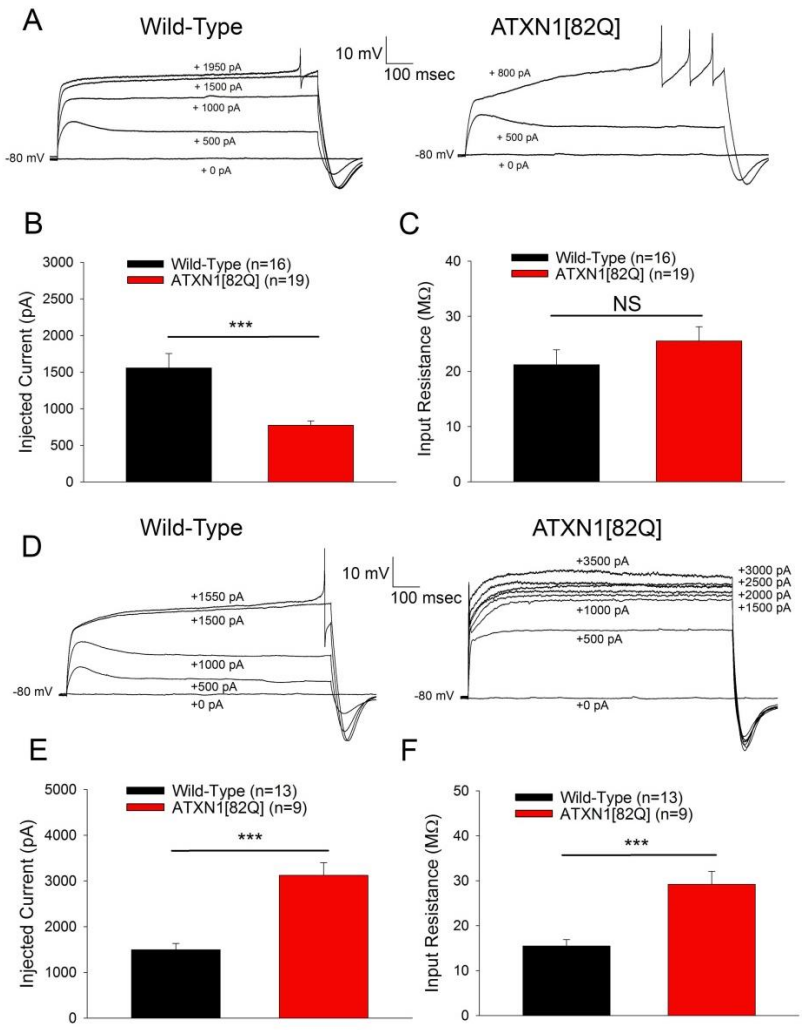

Figure 3.2 Measuring intrinsic dendritic excitability using dendritic calcium spikes in wild-type and ATXN1[82Q] Purkinje neurons. **(A)** Representative traces where dendritic calcium spikes were evoked with somatic current injection (injected current amount indicated on the trace) from five week old wild-type Purkinje neurons (left) and ATXN1[82Q] Purkinje neurons (right). ATXN1[82Q] Purkinje neurons require less injected current to elicit a dendritic calcium spike than wild-type Purkinje neurons, summarized **(B)**. **(C)** At five weeks of age, the input resistances of wild-type and ATXN1[82Q] Purkinje neurons do not differ when measured in normal aCSF with 1 µm TTX. **(D)** Representative traces where dendritic calcium spikes were evoked with somatic current injection (injected current amount indicated on the trace) from fifteen week old wild-type Purkinje neurons (left) and ATXN1[82Q] Purkinje neurons (right). In this case, the ATXN1[82Q] Purkinje neuron did not elicit a dendritic calcium spike up to a maximum of +3.5 nA. The current threshold for a calcium spike is higher in ATXN1[82Q] Purkinje neurons, summarized in **(E)**. **(F)** At fifteen weeks of age, the input resistance of ATXN1[82Q] Purkinje neurons is significantly greater than wild-type Purkinje neurons when measured in normal aCSF with 1 µm TTX. Throughout, data are mean ± SEM. NS = not significant, *** = P<0.001. Statistical significance derived by unpaired two-tailed Student's T-Test (**B**, **C**, **E**, **F**).

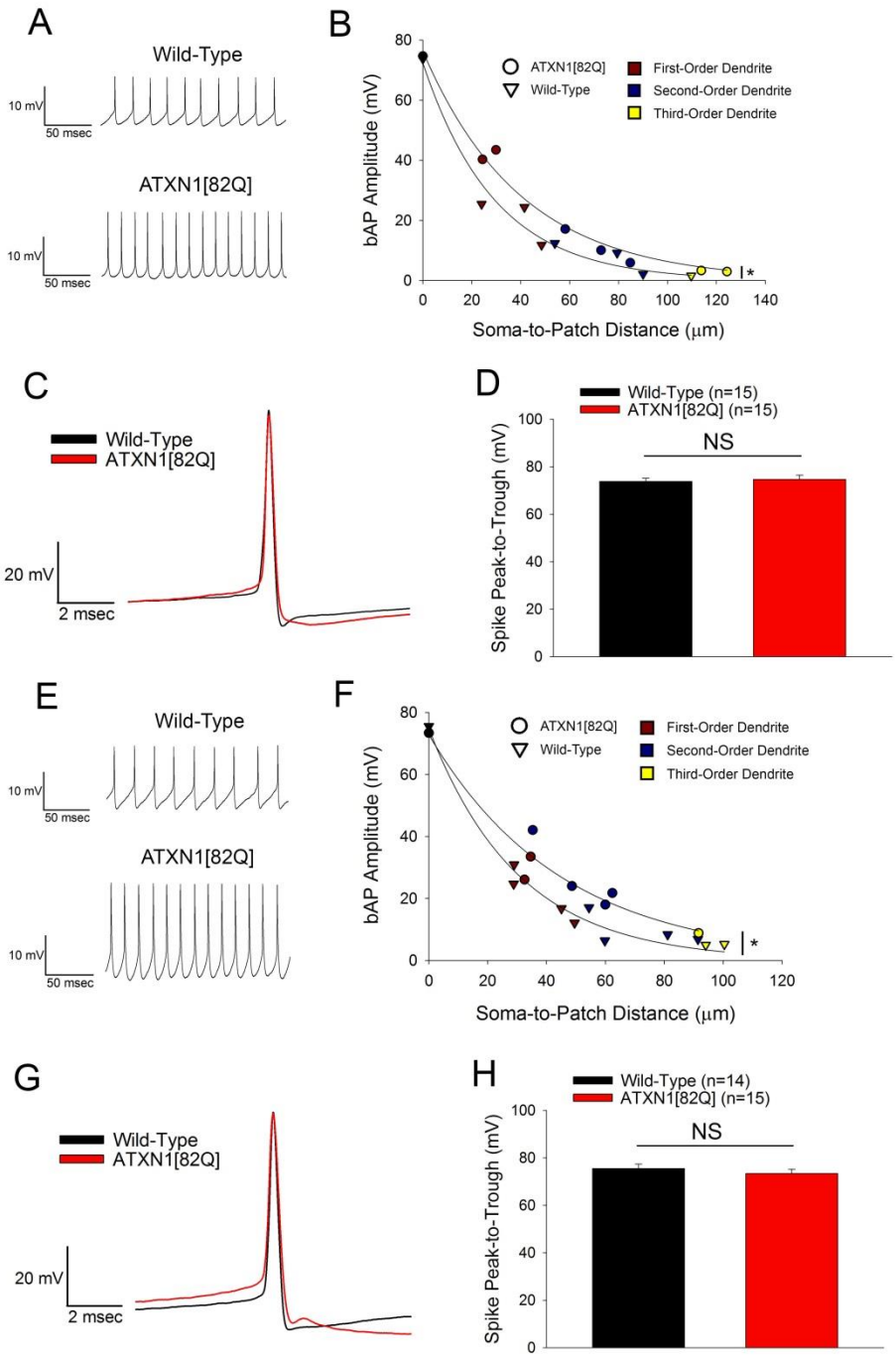

Figure 3.3 Measuring intrinsic dendritic excitability using backpropagating action potentials in wild-type and ATXN1[82Q] Purkinje neurons. **(A)** Representative dendritic whole-cell patch clamp recordings from a five week old wild-type Purkinje neuron (soma-to-patch distance: 53.9 μm) and five week old ATXN1[82Q] Purkinje neuron (soma-to-patch distance: 58.2 μm). **(B)** Scatter-plots with single-exponent decay best-fit lines for back-propagating action potential (bAP) amplitude measurements in wild-type and ATXN1[82Q] Purkinje neurons at five weeks of age show less attenuation of back-propagating action

potentials in ATXN1[82Q] mice. Each data point represents a recording from a separate cell, and the color of the data point represents the order of the dendrite from which the recording was performed. **(C)** Representative action potential from a somatic whole-cell recording in wild-type and ATXN1[82Q] Purkinje neurons at five weeks of age. The peak-to-trough amplitude of action potentials does not differ significantly between wild-type and ATXN1[82Q] Purkinje neurons at five weeks of age, summarized in **(D)**. **(E)** Representative dendritic whole-cell patch clamp recordings from a fifteen week old wild-type Purkinje neuron (soma-to-patch distance: 45.0 µm) and fifteen week old ATXN1[82Q] Purkinje neuron (soma-to-patch distance: 48.6 µm). **(F)** Scatter-plots with single-exponent decay best-fit lines for back-propagating action potential (bAP) amplitude measurements in wild-type and ATXN1[82Q] Purkinje neurons at fifteen weeks of age show less attenuation of back-propagating action potentials in ATXN1[82Q] mice. Each data point represents a recording from a separate cell, and the color of the data point represents the order of the dendrite from which the recording was performed. **(G)** Representative action potential from a somatic whole-cell recording in wild-type and ATXN1[82Q] Purkinje neurons at fifteen weeks of age. The peak-to-trough amplitude of action potentials does not differ significantly between wild-type and ATXN1[82Q] Purkinje neurons at fifteen weeks of age, summarized in **(H)**. Where there are error bars, data are mean ± SEM. Throughout, NS = not significant; * = $P < 0.05$. Statistical significance derived by unpaired two-tailed Student's T-Test (**D**, **H**) or extra sum of squares F test to determine whether one should reject the null hypothesis that data are best described by a single curve rather than two curves separated by genotype (**B**, **F**).

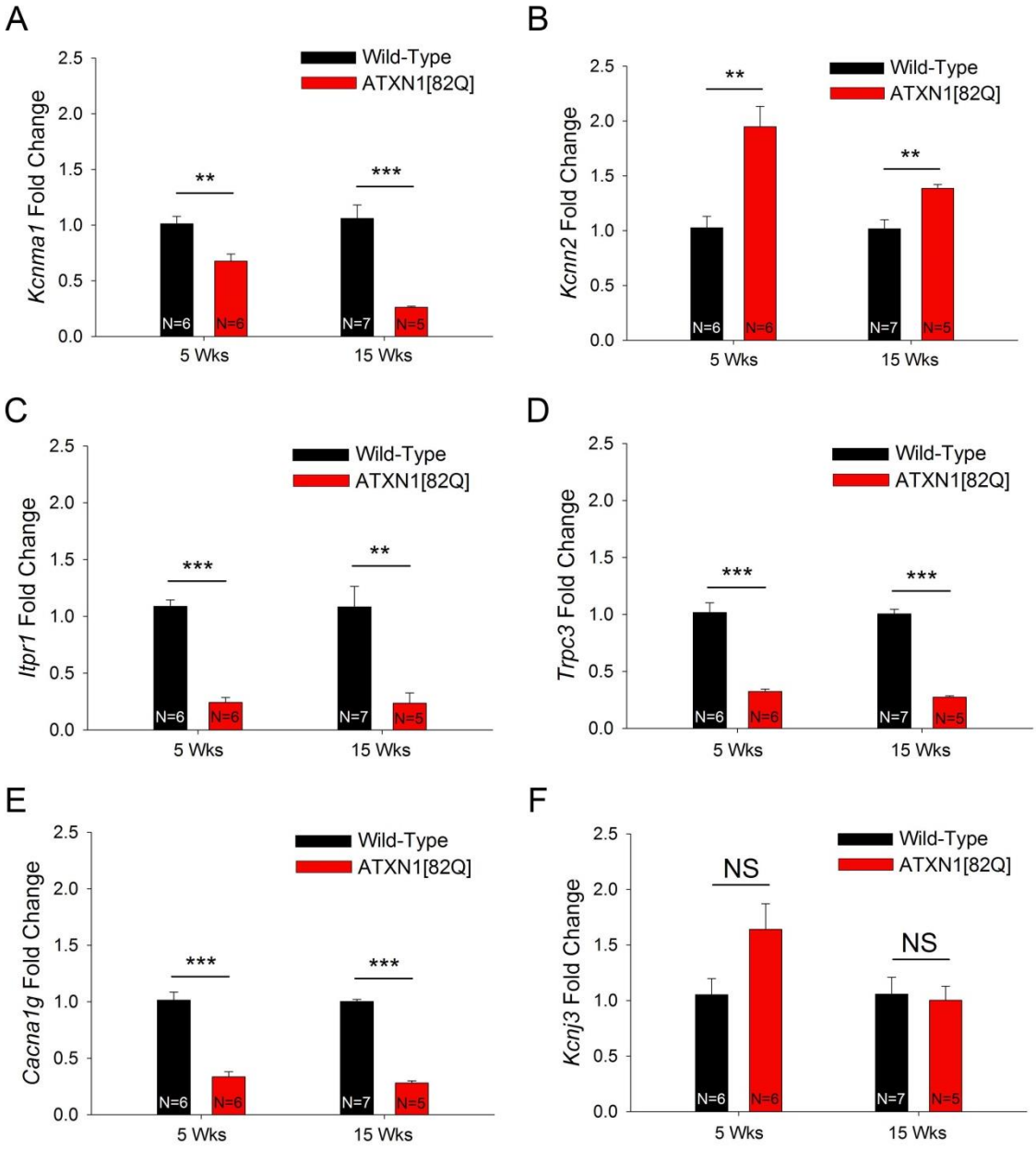

Figure 3.4 Measuring mRNA transcript expression for ion channels important in dendritic physiology. mRNA transcript levels for *Kcnma1* **(A)**, *Kcnn3* **(B)**, *Itpr1* **(C)**, *Trpc3* **(D)**, *Cacna1g* **(E)**, *Kcnj3* **(F)**,Throughout, data are mean ± SEM. Throughout, NS = not significant; ** = P < 0.01; *** = P < 0.001. Statistical significance derived by unpaired two-tailed Student's T-Test (**A**, **B**, **C**, **D**, **E**, **F**).

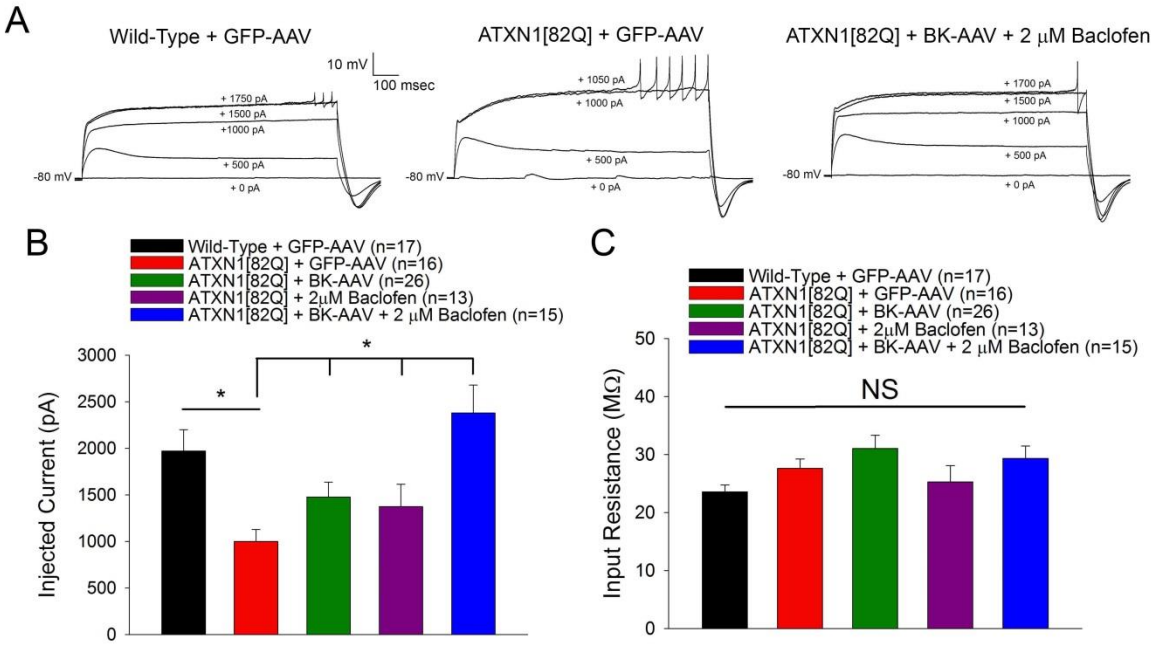

Figure 3.5 Measuring the effect of BK-AAV and baclofen treatment on dendritic calcium spike threshold in ATXN1[82Q] Purkinje neurons at 5 weeks of age. **(A**) Representative traces from Purkinje neurons at 5 weeks of age where dendritic calcium spikes were evoked with somatic current injection (injected current amount indicated on the trace). Recordings are from wild-type mice treated with GFP-AAV (left), ATXN1[82Q] mice treated with GFP-AAV (middle), and ATXN1[82Q] mice treated with BK-AAV and recordings were performed in the presence of 2 μm baclofen (right). **(B)** At five weeks of age, Purkinje neurons from ATXN1[82Q] mice which had been injected with BK-AAV with recordings performed in the presence of 2 μm baclofen show a normalization of their dendritic calcium spike threshold. **(A)** Input resistances are plotted from Purkinje neurons from five week old wild-type mice injected with GFP-AAV, Purkinje neurons from five week old ATXN1[82Q] mice injected with GFP-AAV, Purkinje neurons from five week old ATXN1[82Q] mice injected with BK-AAV, Purkinje neurons from five week old ATXN1[82Q] mice injected with GFP-AAV and exposed acutely to 2 μm baclofen, and Purkinje neurons from five week old ATXN1[82Q] mice injected with BK-AAV and exposed acutely to 2 μm baclofen. Throughout, data are mean ± SEM. Throughout, NS = not significant, * = $P<0.05$. Statistical significance derived by one-way ANOVA with Holms-Sidak multiple comparison test (**B**, **C**).

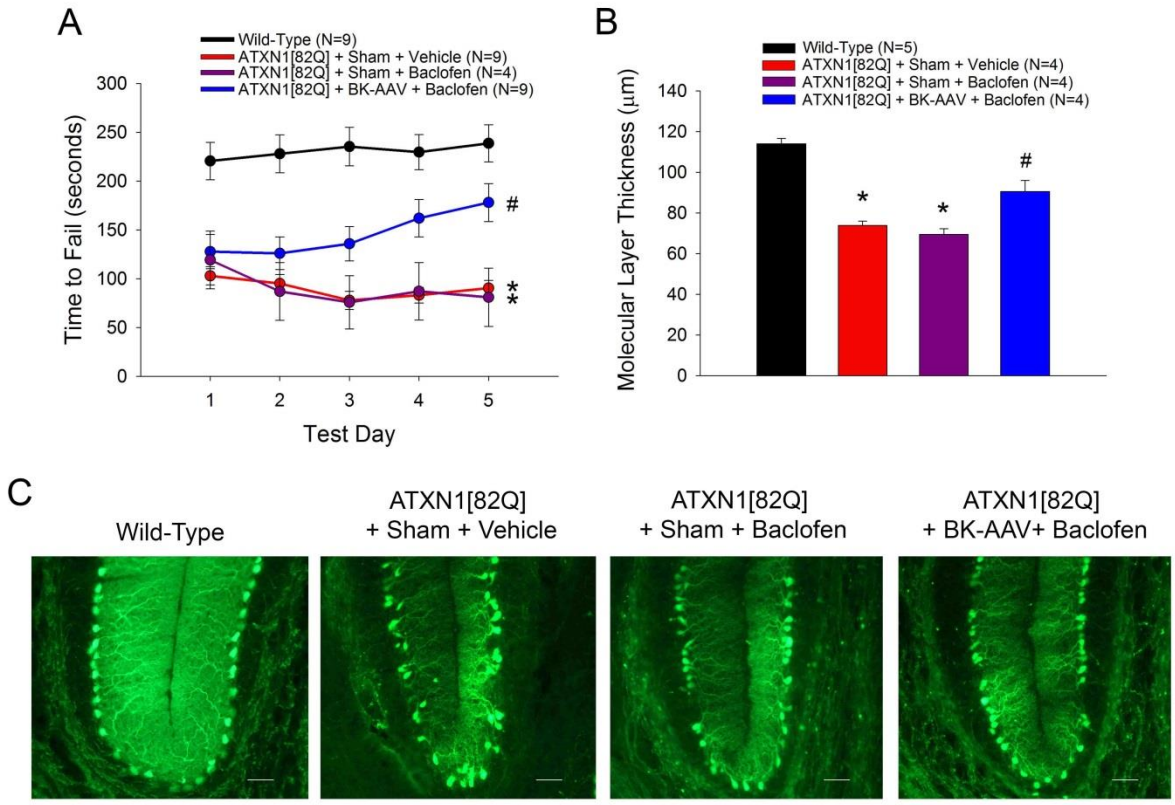

Figure 3.6 Measuring the effect of BK-AAV and baclofen treatment on rota-rod performance and dendritic degeneration in ATXN1[82Q] mice. **(C)** Rotarod performance was improved in ATXN1[82Q] mice injected with BK-AAV and treated with baclofen. * = statistically significant difference from wild-type and ATXN1[82Q] BK-AAV + Baclofen groups; # = statistically significant difference from all other groups. Statistical significance derived by repeated-measures two-way ANOVA with Holms-Sidak multiple comparison test. **(D)** Molecular layer thickness was preserved at fifteen weeks in ATXN1[82Q] mice injected with BK-AAV and treated with baclofen. * = statistically significant difference from wild-type and ATXN1[82Q] BK-AAV + Baclofen groups; # = statistically significant difference from all other groups. Statistical significance derived by one-way ANOVA with Holms-Sidak multiple comparison test. **(E)** Representative images at the cerebellar primary fissure in wild-type mice, ATXN1[82Q] mice exposed to sham surgery and vehicle, ATXN1[82Q] mice exposed to sham surgery and baclofen, and ATXN1[82Q] mice exposed to BK-AAV and baclofen. Scale bar, 50 µm.

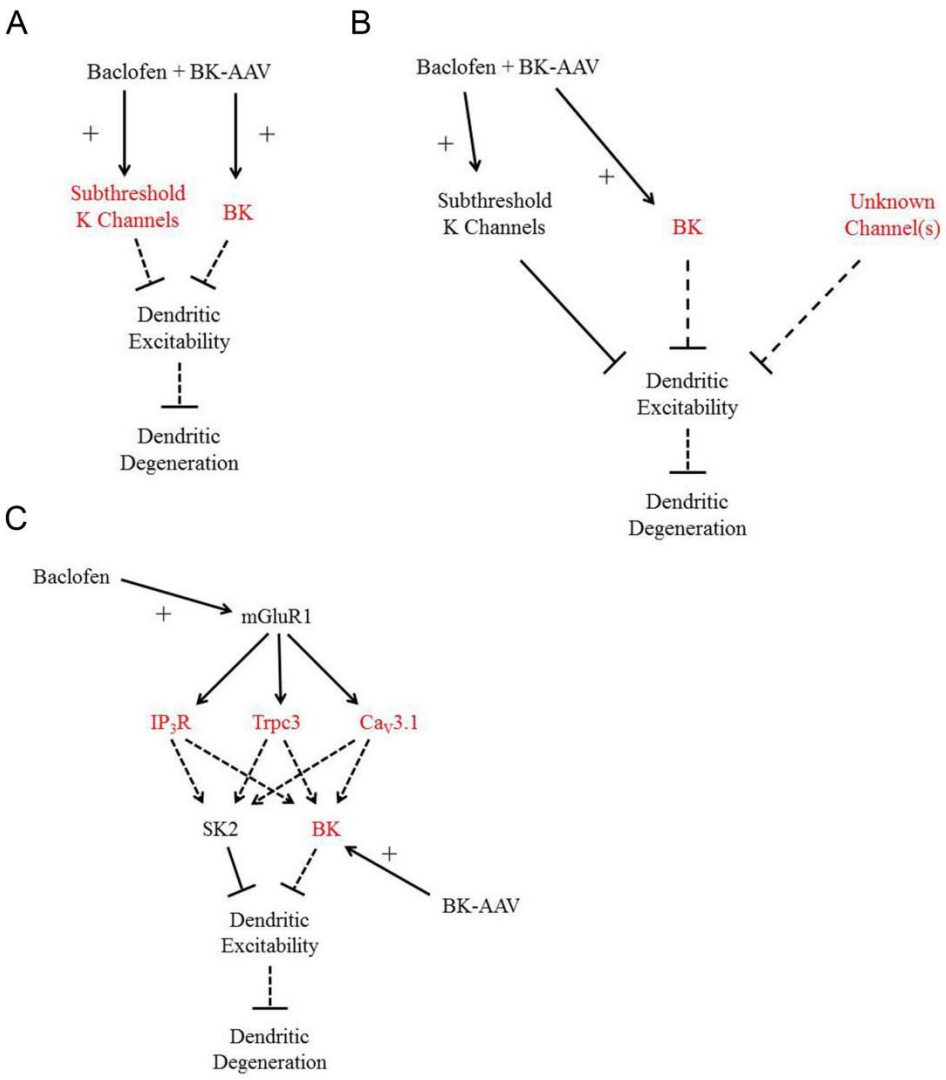

Figure 3.7 Possible pathways underlying increased intrinsic dendritic excitability. **(A)** Pathway outlining increased dendritic excitability in ATXN1[82Q] Purkinje neurons as arising from reduced transcript levels for subthreshold K channel genes and the BK channel. In this model, baclofen acts on remaining subthreshold K channels and BK-AAV restores expression of BK to normalize dendritic excitability. **(B)** Pathway outlining increased dendritic excitability in ATXN1[82Q] Purkinje neurons as arising from reduced transcript levels for BK and reduced function or expression of unknown channels in a parallel pathway. In this model, baclofen acts on unaffected subthreshold K channels and BK-AAV restores expression of BK to normalize dendritic excitability. **(C)** Pathway outlining increased dendritic excitability in ATXN1[82Q] Purkinje neurons as arising from two hits: 1) reduced transcript levels for BK, and 2) reduced expression of mGluR1-dependent dendritic calcium sources (IP_3 receptor, Trpc3, and $Ca_V3.1$). In this model, baclofen acts by potentiating mGluR1 and BK-AAV restores expression of BK to normalize dendritic excitability. In all cases, channels whose transcript levels are reduced in ATXN1[82Q] Purkinje neurons are marked in red.

Chapter 4

The ATXN1[82Q] model of SCA1 shows increased protein kinase C (PKC) substrate phosphorylation that opposes increased Purkinje neuron dendritic excitability and dendritic degeneration

4.1 Abstract

Purkinje neuron dendrite degeneration is a common histopathologic finding in ataxia, and models of spinocerebellar ataxias suggest that dendritic degeneration is an important structural correlate of motor impairment. Establishment and maintenance of mature Purkinje neuron dendrite structure depends heavily on neuronal activity and downstream activity-dependent pathways that act on the dendritic cytoskeleton to specify dendritic structure. Although a role for altered Purkinje neuron physiology in dendritic degeneration has been demonstrated in some models of spinocerebellar ataxia, the activity-dependent pathways that would act downstream of these changes to execute pathogenic dendrite remodeling are not well understood. To address this issue, we investigated activity-dependent regulators of dendritic structure in the ATXN1[82Q] model of SCA1, motivated in part by the finding that ATXN1[82Q] Purkinje neurons show increased intrinsic dendritic excitability that drives dendritic degeneration (chapter 3). We began by exploring changes in several pathways that respond to neuronal activity and regulate dendrite structure, and found a persistent increased in phosphorylation of PKC substrates throughout the course of dendritic degeneration, indicating that there is increased PKC

activation in ATXN1[82Q] Purkinje neurons. Increased PKC substrate phosphorylation was observed in Purkinje neurons from SCA1 patient autopsy tissue, confirming the relevance of this observed finding to human disease. Study of the cause for this increase in PKC substrate phosphorylation revealed that it depends on calcium, implicating conventional PKC isozymes. Suppression of PKC activation in ATXN1[82Q] mice by interbreeding with a mouse expressing a PKC peptide inhibitor in Purkinje neurons (the PKCi mouse) resulted in accelerated dendritic degeneration in ATXN1[82Q] mice, suggesting that increased PKC activity prevents dendrite degeneration. Analysis of dendritic physiology in ATXN1[82Q] mice expressing the PKCi transgene revealed increased intrinsic dendritic excitability, suggesting that increased PKC activity may exert its dendroprotective role by limiting increases in dendritic excitability. These findings identify PKC isozymes as novel protective modifiers of dendritic degeneration in SCA1, and they also suggest PKC isozymes may influence dendritic degeneration in ataxia through regulation of dendritic excitability. The findings from this chapter are included in a paper that is currently under review.

4.2 Introduction

Much is known about the pathways that regulate dendritic structure in developing and mature Purkinje neurons, but little is understood about how these pathways are affected in spinocerebellar ataxias. Purkinje neuron dendrite development depends significantly on Purkinje neuron electrophysiologic activity[84, 85] and there are many studies identifying changes in Purkinje neuron physiology in ataxia (see section 1.3.1-1.3.3). These findings suggest that activity-dependent pathways regulating dendrite structure might be implicated in dendrite degeneration in cerebellar ataxia.

Among the many activity-dependent regulators of dendrite structure (see section 1.3.4), several candidates have already been implicated in different forms of spinocerebellar ataxia. Studies of SCA3 and SCA5 have demonstrated that there is increased activation of calpain family proteases[188, 189], and in SCA3 calpain activity has been demonstrated to be a modifier of Purkinje neuron dendrite degeneration[187]. Studies of hippocampal neurons in the *Atxn1*^{154Q} have suggested that increased activation of GSK-3β plays a role in dendrite degeneration. Finally, protein kinase C activity has been demonstrated to modulate Purkinje neuron dendrite development in an activity-dependent fashion[183], and several studies have suggested that SCA14-causing mutations result in a mutant PKCγ with reduced function and a reduced capacity to phosphorylate targets[185, 265]. We therefore sought to determine whether any of these pathways were altered in the ATXN1[82Q] model of SCA1.

We began by assessing whether there were consistent changes in activation of GSK-3β, calpain family proteases, and PKC isozymes. Having only identified a consistent increase in PKC substrate phosphorylation in ATXN1[82Q], we investigated PKC substrate phosphorylation in autopsy tissue from patients with SCA1 and found that SCA1 patient Purkinje neurons also showed increased PKC substrate phosphorylation. We explored the causes for increased PKC activation in ATXN1[82Q] Purkinje neurons and demonstrated that it required calcium, implicating the conventional PKC isozyme subfamily, and also demonstrated that it was likely a change in activity of these isozymes rather than expression. In order to investigate the consequence for increased PKC activity on dendritic structure in ATXN1[82Q] Purkinje neurons, we inhibited PKC activity in ATXN1[82Q] mice *in vivo* by interbreeding them with PKCi mice that express a pseudosubstrate peptide inhibitor, and we found that inhibition of PKC activity accelerated dendritic degeneration. In our efforts to understand the mechanisms by

which PKC activity modulated dendritic degeneration, we identified increased intrinsic dendritic excitability in ATXN1[82Q] mice expressing the PKCi transgene, suggesting that PKC isozymes may act to limit the pathological increases in dendritic excitability identified in chapter 3. In summary, we have found that increased PKC activation in ATXN1[82Q] mice is dendro-protective, potentially by limiting increases in intrinsic dendritic excitability.

4.3 Results

In experiments outlined in sections 4.3.1, 4.3.2, and 4.3.4, ATXN1[82Q] mice[27] were maintained homozygous for the ATXN1[82Q] transgene. Age- and sex-matched FvB/NJ mice were used as wild-type controls.

In experiments outlined in sections 4.3.5-4.3.7, experimental mice originated from crosses between ATXN1[82Q] (tg/-) mice on an FVB/NJ background and PKCi (tg/-) mice on a C57B6J background, such that all experimental animals were F1 hybrids. The genotypes of mice used are specified as follows:

Wild-Type: ATXN1[82Q] (-/-); PKCi (-/-)

PKCi: ATXN1[82Q] (-/-); PKCi (tg/-)

ATXN1[82Q]: ATXN1[82Q] (tg/-); PKCi (-/-)

ATXN1[82Q] Bigenic: ATXN1[82Q] (tg/-); PKCi (tg/-)

It is important to note that in the experiments discussed in sections 4.3.5-4.3.7, ATXN1[82Q] mice are on a different genetic background and are ATXN1[82Q](tg/-), rather than being ATXN1[82Q](tg/tg) on a pure FvB background as the mice are in section 4.3.1, 4.3.2, and 4.3.4. ATXN1[82Q] mice used for sections 4.3.5-4.3.7 show a slower progression of neurodegeneration (compare molecular layer measurements from Figure 4.5B to molecular layer measurements from Figure 3.6B), which we hypothesize is a result of the lower transgene dose

and different genetic background. All data presented using these mice are from mice at 20 weeks of age. In all experiments, animals were compared to littermate controls.

4.3.1 ATXN1[82Q] cerebella show increased PKC substrate phosphorylation throughout the course of dendritic degeneration

We investigated activation of four activity-dependent dendrite remodeling pathways in ATXN1[82Q] mice: GSK-3β, calpain family proteases, caspase-3, and PKC isozymes. In hippocampal neurons, activity-dependent dendrite remodeling through GSK-3β involves loss of constitutive inhibitory phosphorylation on Serine 9[58]. Investigation of serine 9 phosphorylation on GSK-3β in ATXN1[82Q] cerebella did not reveal a decrease in phosphorylation at 15 weeks (Figure 4.1A-B), suggesting that such activity-dependent disinhibition of GSK-3β is not taking place in ATXN1[82Q] Purkinje neurons. This finding suggests that activity-dependent dendrite remodeling is likely not occurring through GSK-3β.

Both calpain family proteases[206] and caspase-3[204] have been identified as important activity-dependent regulators of the dendritic cytoskeleton. Activation of calpain family proteases and caspase-3 can both be assessed by looking at cleavage of αII-spectrin: calpain activity will produce a unique 145 kDa cleavage product, while caspase-3 activity will produce a unique 120 kDa cleavage product[230]. Investigation of αII-spectrin breakown products in fifteen week old ATXN[82Q] cerebella did not reveal an increase in production of either the caspase-3-specific 120 kDa fragment or the calpain-specific 145 kDa fragment (Figure 4.1C-E), suggesting that there is not increased activation of either pathway. These findings indicate that activity-dependent dendrite remodeling is not occurring through activation of calpain proteases or caspase-3.

Activity-dependent PKC isozyme function profoundly influences Purkinje neuron dendrite development[183], and mutations in PKCγ result in SCA14, a spinocerebellar ataxia with prominent Purkinje neuron dendrite degeneration[186]. Using an antibody that recognizes phosphorylated serine residues within the PKC consensus motif on substrates[266], we assessed whether phosphorylation of PKC substrates was altered in ATXN1[82Q] cerebella at 15 weeks, and found a striking increase in PKC substrate phosphorylation (Figure 4.1F-G). We then assessed PKC substrate phosphorylation at 5 weeks of age to determine whether this change was observed throughout the course of dendritic degeneration, and found a similar increase in PKC substrate phosphorylation (Figure 4.1H-I). These findings demonstrate that PKC substrate phosphorylation is increased throughout the course of ATXN1[82Q] Purkinje neuron dendrite degeneration, suggesting an increase in activation of PKC isozymes. These findings support a potential role for PKC isozyme activation in activity-dependent dendrite remodeling in ATXN1[82Q] Purkinje neurons.

4.3.2 Increased PKC substrate phosphorylation likely represents increased PKC isozyme activity in ATXN1[82Q] Purkinje neurons

The ATXN1[82Q] model of SCA1 is a transgenic model expressing cDNA for human ATXN1 with 82 CAG repeats, and the expression is limited to Purkinje neurons with the *Pcp2 (L7)* promoter. This suggests that the observed changes in PKC substrate phosphorylation might originate from cell-autonomous effects of ATXN1[82Q] expression on Purkinje neurons; however, the data presented in Figure 4.1 are from whole cerebellar extracts, raising the possibility that observed increases in PKC substrate phosphorylation reflect a cell non-autonomous effect such as gliosis[267]. To assess the cell type from which phosphorylated PKC substrate signal originates, immunohistochemistry was performed with the same antibody used to

detect phosphorylated PKC substrates by immunoblotting (Figure 4.2A). Signal is visible in all cell types, consistent with the widespread expression and function of PKC isozymes in the cerebellum; however, the strongest signal originates from Purkinje neurons. The fact that the most robust PKC substrate phosphorylation is observed in Purkinje neurons relative to other cell types suggests that a significant proportion of the observed immunoblot signal originates from Purkinje neurons.

In addition to assessing the cell type in PKC substrate phosphorylation is observed, we aimed to assess whether the increase in substrate phosphorylation represented a true increase in activity, as opposed to changes in the expression of PKC substrates. This is particularly important given that the identity of substrates detected by immunoblotting is not known. Use of protein kinase C inhibitors in organotypic cerebellar slice cultures largely eliminated the immunoblot signal (Figure 4.2B), supporting the conclusion that signal detected using this antibody is an indicator of steady-state PKC activity. We concluded from this that the observed immunoblot signal in figure 4.1F-I represents an increase in PKC activity in ATXN1[82Q] Purkinje neurons.

4.3.3 Increased PKC substrate phosphorylation is observed in Purkinje neurons from SCA1 patient autopsy tissue

In order to ensure that observed increases in PKC activity from the ATXN1[82Q] model are relevant to human SCA1, immunohistochemistry experiments were performed in autopsy tissue from SCA1 patients and age-matched controls (demographic information for patient and control tissue is outlined in Table 4.1). Purkinje neurons were identified with calbindin, and phosphorylated PKC substrates were visualized using the same antibody employed in figures 4.1F-I and 4.2. Consistent with the findings in ATXN1[82Q] mice, there was a significant

increase in PKC substrate phosphorylation (Figure 4.3A) in the dendritic (Figure 4.3B) and somatic (Figure 4.3C) compartments of SCA1 Purkinje neurons compared to healthy controls.

Among the SCA1 patient samples, 4/11 SCA1 samples showed strikingly high PKC substrate phosphorylation. The significance of this heterogeneity is unclear: there is no correlation between increased PKC substrate phosphorylation and CAG repeat length or age of death, and clinical information is not available to determine whether increased PKC substrate phosphorylation predicts worse or improved cerebellar function. Additionally, subjective assessment of Purkinje neuron degeneration (specifically with respect to the number of Purkinje neurons per high power field and apparent dendritic integrity) did not suggest that SCA1 samples with higher PKC activity in Purkinje neurons showed more or less pathology. Additional studies are required to understand the reasons behind the significant variability in SCA1 Purkinje neuron PKC activity observed in patient autopsy tissue. Nevertheless, these studies recapitulate the findings in the ATXN1[82Q] model, supporting the use of this model for understanding any role that increased PKC activity may play in SCA1 Purkinje neuron dendrite degeneration.

4.3.4 Increased PKC substrate phosphorylation reflects increased conventional PKC isozyme activation in ATXN1[82Q] Purkinje neurons

The PKC family of enzymes is subdivided into four sub-families that are distinguished by the regulatory signals to which they respond[268]. The conventional PKC isozyme sub-family (made up of PKCα, PKCβI/II, and PKCγ) requires Ca^{2+} for activation. Cerebellar organotypic slice culture experiments from ATXN1[82Q] and wild-type mice revealed that the increased PKC activity which was observed in SCA1 Purkinje neurons at fifteen weeks could be eliminated by using 5 mM ethylene glycol-bis(β-aminoethyl ether)-N,N,N',N'-tetraacetic acid (EGTA) to chelate extracellular Ca^{2+} ions (Figure 4A-B). This suggests that the observed

changes in PKC substrate phosphorylation reflect increased function of one of the conventional PKC isozymes. Purkinje neurons express both PKCα and PKCγ[269, 270]. ATXN1[82Q] Purkinje neurons show unchanged PKCα expression and reduced PKCγ expression, consistent with previous reports[32] (Figure 2C-G). These data indicate that the observed steady-state increases in conventional PKC activity are due to increased activation rather than increased isozyme expression.

The trigger for increased conventional PKC isozyme activity remains unclear. Multiple calcium sources and PKC activation pathways were inhibited in ATXN1[82Q] organotypic cerebellar slices, including mGluR1, AMPA receptors, and the P/Q-, T-, and L-type voltage-gated calcium channels, but none of these inhibition strategies were able to recapitulate the observed reduction in PKC substrate phosphorylation when slices were treated with EGTA (data not shown). As such, the mechanism by which PKC activity is increased in ATXN1[82Q] Purkinje neurons remains as yet unknown.

4.3.5 Normalizing PKC activity in ATXN1[82Q] Purkinje neurons accelerates dendrite degeneration

As discussed previously, PKC activity plays a major role in determining Purkinje neuron dendritic structure[182, 185]. However, the data from studies of Purkinje neuron dendrite development demonstrate that use of phorbol esters to activate PKC isosymes results in atrophic dendrites[182], while studies of SCA14 suggest that mutations in PKCγ produce an enzyme which is functionally defective[185] or even exerts dominant negative effects[265] to drive Purkinje neuron dendrite degeneration, making it difficult to predict how increased PKC activity might contribute to dendrite degeneration in SCA1 Purkinje neurons. To assess the significance of increased PKC activity in SCA1 Purkinje neurons, we aimed to normalize PKC activity in ATXN1[82Q] mice

and assessed the effect on Purkinje neuron dendritic integrity. We inhibited PKC activity by intercrossing ATXN1[82Q] mice with PKCi mice that express a pseudosubstrate PKC inhibitor peptide under the control of the Purkinje neuron-specific L7/Pcp2 promoter[224] (mice expressing both transgenes are hereafter referred to as ATXN1[82Q] bigenic mice). ATXN1[82Q] bigenic mice showed a normalization of cerebellar PKC substrate phosphorylation (Figure 4.5A).

Importantly, dendrite degeneration at twenty weeks was accelerated in ATXN1[82Q] bigenic mice. Molecular layer thickness, a measure of Purkinje neuron dendritic integrity, was significantly decreased in ATXN1[82Q] bigenic mice compared to both wild-type and PKCi mice (Figure 4.5B&D). The increased dendrite loss in ATXN1[82Q] bigenic mice was also confirmed with whole-cell capacitance measurements, which revealed that the severity of Purkinje neuron atrophy was significantly greater in ATXN1[82Q] bigenic mice compared to ATXN1[82Q] mice (Figure 4.5C). In both molecular layer thickness measurements and whole-cell capacitance measurements, no dendrite surface area changes were observed in PKCi mice, suggesting that the observed effect is specific to increased PKC activation in the disease state. These data suggest that the increased PKC activity observed in ATXN1[82Q] mice protects against dendritic degeneration.

4.3.6 Increased PKC activity does not protect Purkinje neuron dendrites in SCA1 by modulating somatic spiking

Previous studies have suggested that altered spiking is an important driver of neurodegeneration in the ATXN1[82Q] model of SCA1[114, 116] and in other models of cerebellar ataxia[115, 271]. Protein kinase C family members influence the function of a number of ion channels that regulate membrane excitability[272-275]. We therefore sought to investigate whether

increased PKC activity might exert its dendro-protective effect on ATXN1[82Q] Purkinje neurons by altering Purkinje neuron spiking.

To assess this possibility, cell-attached and whole-cell patch clamp somatic recordings were performed from ATXN1[82Q] bigenic and litter-mate control Purkinje neurons in acute cerebellar slices at twenty weeks of age. Baseline firing properties were abnormal in both ATXN1[82Q] bigenic mice and ATXN1[82Q] mice as compared to litter-mate wild-type and PKCi controls (Figure 4.6A). Both ATXN1[82Q] and ATXN1[82Q] bigenic Purkinje neurons exhibited reduction in firing frequency (Figure 4.6B) and increased spike irregularity (Figure 4.6C). Analysis of spikes from whole-cell patch clamp recordings of baseline spiking (Figure 4.6E) revealed reduced amplitude (Figure 4.6F) and increased variability (Figure 4.6G) of the anti-peak after-hyperpolarization potential (AHP) reached during each spike, and abnormalities in the AHP have been previously demonstrated to underlie irregular spiking in Purkinje neurons[105, 276]. The alterations in spiking in ATXN1[82Q] Purkinje neurons are consistent with our prior work in this model of SCA1[116] identifying altered spiking and a reduction in the AHP due to reduced expression and function of the large-conductance calcium-activated potassium (BK) channel. Consistent with these data, we observed reduced expression of *Kncma1*, the gene that encodes the BK channel (Figure 4.6D).

Importantly, all of these spiking parameters were similarly altered in both ATXN1[82Q] and ATXN1[82Q] bigenic Purkinje neurons. The lack of differences in basal Purkinje neuron spiking between ATXN1[82Q] and ATXN1[82Q] bigenic Purkinje neurons indicate that PKC activity does not exert its dendro-protective effect by modulating Purkinje neuron somatic spiking.

4.3.7 Increased PKC activity may protect Purkinje neuron dendrites in SCA1 by reducing intrinsic dendritic excitability

The studies outlined in section 4.3.6 demonstrate that PKC activity is unlikely to exert its dendroprotective effect in SCA1 by regulating somatic spiking. Importantly, studies presented in chapter 3 demonstrate that increased intrinsic dendritic excitability is a driver of Purkinje neuron dendrite degeneration in SCA1. Protein kinase C isozymes phosphorylate a number of channels that are known to regulate Purkinje neuron dendrite excitability, notably $K_V3.3$[272] and $Ca_V3.1$[277], raising the possibility that increased PKC activity may protect ATXN1[82Q] Purkinje neuron dendrites by influencing dendritic excitability.

Despite the similarity in basal spiking between ATXN1[82Q] and ATXN1[82Q] bigenic Purkinje neurons, ATXN1[82Q] bigenic Purkinje neurons could not sustain spiking in response to depolarizing current injection to the same level as ATXN1[82Q] Purkinje neurons (Figure 4.7A-B). This abnormality occurred despite a similar input resistance for ATXN1[82Q] bigenic Purkinje neurons and ATXN1[82Q] Purkinje neurons (Figure 4.7C). Importantly, in some Purkinje neurons from ATXN1[82Q] bigenic mice, dendritic calcium spikes appeared after a small number of sweeps and appeared to compete with somatic sodium action potentials (Figure 4.7A). It is known that dendritic calcium spikes can influence somatic spiking in Purkinje neurons[154, 278], raising the possibility that ATXN1[82Q] bigenic Purkinje neurons required less injected current to elicit a dendritic calcium spike than ATXN1[82Q] Purkinje neurons. As discussed in section 3.3.2, this would suggest an increase in intrinsic dendritic excitability.

To directly test the intrinsic dendritic excitability of ATXN1[82Q] bigenic Purkinje neurons, the same calcium spike experiment utilized in section 3.3.2 was performed in ATXN1[82Q] bigenic and ATXN1[82Q] Purkinje neurons (Figure 4.7D). Consistent with the

conclusion that ATXN1[82Q] Purkinje neurons show increased intrinsic dendritic excitability, they required less injected current to elicit dendritic calcium spikes (Figure 4.7E) in the absence of changes in input resistance (Figure 4.7F). As discussed in chapter 3, a reduced threshold to dendritic calcium spikes suggests increased intrinsic dendritic excitability. Because of the role established in chapter 3 for increased intrinsic dendritic excitability as a driver of ATXN1[82Q] Purkinje neuron dendrite degeneration, these data raise the possibility that increased PKC activity opposes SCA1 Purkinje neuron dendrite degeneration by reducing intrinsic dendritic excitability.

4.4 Discussion

Here we report that Purkinje neurons from the ATXN1[82Q] model of SCA1 show increased activation of PKC isozymes, which are important regulators of Purkinje neuron dendrite structure that are responsive neuronal activity. Increased PKC isozyme activity is recapitulated in Purkinje neurons from SCA1 patient post-mortem tissue, demonstrating that observations in the ATXN1[82Q] model recapitulate human disease. Investigation of the mechanism behind increased PKC activity reveal that it is specifically the conventional PKC isozymes which are activated in ATXN1[82Q] Purkinje neurons. Importantly, normalizing PKC activity in ATXN1[82Q] mice by interbreeding with mice expressing a PKC pseudosubstrate inhibitor in Purkinje neurons results in accelerated dendrite degeneration, demonstrating that increased PKC activity protects ATXN1[82Q] Purkinje neuron dendrite structure. Efforts to understand the mechanism behind this dendroprotection revealed that increased PKC activity opposes intrinsic dendritic excitability but has no effect on somatic spiking, further supporting a role for dendritic excitability independent of somatic spiking as a driver of dendrite degeneration in SCA1 Purkinje neurons.

As discussed in section 1.3.4, studies of Purkinje neuron development have found that PKC activation suppresses dendrite outgrowth[182], while studies of SCA14 have suggested that the Purkinje neuron dendrite degeneration observed in SCA14[186] arises from a mutated PKCγ with reduced *in vivo* kinase activity[185] or even dominant negative action[265]. These data have suggested that PKC activity might have distinct roles in developing vs. mature neurons, with PKC activity inhibiting dendrite outgrowth in developing Purkinje neurons but supporting dendrite stability in mature Purkinje neurons. The findings from this study lend support to the idea that increased PKC activity stabilizes mature Purkinje neuron dendrites, and they suggest that increased PKC activation in ATXN1[82Q] Purkinje neurons is an induced protective pathway that slows the rate of dendrite degeneration. These findings are not only relevant to SCA1, but they also provide insight into the Purkinje neuron degeneration observed in SCA14[186], suggesting that the adult-onset dendrite degeneration in this disease reflects the loss of a factor (PKCγ) that sustains mature Purkinje neuron dendrites.

How increased PKC activity opposes dendritic degeneration in ATXN1[82Q] Purkinje neurons is at this point not clear. However, it is very likely a Purkinje cell-autonomous effect, as both the ATXN1[82Q] transgene and the PKCi transgene are expressed only in Purkinje neurons. As such, the ATXN1[82Q] bigenic mouse lends itself to –omics approaches for exploring the dendro-protective pathway(s) downstream of PKC in SCA1. PKC isozymes act not just on direct substrates but also influence transcription[279], suggesting that there may be utility in both phosphoproteomic and transcriptomic approaches. Ideally, such a study might identify novel modifiers of dendritic degeneration relevant to SCA1 and other SCAs.

Because of the data in chapter 3 indicating that increased dendritic excitability drives SCA1 Purkinje neuron dendrite degeneration, the reduced threshold to calcium spikes in

ATXN1[82Q] bigenic Purkinje neurons suggests that increased PKC activity in ATXN1[82Q] Purkinje neurons protects Purkinje neuron dendrites by limiting increases in dendritic excitability. If this were confirmed to be the mechanism, the fact that no other changes in baseline spiking were identified between ATXN1[82Q] and ATXN1[82Q] bigenic Purkinje neurons would demonstrate that increased intrinsic dendritic excitability can drive dendrite degeneration independent of changes in spiking. This would add more weight to the arguments put forth in chapter 3, and it would address the lack of dendrite specificity for the BK-AAV and baclofen experiment.

Further exploration of this mechanism would require identification of the channel(s) acted on by PKC to limit dendrite degeneration. Among the many channel targets of PKC, three channel candidates are of particular interest because they are expressed at high levels in PN dendrites and are affected by PKC phosphorylation in a manner which would be predicted to reduce dendritic excitability. The first channel of interest is the Slack channel, which is a sodium-activated potassium channel whose current is increased two- to three-fold in response to PKC phosphorylation at Ser407[280, 281]. The second channel of interest is Kv3.3, a channel which has been shown to suppress dendritic excitability[152] and which shows slowing of inactivation upon PKC phosphorylation at either Ser3 or Ser9[272]. The final channel candidate is the T-Type voltage-gated calcium channel subfamily, which shows a two- to three-fold increase in peak current upon PKC phosphorylation[277]; the prediction would be that increased T-Type channel activity would reduce excitability by activating calcium-activated potassium channels, since the predominant effect of calcium channel function in Purkinje neurons is to produce a hyperpolarizing current through activation of calcium-activated potassium channels[96]. Identifying which of these channels are modulating dendritic excitability downstream of PKC

will not only reveal dendro-protective channel targets for SCA1 and possibly SCA14, but will also provide insight into how specific channels regulate activity-dependent dendrite remodeling in Purkinje neurons.

An important question not answered in this study is the mechanism by which increased PKC activity is triggered in SCA1 Purkinje neurons. The fact that calcium chelation eliminates PKC substrate phosphorylation in ATXN1[82Q] cerebella demonstrates that increased PKC activity is mediated by conventional PKC isozymes; however, conventional PKC isozymes expressed in Purkinje neurons (PKCα and PKCγ) are not increased in expression, and PKCγ in fact has significantly reduced expression. Furthermore, a well-characterized pathway for activation of conventional PKC isozymes is from studies of parallel fiber LTD, wherein Purkinje neuron cPKC isozymes (most likely PKCα[282]) are activated downstream of mGluR1 through the action of both DAG and IP_3-mediated calcium[283]; however, ATXN1[82Q] Purkinje neurons show reduced mGluR1-mediated current and cytosolic [Ca^{2+}] changes[135]. These findings demonstrate that to explain increased PKC activity in ATXN1[82Q] Purkinje neurons, one cannot invoke changes in expression of PKCα or PKCγ and also cannot invoke increased mGluR1-dependent activation.

We propose several hypotheses for increased PKC activity in ATXN1[82Q] Purkinje neurons. One possibility is that despite reduced expression of calcium sources downstream of mGluR1 (section 3.3.4), cytosolic [Ca^{2+}] might still be increased from another calcium source that has not yet been tested, resulting in secondary DAG production and consequent PKC activation[284]. A second possibility is that the observed increase in PKC activity reflects ectopic expression of PKCβI or PKCβII in Purkinje neurons as a result of ATXN1[82Q] transgene

expression, a possibility best assessed by immunohistochemistry analysis of PKCβI and PKCβII expression in ATXN1[82Q] Purkinje neurons.

A third possibility is that as PKCγ expression is suppressed, signals for activation of both PKCγ and PKCα result in disproportionate activation of PKCα, with the differences in phosphorylation efficiency and substrate pool that have been reported for individual PKC isozymes[285] resulting in the observed increase in PKC substrate phosphorylation. Several lines of evidence support this hypothesis. In studies of Purkinje neuron dendrite development it has been suggested that PKCα forms a "reserve pool" that is only activated in response to strong stimuli[286], and in ATXN1[82Q] Purkinje neurons it might be possible that this reserve pool is recruited more readily as PKCγ expression is reduced. Furthermore, immunohistochemistry experiments in ATXN1[82Q] Purkinje neurons (see figure 4.4F-G) show that PKCγ is particularly suppressed in the dendritic arbor and PKCα expression is intact throughout both the soma and dendrite, such that if such a mechanism were active it might arise through regional differences in the availability of each isozyme. This possibility would be best assessed by crossing ATXN1[82Q] mice to PKCα knockout mice; if this hypothesis were correct then ATXN1[82Q] mice interbred with PKCα knockout mice should also have accelerated dendritic degeneration.

4.5 Acknowledgements

I thank members of the Shakkottai laboratory for helpful comments. I thank Aaron Wasserman for technical assistance performing SCA1 patient sample immunohistochemistry, as well as molecular layer thickness measurements. I thank Dr. Arnulf Koeppen for providing autopsy tissue slides from SCA1 patients and the University of Michigan Brain Bank and Matthew Perkins for providing autopsy tissue slides from an SCA1 patient and age-matched

healthy controls. I thank Dr. Chris De Zeeuw for providing the PKCi transgenic mice. This work was supported by the National Institutes of Health [R01NS085054 to V.G.S., T32GM007863 to R.C.].

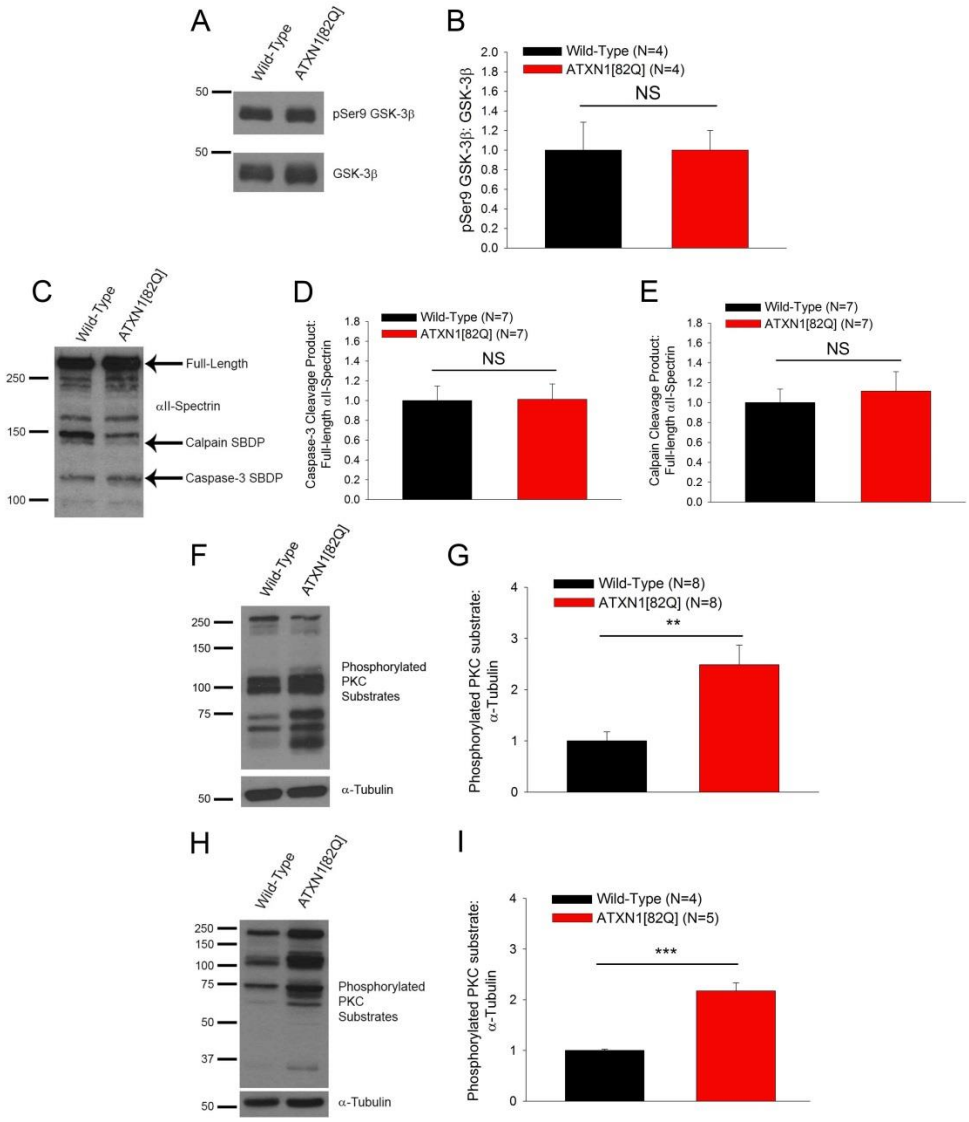

Figure 4.1 Activity-dependent dendrite remodeling pathways in whole cerebellar lysates from ATXN1[82Q] mice. **(A)** Representative Western blot for phospho-Ser9 GSK-3β at fifteen weeks of age showing unchanged phosphorylation of serine 9 on GSK-3β in ATXN1[82Q] cerebella, summarized in **(B)**. **(C)** Representative Western blot for αII-spectrin breakdown products (SBDPs) produced by the activity of calpain family proteases and caspase-3. These blots show unchanged levels of the caspase-3-specific 120 kDa fragment relative to full-length αII-spectrin (summarized in **(D)**) and unchanged levels of the calpain-specific 145 kDa fragment relative to full-length αII-spectrin (summarized in **(E)**) at fifteen weeks of age in ATXN1[82Q] cerebella. **(F)** Representative Western blot for phosphorylated PKC substrates at fifteen weeks of age showing increased PKC substrate phosphorylation in cerebella from ATXN1[82Q] mice, summarized in **(G)**. **(H)** Representative Western blot for phosphorylated PKC substrates at five weeks of age show increased PKC substrate phosphorylation in cerebella from ATXN1[82Q] mice, summarized in **(I)**. Throughout, data are mean ± SEM. ** = P<0.01; *** = P<0.001. Statistical significance derived by unpaired two-tailed Student's T-Test (**B**, **D**, **E**, **G**, **I**).

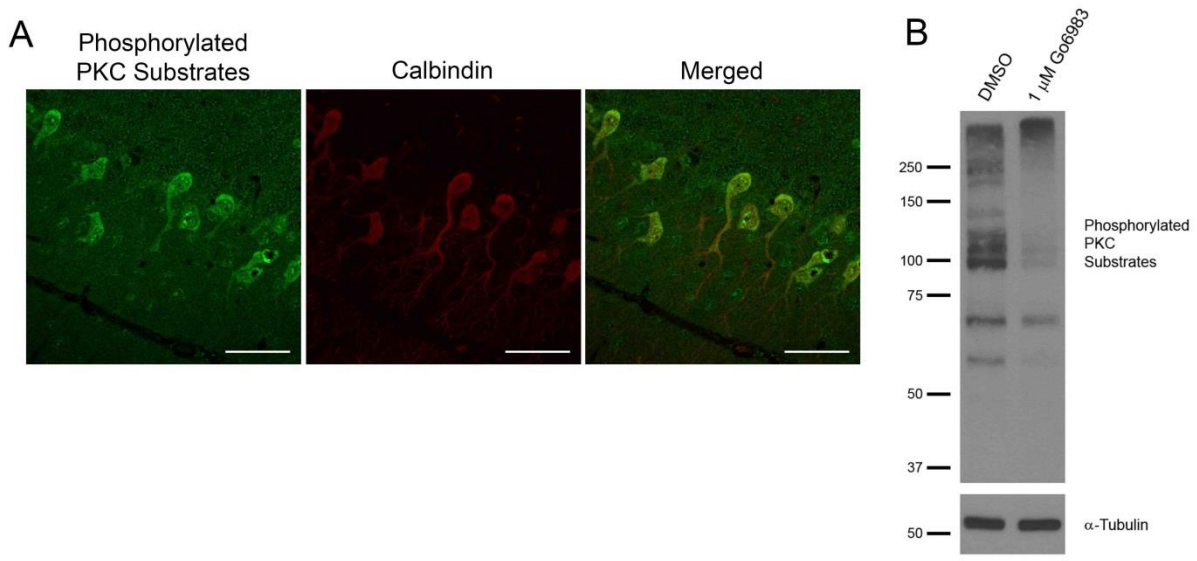

Figure 4.2 Increased PKC substrate phosphorylation in ATXN1[82Q] mice reflects increased PKC isozyme activity in Purkinje neurons. **(A)** Representative immunohistochemistry experiment showing PKC substrate phosphorylation in Purkinje neurons from a fifteen week old ATXN1[82Q] mice. Scale bars, 50 μm. **(B)** Western blot demonstrating the effect of the PKC inhibitor Go6983 on PKC substrate phosphorylation in cerebellar slice cultures from ATXN1[82Q] mice at fifteen weeks of age.

SCA1 Samples

Patient No	Age	Repeat Size (pathogenic allele)	Sex
S1	47	47	Male
S2	52	Not Available	Male
S3	54	50	Male
S4	59	47	Male
S5	61	46	Male
S6	63	41	Female
S7	64	45	Male
S8	64	44	Male
S9	65	42	Male
S10	66	46	Female
S11	73	Not Available	Female
S12	81	38	Female

Control Samples

Patient No	Age	Repeat Size	Sex
C1	48	N/A	Female
C2	59	N/A	Male
C3	61	N/A	Male
C4	65	N/A	Male
C5	70	N/A	Male
C6	73	N/A	Female
C7	80	N/A	Female

Table 4.1 Demographic information on SCA1 patients and age-matched healthy controls. Presented above is relevant demographic information from SCA1 patients and age-matched controls for data presented in figure 4.3.

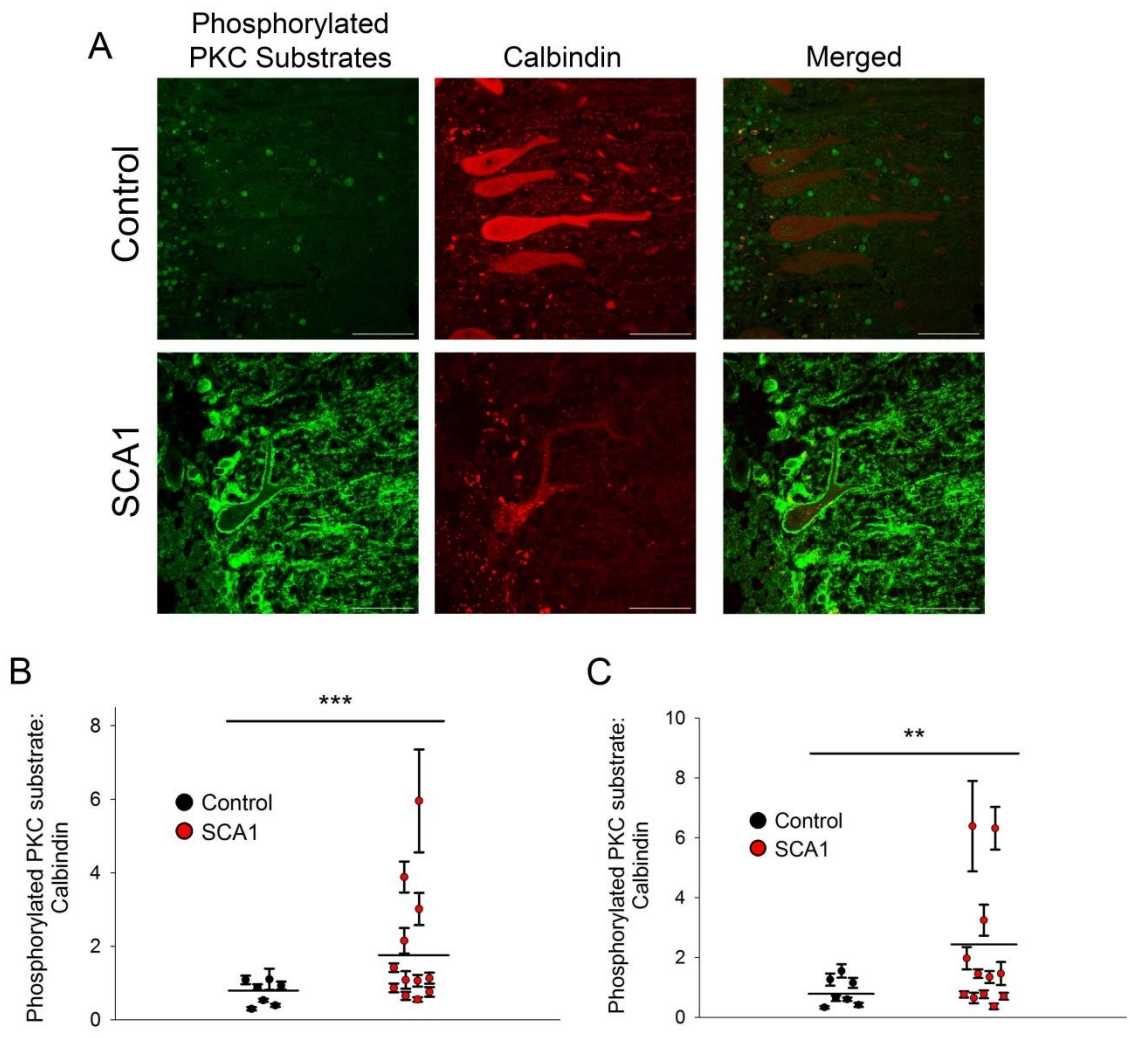

Figure 4.3 Increased PKC substrate phosphorylation is observed in Purkinje neurons from SCA1 patient autopsy tissue. **(A)** Representative images of phosphorylated PKC substrate staining (green) in Purkinje neurons (red) from SCA1 patient samples and age-matched healthy controls. Scale bars, 50 µm. Summarized data show increased phosphorylated PKC substrate staining relative to calbindin staining in the dendritic **(B)** and somatic **(C)** compartment of Purkinje neurons from SCA1 patient samples and age-matched healthy control samples. Each data point represents an individual patient, with error bars representing SEM for measurements from multiple Purkinje neurons in that individual. ** = P<0.01; *** = P<0.001. Statistical significance derived by two-way ANOVA demonstrating an independent impact of disease state on phosphorylated PKC substrate-to-calbindin ratio (**B**, **C**).

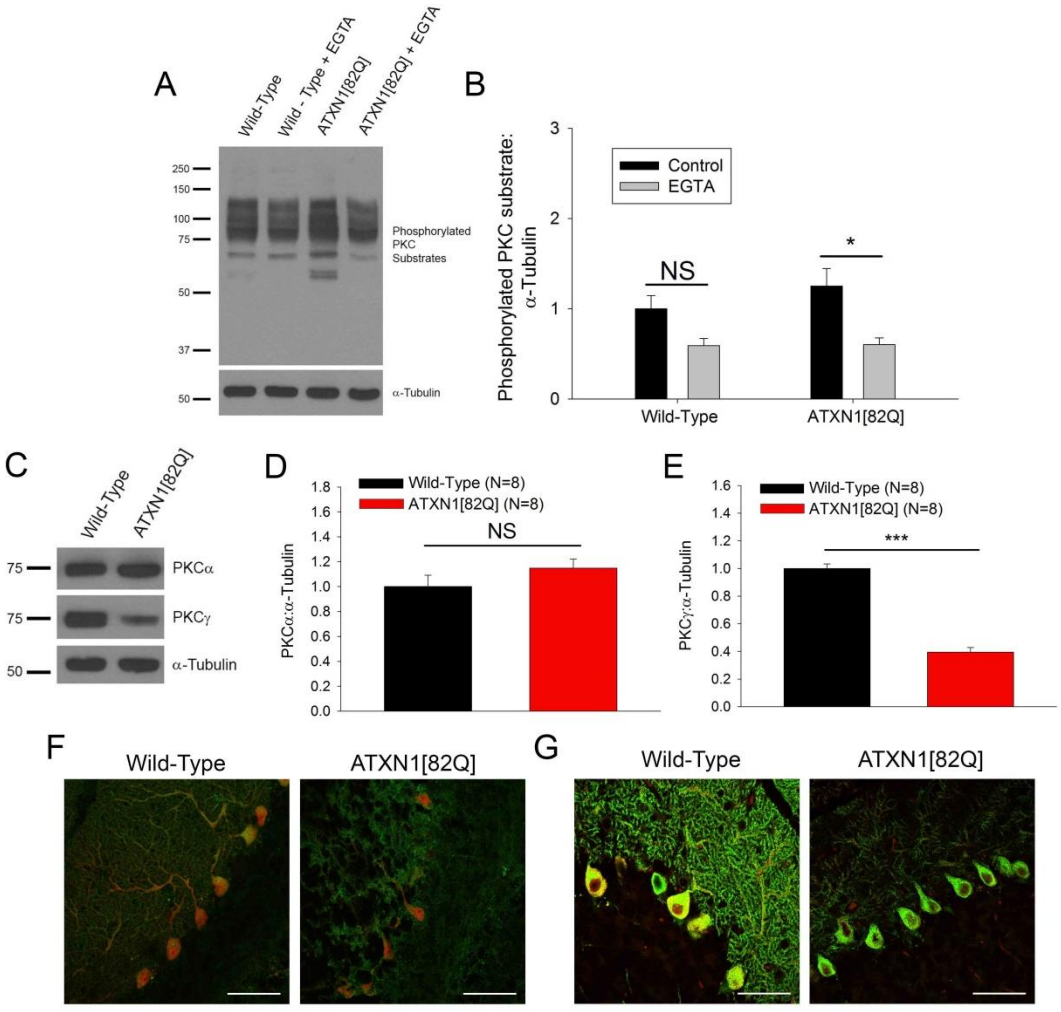

Figure 4.4 Conventional PKC isozyme activity is increased in ATXN1[82Q] Purkinje neurons. **(A)** Representative Western blot for phosphorylated PKC substrates in organotypic cerebellar slice cultures treated with 5 mM EGTA from fifteen week old mice. Calcium chelation with EGTA reduced PKC substrate phosphorylation in ATXN1[82Q] slice cultures but not wild-type slice cultures, summarized in **(B)**. **(C)** Representative Western blot for PKCα and PKCγ in fifteen week old mice. Unchanged expression of PKCα in ATXN1[82Q] cerebella at fifteen weeks of age is summarized in **(D)**, while reduced expression of PKCγ in ATXN1[82Q] cerebella at fifteen weeks of age is summarized in **(E)**. **(F)** Representative image of PKCα expression (green) in ATXN1[82Q] and wild-type Purkinje neurons (labelled with calbindin, red) at fifteen weeks of age. Scale bars, 50 µm **(G)** Representative image of PKCγ expression (green) in ATXN1[82Q] and wild-type Purkinje neurons (labelled with calbindin, red) at fifteen weeks of age. Scale bars, 50 µm. Throughout, data are mean ± SEM. NS = Not Significant; * = $P<0.05$; *** = $P<0.001$. Statistical significance derived by two-way ANOVA with Sidak's multiple comparison test with statistically significant differences after multiple comparisons indicated (**B**) or unpaired two-tailed Student's T-Test (**D**, **E**).

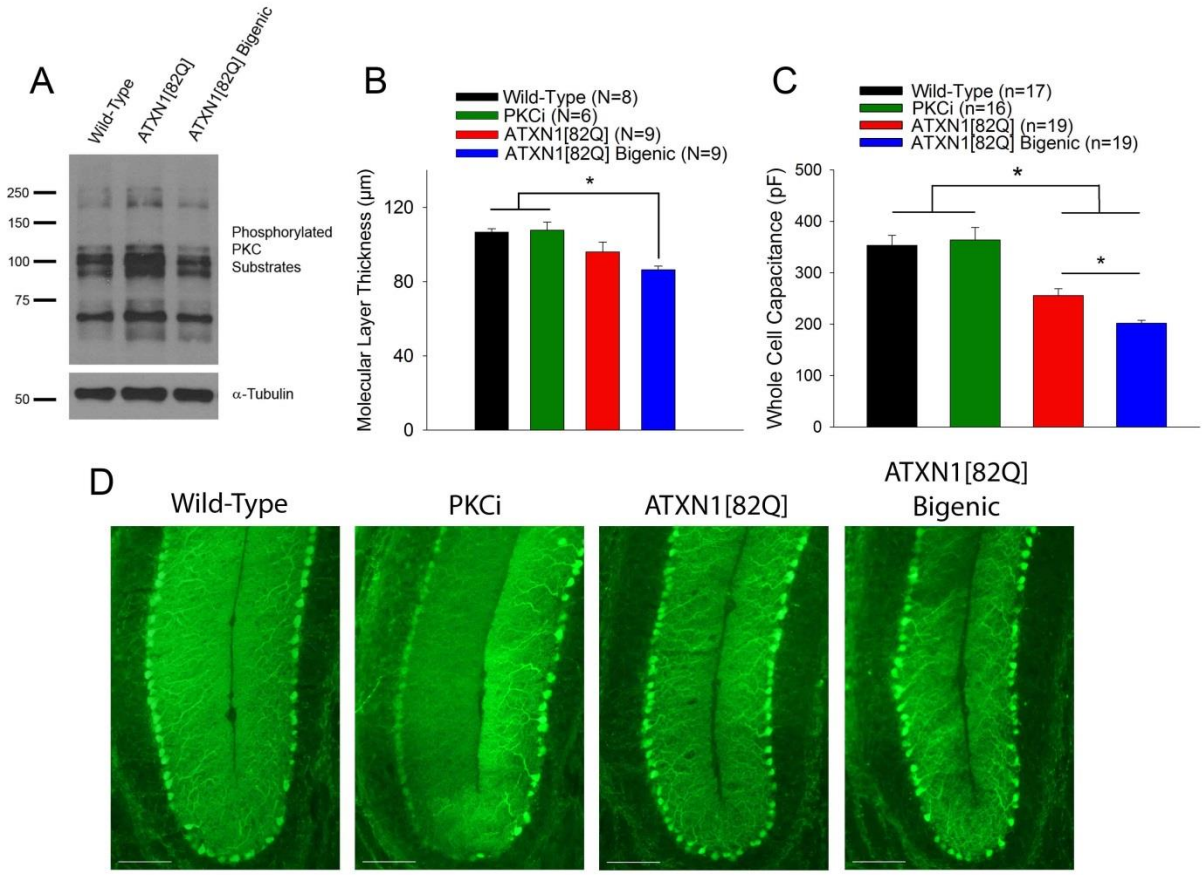

Figure 4.5 Increased PKC activity protects against dendritic degeneration in ATXN1[82Q] mice. **(A)** Representative Western blot for PKC substrate phosphorylation in wild-type, ATXN1[82Q], and ATXN1[82Q] bigenic mice at twenty weeks of age demonstrating normalization of PKC substrate phosphorylation in ATXN1[82Q] bigenic mice. **(B)** Reduced molecular layer thickness in lobule V of ATXN1[82Q] bigenic mice at twenty weeks of age. **(C)** Whole-cell capacitance measurements in ATXN1[82Q] bigenic Purkinje neurons show a greater reduction in cell size relative to ATXN1[82Q] Purkinje neurons, which are atrophied relative to wild-type and PKCi Purkinje neurons at twenty weeks of age. **(D)** Representative images at the cerebellar primary fissure in wild-type, PKCi, ATXN1[82Q], and ATXN1[82Q] bigenic mice stained with calbindin at twenty weeks of age. Scale bar, 100 μm. Throughout, data are mean ± SEM. * = $P<0.05$. Statistical significance derived by one-way ANOVA with Holms-Sidak multiple comparison test (**B**, **C**).

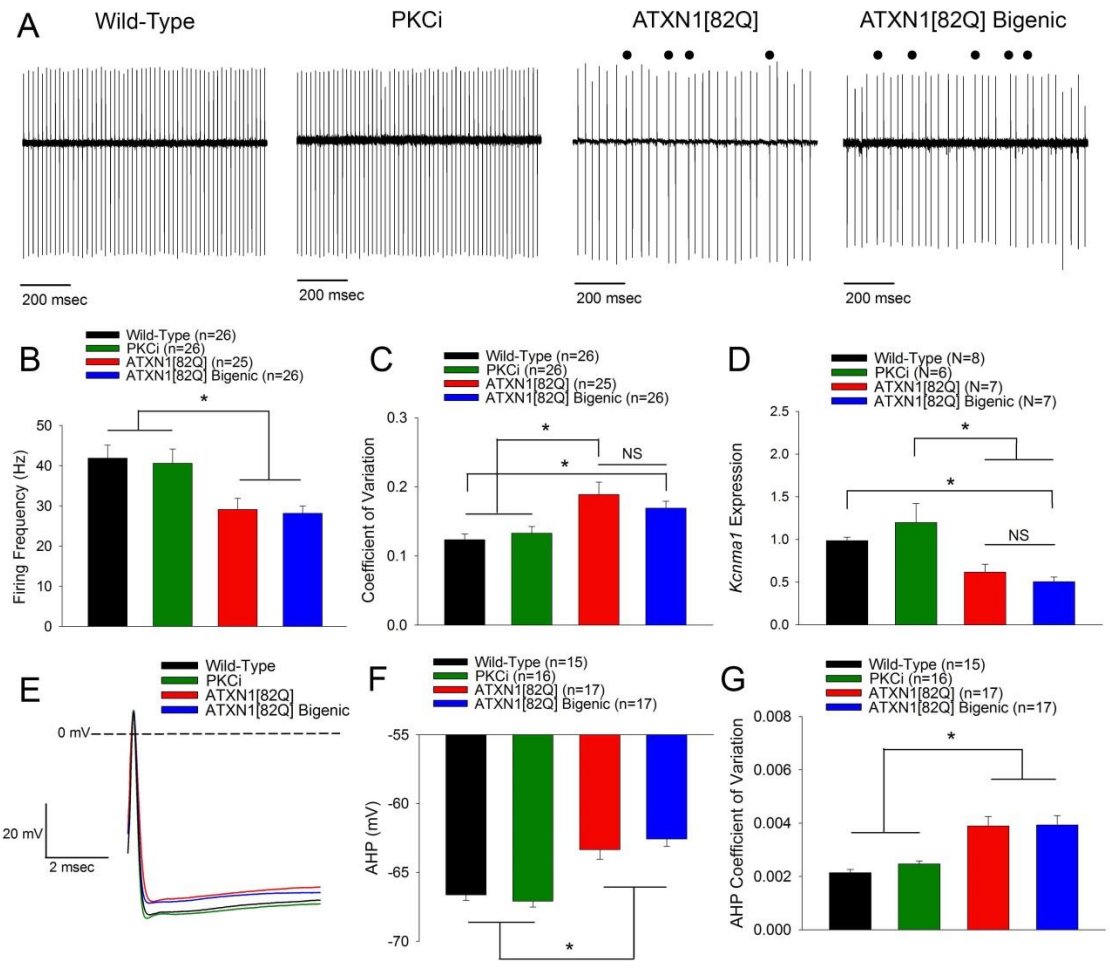

Figure 4.6 Increased PKC activity does not influence baseline action potential firing in ATXN1[82Q] Purkinje neurons. **(A**) Representative firing from wild-type, PKCi, ATXN1[82Q], and ATXN1[82Q] bigenic (expressing both the ATXN1[82Q] and PKCi transgenes) Purkinje neurons. ATXN1[82Q] and ATXN1[82Q] bigenic mice show irregular spiking, with abnormal pauses marked with ●. **(B)** ATXN1[82Q] and ATXN1[82Q] bigenic Purkinje neurons show reduced firing frequency. **(C)** ATXN1[82Q] and ATXN1[82Q] bigenic Purkinje neurons show more irregular firing, indicated by a higher coefficient of variation. **(D)** ATXN1[82Q] and ATXN1 [82Q] bigenic mice show reduced expression of *Kcnma1*, the gene encoding the BK channel. **(E)** Representative spontaneous action potentials from wild-type, PKCi, ATXN1[82Q], and ATXN1[82Q] bigenic Purkinje neurons. ATXN1[82Q] and ATXN1[82Q] bigenic Purkinje neurons have an AHP which does not achieve the same degree of hyperpolarization as wild-type and PKCi Purkinje neurons, summarized in **(F)**. **(G)** During spontaneous spiking, the membrane potential reached by the AHP of each spike varies more in ATXN1[82Q] and ATXN1[82Q] bigenic Purkinje neurons relative to wild-type and PKCi Purkinje neurons, indicated by a higher coefficient of variation for AHP measurements. Throughout, data were acquired from Purkinje neurons in mice at twenty weeks of age. Throughout, data are mean ± SEM. NS = not significant; * = $P < 0.05$. Statistical significance derived by one-way ANOVA with Holms-Sidak multiple comparison test (**B**, **C**, **D**, **F**, **G**).

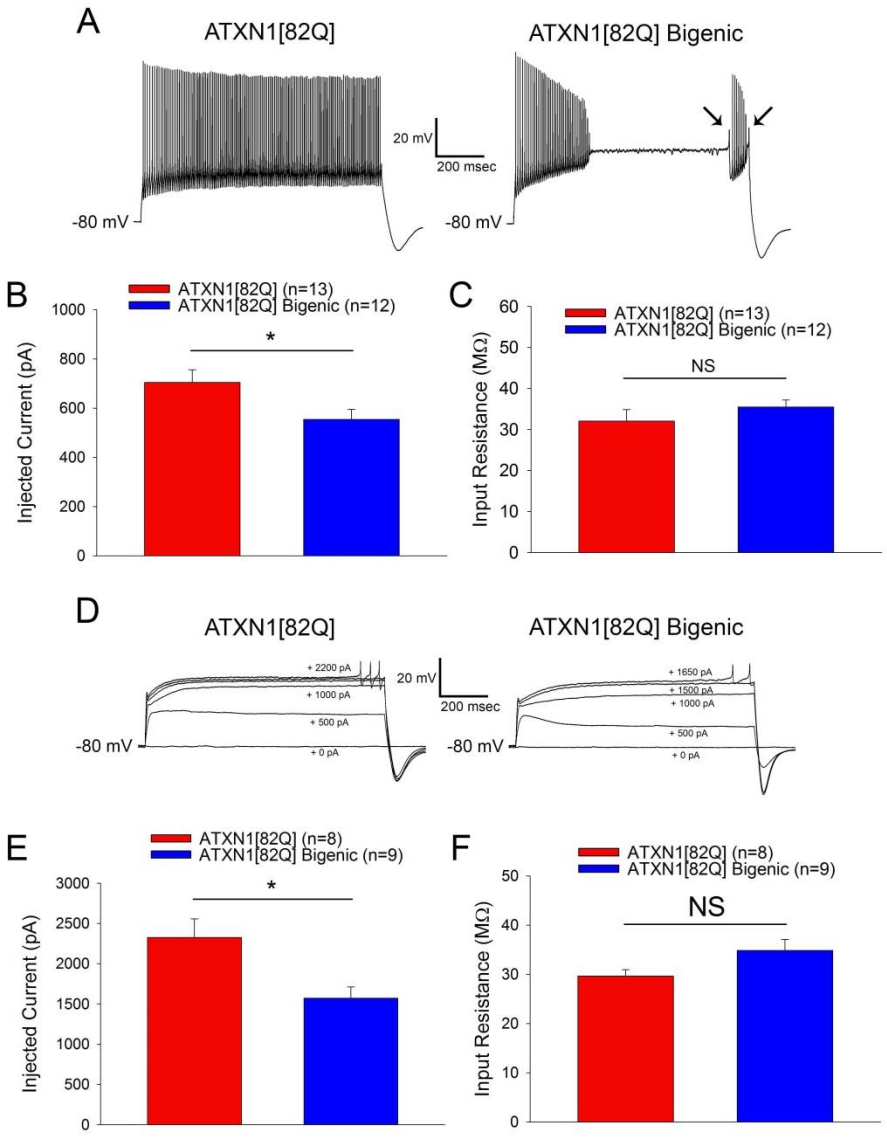

Figure 4.7 Increased PKC activity opposes increases in dendritic excitability in ATXN1[82Q] Purkinje neurons. **(A)** Representative traces from ATXN1[82Q] and ATXN1[82Q] bigenic Purkinje neurons injected with +700 pA of current. Dendritic calcium spikes in the ATXN1[82Q] bigenic Purkinje neuron are marked with arrows. ATXN1[82Q] bigenic Purkinje neurons undergo depolarization block of repetitive spiking at lower levels of injected current than ATXN1[82Q] Purkinje neurons, summarized in **(B)**. **(C)** Representative traces where dendritic calcium spikes were evoked with somatic current injection (injected current amount indicated on the trace) from ATXN1[82Q] (left) and ATXN1[82Q] bigenic (right) Purkinje neurons treated with 1 μm TTX. ATXN1[82Q] bigenic Purkinje neurons require less injected current to elicit a dendritic calcium spike than ATXN1[82Q] Purkinje neurons, summarized in **(D)**. Throughout, data were acquired from Purkinje neurons in mice at twenty weeks of age. Throughout, data are mean ± SEM. NS = not significant; * = $P < 0.05$. Statistical significance derived by unpaired two-tailed Student's T-Test (**B**, **D**).

Chapter 5

Increased protein kinase C (PKC) substrate phosphorylation is a shared modifier of Purkinje neuron degeneration in some forms of ataxia

5.1 Abstract

Purkinje neuron dendrite degeneration is a common histopathologic finding in many spinocerebellar ataxias and sporadic forms of ataxia. Purkinje neuron dendrite structure is heavily regulated by the activity of PKC isozymes in developing Purkinje neurons and the studies outlined in chapter 4 demonstrate that altered PKC function modulates Purkinje neuron dendrite degeneration in spinocerebellar ataxia type 1 (SCA1). We were interested in exploring the extent to which a role for PKC isozymes in regulating dendrite degeneration was common to inherited and sporadic ataxias. To explore a role for PKC in another spinocerebellar ataxia, we assessed whether there were changes in PKC activity in the ATXN2[127Q] model of spinocerebellar ataxia type 2 (SCA2), and found that there was increased PKC activity at the onset of Purkinje neuron dendrite degeneration. Suppression of PKC activation in ATXN2[127Q] mice by interbreeding with a mouse expressing a PKC peptide inhibitor in Purkinje neurons (the PKCi mouse) resulted in accelerated dendrite degeneration and cell loss in ATXN2[127Q] mice, suggesting that increased PKC activity is also neuroprotective in SCA2. Analysis of PKC substrate phosphorylation in multiple system atrophy (MSA), a sporadic

neurodegenerative disease that can involve Purkinje neurons, revealed that post-mortem human MSA tissue with heavy Purkinje neuron involvement showed increased Purkinje neuron PKC substrate phosphorylation, raising the possibility that dendro-protective increases in PKC activity may be observed in sporadic forms of ataxia as well. These data support increased PKC activity as an important neuroprotective pathway in some forms of inherited and sporadic ataxia. Some of the findings from this chapter are included in a paper that is currently under review.

5.2 Introduction

As discussed in section 1.1.1, cerebellar ataxia is a clinical entity rather than a discrete disease, and there are a large number of causes of ataxia, including ischemic, toxic, metabolic, paraneoplastic, or genetic etiologies. For many[4, 5, 287] but not all[288] forms of progressive ataxia, autopsy studies suggest degeneration of Purkinje neuron dendrites preceding cell death. From studies of spinocerebellar ataxias there is evidence to suggest that progressive dendrite degeneration is capable of contributing substantially to motor impairment, underlining the importance of understanding this phase in Purkinje neuron pathology.

In exploring this diverse set of diseases, each of which show varying amount of clinical and histopathologic overlap, an important question emerges: are there common mechanisms of disease across multiple forms of ataxia? Studies of protein-protein interaction networks[289] and distinguishing features of specific brain regions' transcriptomes[290] have demonstrated that there are relatively small clusters of interacting proteins or pathways that emerge when one considers ataxias as a group. These findings suggest that distinct pathogenic insults may ultimately feed into constrained pathways by which Purkinje neurons can degenerate. They also suggest that common features of disease, such as dendrite degeneration, may be executed through a similarly constrained set of intracellular actors.

As discussed in chapter 4, our studies have identified increased PKC activation as a modifier of Purkinje neuron dendrite degeneration in SCA1. Given the role that PKC activity plays as a potent regulator of normal Purkinje neuron dendrite development[182], we were interested in investigating whether this role for PKC extended beyond SCA1. We began with studies of SCA2, a form of ataxia that appears to be closely linked to SCA1.

SCA2 is caused by CAG tract expansions in ATXN2[291], resulting in a protein product (Ataxin-2) with an expanded polyglutamine tract. All patients with SCA2 present with ataxia and many with eye movement abnormalities, while additional symptoms such as dementia, neuropathy, and chorea can be observed[292]. As with SCA1, patients with more CAG repeats in ATXN2 will show an earlier onset of disease[292]. Severe Purkinje neuron dendrite degeneration has been observed in autopsy tissue from SCA2 patients[5], and studies in a mouse model of SCA2 have confirmed that dendrite degeneration is likely an important contributor to motor impairment[11].

In addition to both being polyglutamine diseases, SCA1 and SCA2 appear mechanistically linked. A study in a drosophila model of SCA1 revealed that increasing levels of the drosophila homologue of ATXN2 (dAtx2) results in accelerated pathology and demonstrated a direct protein-protein interaction between dAtx2 and Ataxin-1[293]. Importantly, changes in Purkinje neuron excitability have been described in models of both diseases[11, 114, 116] and treatments which improve spiking but also reduce dendritic excitability have been shown to limit neuropathology in models of SCA1[116] and SCA2[115]. Because Purkinje neuron pathology appears to be realized through similar pathways in SCA1 and SCA2, we aimed to investigate a potential role for PKC activity as a modulator of Purkinje neuron dendrite pathology in SCA2.

We began by assessing PKC substrate phosphorylation in the ATXN2[127Q] model of SCA2[11] and found that PKC activity was increased at the onset of Purkinje neuron dendrite degeneration. We found that as with SCA1, calcium chelation with EGTA resulted in a significant reduction in PKC substrate phosphorylation in ATXN2[127Q] cerebella, implicating conventional PKC isozymes. Suppression of PKC activation in ATXN2[127Q] mice by interbreeding with a mouse expressing a PKC peptide inhibitor in Purkinje neurons (the PKCi mouse) resulted in accelerated dendrite degeneration and cell loss in ATXN2[127Q] mice, suggesting that increased PKC activity is also neuroprotective in SCA2.

We also explored a role for PKC activation in other forms of cerebellar ataxia. Analysis of PKC substrate phosphorylation in the sporadic neurodegenerative disease MSA revealed that post-mortem human MSA tissue with heavy Purkinje neuron involvement showed increased Purkinje neuron PKC substrate phosphorylation, raising the possibility that dendro-protective increases in PKC activity may be observed in this disease. Our findings shed light on a role for increased PKC activity as a modifier of Purkinje neuron degeneration beyond SCA1, but they also highlight the fact that this role is not universal to diseases affecting Purkinje neurons.

5.3 Results

In experiments outlined in section 5.3.1, ATXN2[127Q] mice were maintained by crossing to the B6D2F1 hybrid background (Jackson Labs) on which the mouse was originally generated. Experiments using ATXN2[127Q] mice were done using hemizygous ATXN2[127Q] (tg/-) mice compared to wild-type ATXN2[127Q] (-/-) littermate controls. Mice used for these experiments were twelve weeks old.

In the experiments outlined in section 5.3.2, experimental mice originated from crosses between ATXN2[127Q] (tg/-) mice on a mixed background and PKCi (tg/-) mice on a C57B6J

background, such that all experimental animals were on a mixed background. The genotypes of mice used are specified as follows:

Wild-Type: ATXN2[127Q] (-/-); PKCi (-/-)

PKCi: ATXN2[127Q] (-/-); PKCi (tg/-)

ATXN2[127Q]: ATXN2[127Q] (tg/-); PKCi (-/-)

ATXN2[127Q] Bigenic: ATXN2[127Q] (tg/-); PKCi (tg/-)

All data presented from these experiments were from mice at twenty-five weeks of age. In all experiments, animals were compared to littermate controls.

5.3.1 ATXN2[127Q] cerebella show increased conventional PKC isozyme activity at the onset of Purkinje neuron dendrite degeneration

The ATXN2[127Q] mouse[11] is a transgenic model which overexpresses mutant human ATXN2 with 127 CAG repeats selectively in cerebellar Purkinje neurons under the *Pcp2 (L7)* promoter. In this model, thinning of the cerebellar molecular layer is first detected at twelve weeks[11]. Although thinning of the molecular layer is a relatively crude measure of dendritic degeneration, we explored PKC substrate phosphorylation at this age, since it is well before the onset of cell loss (previously reported to be forty weeks[11]) such that any observed changes would be occurring during the dendrite degeneration phase.

As was observed with ATXN1[82Q] cerebella (see section 4.3.1), ATXN2[127Q] cerebellar extracts show a significant increase in PKC substrate phosphorylation (Figure 5.1A-B). Organotypic cerebellar slice culture experiments at this age reveal that treatment with 5 mM EGTA produces a reduction in PKC substrate phosphorylation in ATXN2[127Q] samples which is trending towards significance, while producing a noticeable but less substantial reduction in wild-type samples (Figure 5.1C-D). Although the observed effect on wild-type samples in this

experiment is much more striking, these trends are otherwise consistent with what was observed in experiments with ATXN1[82Q] mice (see figure 4.4A-B). The fact that EGTA treatment appears to have a similar effect on PKC substrate phosphorylation suggests that increased PKC substrate phosphorylation is likely attributable to the action of conventional PKC isozymes. Together, these data suggest that there is increased conventional PKC activity in ATXN2[127Q] cerebella at the onset of dendritic degeneration, raising the possibility that a similar mechanism is at work in regulating ATXN2[127Q] Purkinje neuron dendrite degeneration as was observed in ATXN1[82Q] mice.

5.3.2 Normalizing PKC activity in ATXN2[127Q] Purkinje neurons accelerates Purkinje neuron dendrite degeneration

As discussed in section 4.3.5, normalizing PKC activity in ATXN1[82Q] mice by interbreeding with PKCi mice expressing a PKC pseudosubstrate inhibitor results in accelerated dendrite degeneration, suggesting that increased PKC activity in ATXN1[82Q] Purkinje neurons is neuroprotective. We crossed ATXN2[127Q] mice with PKCi mice to generate ATXN2[127Q] bigenic progeny. At twenty-five weeks, ATXN2[127Q] bigenic mice showed significantly greater thinning of the molecular layer in the intermediate zone relative to litter-mate ATXN2[127Q] mice (Figure 5.2A, 5.2C). There was significant cell death in the anterior cerebellum in both ATXN2[127Q] bigenic and litter-mate ATXN2[127Q] mice, but with more prominent disruption of the organization of Purkinje neurons in ATXN2[127Q] bigenic mice (Figure 5.2B). These data demonstrate that increases in PKC activity oppose Purkinje neuron dendrite degeneration in both SCA1 and SCA2.

Based on this analysis, it is clear that at twenty-five weeks of age, ATXN2[127Q] Purkinje neuron pathology is already quite advanced, as there is already robust cell loss detected

in the anterior cerebellum. This is in contrast to previous studies in the ATXN2[127Q] model, which have suggested that statistically significant cell loss is first detected at 40 weeks of age[11]. This discrepancy may have arisen because of the mixed background on which our experiments were performed, or because of differences in the cell counting method utilized. Nevertheless, these data suggest that analysis of dendritic degeneration in ATXN2[127Q] bigenic mice should be performed at an earlier point before cell loss has begun, in order to more accurately isolate any potential role for PKC as a modulator of Purkinje neuron dendrite degeneration in SCA2.

5.3.3 Increased PKC substrate phosphorylation is observed in Purkinje neurons from multiple system atrophy (MSA) patient autopsy tissue

Multiple system atrophy (MSA) is an adult-onset, sporadic neurodegenerative disease characterized by autonomic dysfunction and variable combinations of parkinsonism, cerebellar ataxia, lower motor neuron disease, and brainstem dysfunction[294]. MSA is clinically divided into a Parkinsonian subtype (MSA-P) or a cerebellar subtype (MSA-C), depending on whether the predominant motor symptom is Parkinsonism or cerebellar ataxia. Although the causes and mechanisms of MSA remain poorly understood, it is thought that pathology originates in oligodendrocytes[295] and involves the accumulation of α-synuclein, which deposits in both oligodendroglia and neurons[296]. As with the clinical presentation, the neuropathology can be varied, and a subset of patients will have prominent involvement of Purkinje neurons[297].

As outlined in chapter 4 and sections 5.3.1-5.3.2, PKC activity may be a modifier of Purkinje neuron pathology that extends beyond PKCγ mutations in SCA14 to include other forms of inherited ataxia. We were interested in assessing whether PKC might modify disease pathogenesis in sporadic forms of ataxia, and to that end we examined PKC substrate phosphorylation in surviving Purkinje neurons from post-mortem MSA samples that were noted

at autopsy to have significant Purkinje neuron involvement (demographic information is outlined in Table 5.1). MSA samples were compared to age-matched samples from patients with Alzheimer disease (AD), a neurodegenerative disease with limited cerebellar involvement[298, 299]. Subjective assessment of MSA tissue revealed substantial pathology, such that calbindin-positive Purkinje neurons were in some samples difficult to find, with those Purkinje neurons that were identified often lacking visible dendrite. Importantly, surviving MSA Purkinje neurons showed a significant increase in PKC substrate phosphorylation relative to age-matched AD controls (Figure 3A-3B).

It is important to note that as with the SCA1 patient tissue (see section 4.3.4), there was substantial heterogeneity in PKC substrate phosphorylation both within and between MSA samples. Also as with the SCA1 patient tissue, there was no correlation between increased PKC substrate phosphorylation and subjective assessment of Purkinje neuron degeneration. However, there was an apparent association between clinical features and PKC substrate phosphorylation, with those patients defined clinically as having both MSA-C and MSA-P showing a significantly higher phosphorylated PKC substrate-to-calbindin ratio than those defined as having MSA-C alone (Figure 3C). With such a small number of patients it is difficult to draw firm conclusions from these data, but they raise the possibility that PKC activity correlates with differences in clinical presentation. As such, this study raises the possibility that PKC substrate phosphorylation may act as a disease modifier in MSA as was observed in SCA1 and SCA2. Given the apparent association between clinical presentation and Purkinje neuron PKC substrate phosphorylation, this activity also appears to correlate with clinical presentation, suggesting that the influence of PKC substrate phosphorylation on disease progression is clinically meaningful.

5.4 Discussion

Here we report that increased PKC activity may be a more general feature of degenerative ataxias. As in ATXN1[82Q] mice, increased PKC substrate phosphorylation is observed in cerebellar extracts from the ATXN2[127Q] model of SCA2, and the increase in PKC substrate phosphorylation appears to reflect increases in activity of conventional PKC isozymes. Also as was observed in ATXN1[82Q] mice, normalizing PKC activity in ATXN2[127Q] mice by interbreeding with mice expressing a PKC pseudosubstrate inhibitor in Purkinje neurons results in accelerated dendrite degeneration, demonstrating that increased PKC activity protects ATXN2[127Q] Purkinje neuron dendrite structure. These studies demonstrate that dendroprotective increases in PKC activity are a common feature of SCA1 and SCA2, underscoring the shared pathogenic features of these diseases. Finally, study in autopsy tissue from patients with MSA revealed increased PKC substrate phosphorylation in Purkinje neurons, suggesting that PKC activity may act as a clinically-relevant modifier of disease not just in inherited ataxias but also sporadic forms of ataxia. The mechanism by which PKC activity modulates Purkinje neuron degeneration in these other forms of ataxia warrants further study.

The data outlined in section 5.3.3 suggest not only that PKC substrate phosphorylation is increased in Purkinje neurons from patients with MSA, but they also establish a correlation between PKC substrate phosphorylation and clinical presentation. These data raise the exciting possibility that Purkinje neuron PKC substrate phosphorylation may not only modulate cellular neuropathology but also clinical course. Clinical data on the autopsy samples utilized were limited, and more information on initial presentation and clinical course could provide further information regarding a possible role for PKC activity as a modifier of disease. Additional studies with more patients are required to test this relationship more definitively and to explore

other reasons behind the variability observed in MSA Purkinje neuron PKC activity observed in patient autopsy tissue.

The fact that similar acceleration of dendrite degeneration is observed in ATXN2[127Q] bigenic mice and ATXN1[82Q] bigenic mice presents an exciting opportunity for the application of the –omics approaches discussed in section 4.4. Using either phosphoproteomics or transcriptomics, comparisons both within and between models will allow dendro-protective pathways to be more easily separated from spurious changes by identifying only those pathways that are changed by PKCi expression in both ATXN1[82Q] and ATXN2[127Q] mice (see Figure 5.4). In theory, such an approach has the capacity to identify novel modifiers of Purkinje neuron dendrite degeneration, and these modifiers will not only apply to SCA1 and SCA2 but may apply MSA and potentially to SCA14. Future studies will aim to not only identify these pathways, but to then validate them in SCA1 and SCA2 and then subsequently assess the extent to which those pathways are affected in MSA and potentially other forms of inherited and sporadic ataxia.

In section 4.3.7, it was proposed that PKC activity may exert its dendroprotective effect in ATXN1[82Q] Purkinje neurons by limiting increases in dendritic excitability. There are several reasons to believe that a similar mechanism could be at work in ATXN2[127Q] Purkinje neurons. The first is that abnormalities of Purkinje neuron spiking have been described in models of SCA2[11, 115], indicating that SCA2 is also a condition where Purkinje neuron intrinsic excitability is perturbed. Although intrinsic dendritic excitability has not been explored directly, it has been shown that an activator of SK2 channels, which are highly expressed in Purkinje neuron dendrites[153] and act to reduce intrinsic dendritic excitability[237], is able to improve late-stage Purkinje neuron pathology in a model of SCA2[115]. It is important to note that unlike studies where improvement of spiking produced neuroprotection in SCA1[114, 116], this study did

not assess dendrite pathology at baseline or with SK2 modulation in this model, so there is not a necessary connection between the observed effect on late-stage pathology and dendrite degeneration in SCA2. However, it does establish a role for abnormal intrinsic excitability in SCA2, and it raises the possibility that modulation of dendritic excitability could influence Purkinje neuron dendrite degeneration. Future studies will aim to assess whether ATXN2[127Q] mice have abnormalities in intrinsic dendritic excitability, at which point the difference between ATXN2[127Q] bigenic mice and ATXN2[127Q] mice can also be assessed to determine if PKC activity suppresses dendritic excitability in SCA2 as it does in SCA1.

As with the ATXN1[82Q] model, it is not clear from the studies presented above why PKC activity is increased in ATXN2[127Q] cerebella. The role for conventional PKC isozymes in ATXN2[127Q] mice appears similar to what was observed in ATXN1[82Q] mice, although studies of PKCα and PKCγ protein expression have not yet been performed in ATXN2[127Q] mice. Future studies will aim to determine whether increases in PKCα or PKCγ protein expression might explain the observed increased in ATXN2[127Q] cerebellar PKC activity. If no increase is identified, the same hypotheses proposed for the ATXN1[82Q] model of SCA1 can be pursued in the ATXN2[127Q] mouse, allowing for a more complete understanding of this shared pathway between SCA1, SCA2, and potentially MSA.

5.5 Acknowledgements

I thank members of the Shakkottai laboratory for helpful comments. I thank Aaron Wasserman for technical assistance performing MSA and AD patient sample immunohistochemistry, as well as molecular layer thickness measurements in SCA2 bigenic mice. I thank the University of Michigan Brain Bank and Matthew Perkins for providing autopsy tissue slides from MSA and age-matched Alzheimer disease controls. I thank Dr. Chris

De Zeeuw for providing the PKCi transgenic mice, and I thank Dr. Stefan Pulst for providing the ATXN2[127Q] mice. This work was supported by the National Institutes of Health [R01NS085054 to V.G.S., T32GM007863 to R.C.].

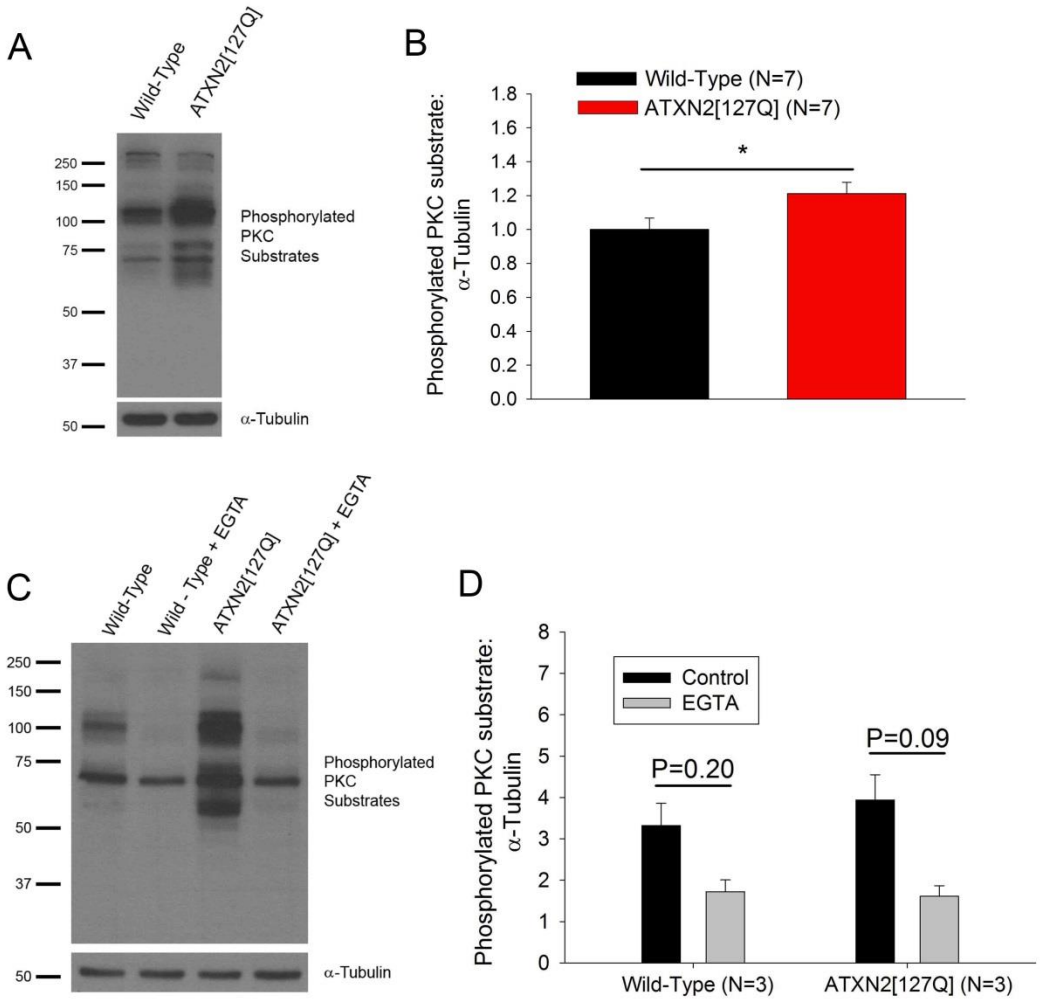

Figure 5.1 ATXN2[127Q] cerebella show increased PKC substrate phosphorylation by conventional PKC isozymes. **(A)** Representative Western blot for phosphorylated PKC substrates at twelve weeks of age showing increased PKC substrate phosphorylation in cerebella from ATXN2[127Q] mice, summarized in **(B)**. **(C)** Representative Western blot for phosphorylated PKC substrates in organotypic cerebellar slice cultures treated with 5 mM EGTA from twelve week old mice. Calcium chelation with EGTA reduced PKC substrate phosphorylation in ATXN2[127Q] slice cultures but not wild-type slice cultures, summarized in **(D)**. Throughout, data are mean ± SEM. NS = not significant; * = P<0.05. Statistical significance derived by unpaired two-tailed Student's T-Test (**B**) or two-way ANOVA with Sidak's multiple comparison test with P-values after multiple comparisons test indicated (**D**).

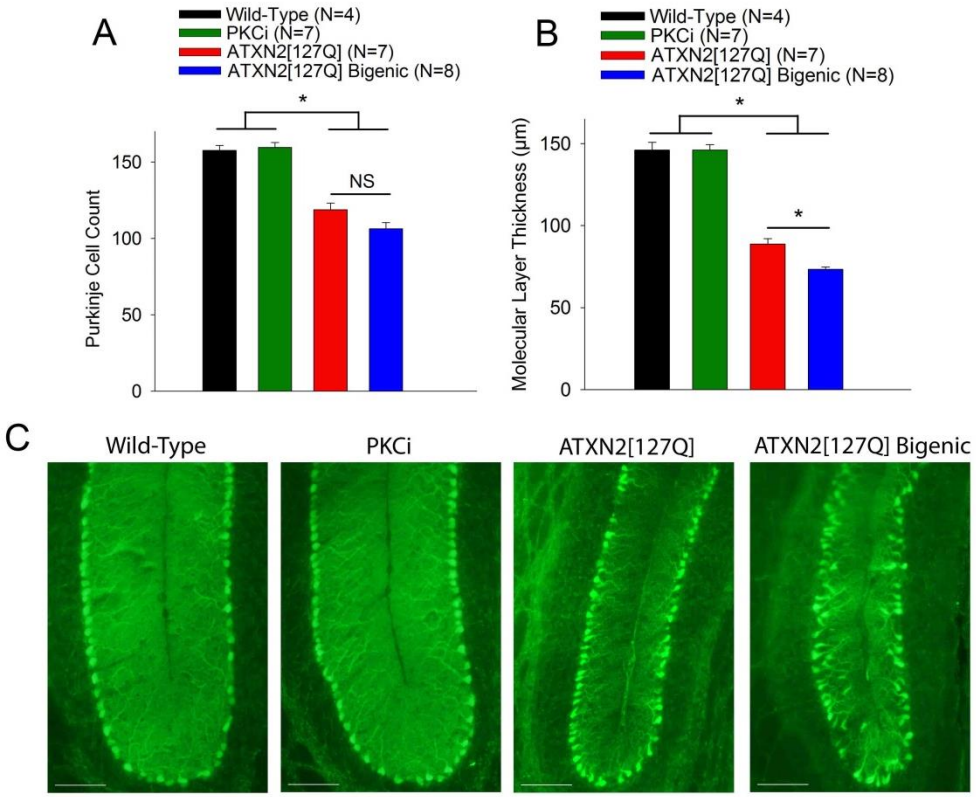

Figure 5.2 Increased PKC activity protects against dendritic degeneration in ATXN1[82Q] mice. **(A)** ATXN2[127Q] bigenic mice and ATXN2[127Q] mice show significant cell loss in lobule IV/V at twenty-five weeks of age. **(B)** Reduced molecular layer thickness in lobule VI of ATXN2[127Q] bigenic mice at twenty-five weeks of age. **(C)** Representative images at the cerebellar primary fissure in wild-type, PKCi, ATXN2[127Q], and ATXN2[127Q] bigenic mice stained with calbindin at twenty-five weeks of age. Scale bar, 100 µm. Throughout, data are mean ± SEM. NS = not significant; * = P<0.05. Statistical significance derived by one-way ANOVA with Holms-Sidak multiple comparison test (**B**, **C**).

MSA Samples

Patient No	Age	Sex	MSA-C vs. MSA-P
BB1427	49	Male	MSA-C
BB666	54	Male	MSA-C
BB39	61	Female	MSA-C & MSA-P
BB822	65	Female	MSA-C & MSA-P
BB1679	72	Female	MSA-C
BB658	72	Male	Not Reported
BB1358	75	Male	MSA-C

AD Samples

Patient No	Age	Sex	MSA-C vs. MSA-P
BB787	51	Female	N/A
BB1302	52	Male	N/A
BB1235	69	Female	N/A
BB325	72	Female	N/A
BB1520	72	Female	N/A
BB460	73	Male	N/A
BB209	77	Female	N/A

Table 5.1 Demographic information on MSA patients and age-matched Alzheimer disease controls. Presented above is relevant demographic information from MSA patients and age-matched Alzheimer disease (AD) controls for data presented in figure 5.3.

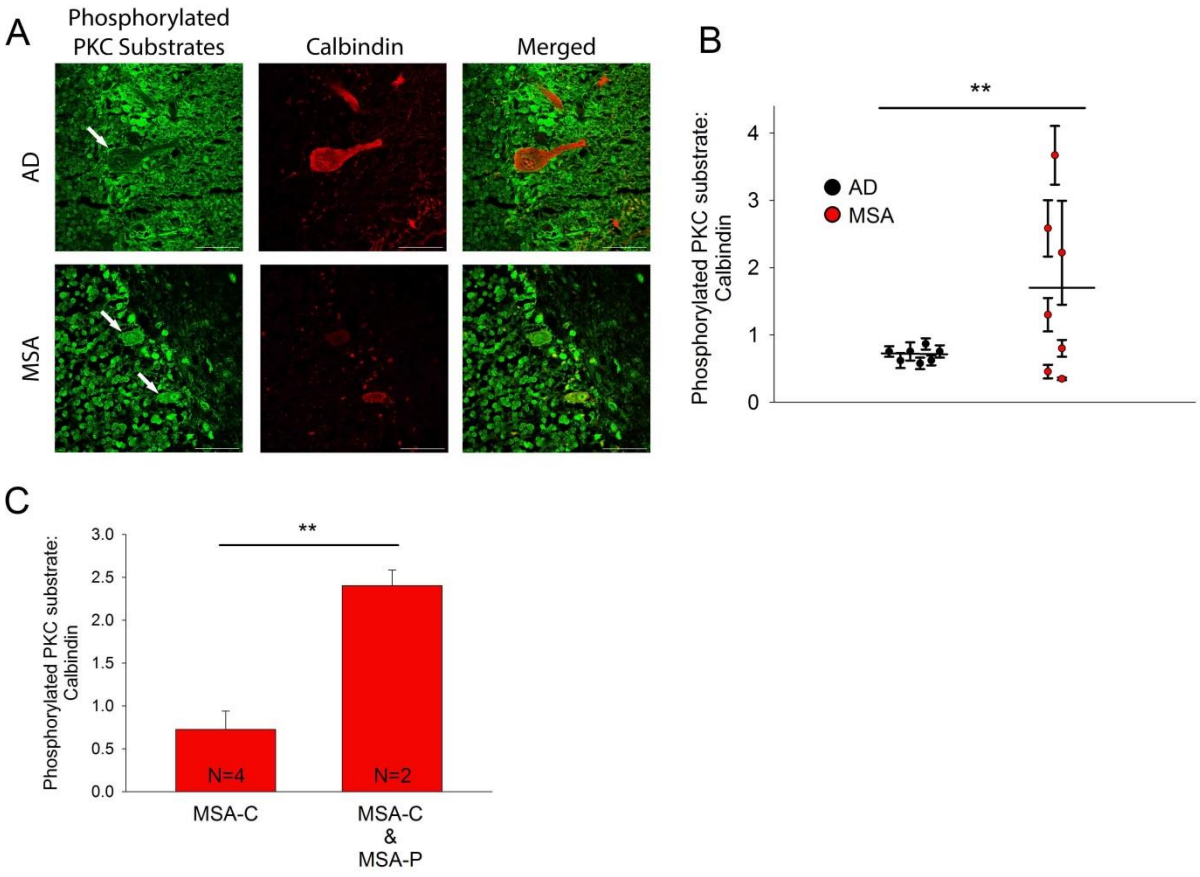

Figure 5.3 Increased PKC substrate phosphorylation is observed in Purkinje neurons from MSA patient autopsy tissue. **(A)** Representative images of phosphorylated PKC substrate staining (green) in Purkinje neurons (red) from MSA patient samples and age-matched Alzheimer disease (AD) controls. In phosphorylated PKC substrate images, Purkinje neurons are marked with arrows. Scale bars, 50 µm. Data showing increased phosphorylated PKC substrate staining relative to calbindin staining in the somatic compartment of Purkinje neurons from MSA patient samples and age-matched healthy control samples is summarized in **(B)**. Each data point represents an individual patient, with error bars representing SEM for measurements from multiple Purkinje neurons in that individual. **(C)** Comparison of phosphorylated PKC substrate staining relative to calbindin staining in patients defined clinically as MSA-C vs. patients defined as both MSA-C & MSA-P; data are from (B). ** = P<0.01. Statistical significance derived by two-way ANOVA detecting an effect of disease state on PKC substrate phosphorylation (**B**) or unpaired two-tailed Student's T-Test **(C)**.

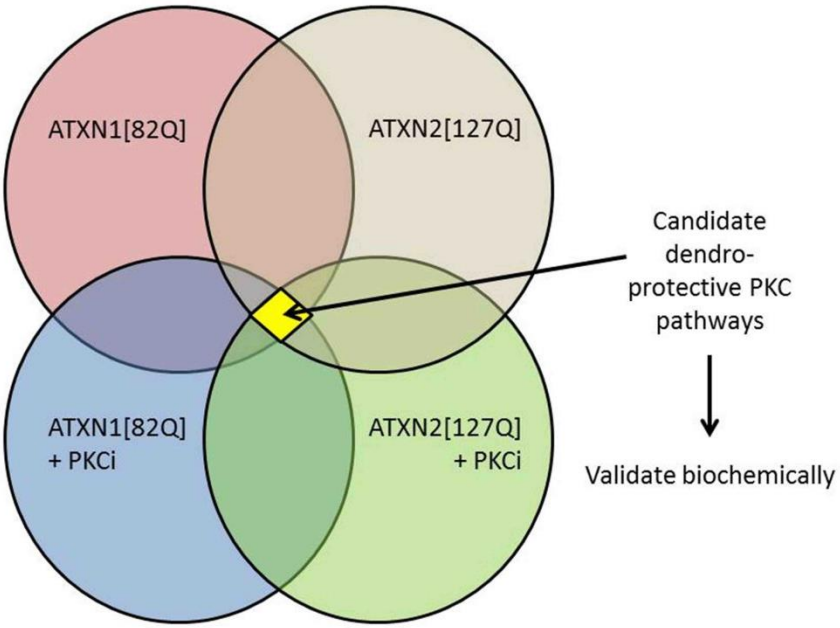

Figure 5.4 Conceptual framework for discovery of PKC-dependent dendro-protective pathways in SCA1 and SCA2. Proteomic or transcriptomic tools are likely to reveal changes between mice expressing the SCA transgene alone vs. mice expressing the SCA transgene and PKCi transgene. If the mechanism for PKC-dependent dendrite protection is shared between SCA1 and SCA2, identifying the area of overlap between PKC-modulated pathways in SCA1 and SCA2 will allow for elimination of spurious hits and foreground those pathways which are likely to be biologically relevant. Those pathways can then be validated biochemically in SCA1 mice, SCA1 patient samples, SCA2 mice, and MSA patient samples

Chapter 6

Conclusions and Future Directions

The results described in this dissertation lead to four main conclusions. The first is that Purkinje neuron dendrite degeneration is associated with increased intrinsic dendritic excitability in the ATXN1[82Q] model of SCA1. Secondly, normalizing intrinsic dendritic excitability by targeting channels whose transcript levels are suppressed by ATXN1[82Q] transgene expression is able to improve motor performance and preserve Purkinje neuron dendrites, establishing a novel role for increased intrinsic dendritic excitability as a driver of Purkinje neuron dendrite degeneration in SCA1. Thirdly, increased PKC activity is observed in the ATXN1[82Q] mouse and SCA1 patient tissue, and the action of this increase in PKC activity is to preserve Purkinje neuron dendrite structure and limit increases in intrinsic dendritic excitability. Finally, increased PKC activity is neuroprotective in the ATXN2[127Q] model of SCA2 and is observed in MSA patient tissue, suggesting that a role for PKC in dendrite degeneration may extend beyond SCA1 to other forms of inherited and sporadic ataxia. Together, the findings of this thesis provide a novel conceptual framework for understanding Purkinje neuron dendrite degeneration in ataxia: instead of being a passive response to toxic insult, it may instead reflect a regulated process where electrophysiologic activity and PKC activity regulate degenerative dendrite remodeling. However, important gaps remain in our understanding of Purkinje neuron dendrite physiology and PKC activity in these diseases. In this section, I will outline what I see as important opportunities for future studies extending from this work.

6.1 Dendritic calcium homeostasis in SCA1 Purkinje neurons

In any discussion of excitability and its relationship to neurodegeneration, considerable thought must be given to calcium dynamics. Ionic Ca^{2+} acts not just as a charge carrier but also an extremely powerful second messenger that impinges upon a myriad of cellular processes[300]. Among these, the importance of calcium as a driver of dendrite remodeling[301] and cell death[302] position it as an essential consideration in neurodegenerative disease.

There is an extensive literature for many neurodegenerative diseases that views neurodegeneration as a consequence of increased cytosolic calcium[167, 303-305]. Additionally, many studies which link increases in membrane excitability to neurodegeneration invoke ionic Ca^{2+} as the second messenger by which abnormalities at the membrane ultimately exert their degenerative effect[306, 307]. Although I do not necessarily disagree with this hypothesis in its relevance to other neurodegenerative diseases, I propose a different hypothesis for Purkinje neuron degeneration in SCA1: dendrite degeneration is driven in part by *reduced* cytosolic calcium availability, which contributes to increased intrinsic dendritic excitability that ultimately exerts its effect on dendrite structure by a different mechanism.

In the soma of Purkinje neurons, the effect of voltage-gated calcium channel opening is actually to hyperpolarize membrane potential because of the action of calcium-activated potassium channels[96]. Indirect evidence suggests that the same principle applies in Purkinje neuron dendrites, because local dendritic perfusion of cadmium chloride to block voltage-gated calcium channels has the same effect on spontaneous spiking as dendritic perfusion of specific blockers of SK2 or BK[101, 308]. These findings have demonstrated that under normal conditions, voltage-gated calcium channels function as stabilizers of Purkinje neuron membrane potential.

However, reducing the function of calcium-activated potassium channels results in increased somatic[308] and dendritic[149, 237] calcium entry through voltage-gated calcium channels, demonstrating that this operates as a negative feedback loop. Our prior work had demonstrated reduced BK channel expression and increased somatic excitability in ATXN1[82Q] Purkinje neurons[116], and our studies showing increased dendritic excitability (see chapter 3) led us to hypothesize that increased calcium dendritic calcium entry might be a driver of dendrite degeneration in SCA1. Our hypothesis was complicated, however, by an early study demonstrating relatively modest and inconclusive changes in ATXN1[82Q] Purkinje neuron synaptically-driven cytosolic [Ca^{2+}] increases[309]. Three findings clarified our understanding: 1) we observed that the combination of BK-AAV and baclofen could normalize dendritic excitability and preserve dendrites, 2) we observed reduced expression of the mGluR1-dependent calcium sources, and 3) a study was published demonstrating that ATXN1[82Q] Purkinje neurons show reduced mGluR1-mediated cytosolic [Ca^{2+}] increases after parallel fiber stimulation that can be normalized by treatment with baclofen[135]. This led us to revise our model, such that reduced expression of calcium sources would limit dendritic calcium entry while simultaneously exacerbating increases in dendritic excitability, such that a strategy targeting both the calcium sources and BK (through the use of baclofen and BK-AAV, respectively) was required to normalize dendritic excitability and preserve dendrite structure.

This "two-hit" model of increased dendritic excitability motivates several future lines of study. The first is to do a thorough and complete analysis of dendritic cytosolic [Ca^{2+}] in ATXN1[82Q] Purkinje neurons. Dendritic cytosolic [Ca^{2+}] should be assessed at five weeks and fifteen weeks during baseline spiking, somatic current injection-evoked spiking, parallel fiber stimulation, and climbing fiber stimulation. Distal and proximal segments should be assessed, in

order to provide a more granular picture of how calcium signaling might be perturbed. Furthermore, the effects of BK-AAV and baclofen treatment on all of these measures should be assessed. Without such a complete characterization of ATXN1[82Q] Purkinje neuron dendritic calcium homeostasis, it will be difficult to generate biologically realistic models of the role that calcium plays in SCA1 dendrites. We currently have the tools for Oregon Green BAPTA-based confocal calcium imaging in slices, and efforts to optimize and then apply the technique are ongoing.

A second key area for further research will be to test a role for mGluR1 and downstream calcium sources in increased dendritic excitability and dendritic degeneration. The role for these calcium sources can be assessed by repeating the BK-AAV + baclofen calcium spike experiment but in the presence of either mGluR1 antagonists or antagonists for one of the calcium sources; if the hypothesis is correct, the effect of baclofen should be occluded entirely by mGluR1 antagonists and partially blocked by IP_3 receptor, T-Type calcium channel, or TRPC3 channel blockers. Conversely, activators of mGluR1 should be able to substitute for baclofen and reduce intrinsic dendritic excitability either by themselves or in conjunction with BK-AAV. If mGluR1 is determined to be upstream of BK in modulation of dendritic excitability *in vitro*, then an *in vivo* experiment should be performed using a specific mGluR1 agonist in conjunction with BK-AAV to assess whether the behavioral and dendrite rescue can be recapitulated in ATXN1[82Q] mice.

Yet another question that arises from this hypothesis is the following: if ionic Ca^{2+} is not the signal by which increased excitability produces changes in dendrite structure, how is it that changes at the membrane are ultimately converted into degenerative changes in the neuron? One possibility is that the signaling occurs through membrane potential-dependent changes in the flux

of another ion; although less well-studied than Ca^{2+}, changes in flux or concentration of other ions has been linked to biological processes as diverse as cell cycle transitions[310, 311], atypical cell death pathways[312], oocyte fertilization[313], and even neural circuit activity[314]. Another possibility is that membrane potential itself is the signal: for example, a recent study demonstrated that membrane potential modulates K-Ras signaling in a manner that is independent of Ca^{2+} by altering the clustering of charged plasma membrane phospholipids[212]. Future studies in this area could leverage insights from a wide range of fields, including studies of cell cycle progression[315], cancer biology[316], and transition metal biology[317], to identify candidate pathways that respond to changes in membrane potential or non-Ca^{2+} ion flux and trigger either cytoskeletal remodeling or transcriptional changes. Validation of pathway activation using downstream gene expression changes or phosphorylation of pathway targets can then serve as a foundation for more comprehensive investigation. Although time-consuming and significant in scope, such studies may lead to significant insights, including identification of novel pathways for regulating dendrite structure not yet considered in neuroscience.

Beyond this, there is an important question not explored in this thesis: by what mechanism is ATXN1[82Q] suppressing transcript levels for these genes? As discussed in section 3.3.4, polyglutamine-expanded Ataxin-1 likely exerts its effect by perturbing transcription, indicating that transcriptional regulators for these genes likely hold the answer. I propose that there are at least two separate transcriptional systems impacted by ATXN1[82Q]: one controlling the expression of *Itpr1*, *Cacna1g*, and *Trpc3*, with another controlling expression of *Kcnma1*. This hypothesis is based on the kinetics of mRNA transcript suppression for these genes (see figure 3.4): *Itpr1*, *Cacna1g*, and *Trpc3*, are all completely suppressed at five weeks of age and remain suppressed, while *Kncma1* shows progressive reduction of expression from five

weeks of age to fifteen weeks of age. Future studies to investigate this hypothesis will require a combination of bioinformatic analysis of gene regulatory elements for identification of candidate regulators and biochemical approaches to validate whether those candidates bind to Ataxin-1 and/or regulatory sequences.

6.2 Dendrite structure and its relationship to dendritic excitability in SCA1

Chapter 4 focuses primarily on the role for reduced ion channel expression as a driver of increased dendritic excitability and downstream dendrite degeneration. A question not explored by this thesis is the extent to which structural changes in the dendrite then feed back to influence dendritic excitability. Cable theory would predict that the substantial changes described in ATXN1[82Q] Purkinje neuron dendrite structure should produce some kind of impact on dendrite signal propagation. We propose two opposing hypotheses for the impact that dendrite remodeling has on ATXN1[82Q] Purkinje neuron dendrite physiology: 1) dendrite degeneration further amplifies increases in dendrite excitability, or 2) dendrite degeneration is homeostatic from the perspective of excitability in that it opposes increases in dendritic excitability.

The first hypothesis is essentially a positive feedback model. Structural changes in dendrite shafts that would be predicted as part of this model include reduced branching, increased cross-sectional surface area, and reduced length for each dendrite segment. If this hypothesis were validated, it would suggest that early intervention would be critical for achieving maximal clinical benefit, as the establishment of structural changes that increase excitability would not only ensure the continued progression of disease but would also frustrate therapeutic strategies which relied solely on targeting dendritic channels.

The second hypothesis is a negative feedback model. Structural changes in dendrite shafts that would be predicted as part of this model include increased branching, reduced cross-

sectional surface, and increased length for each dendrite segment. This hypothesis is interesting because of the robust literature demonstrating that neurons exert homeostatic control over excitability[318]. Although the study of so-called homeostatic plasticity has only demonstrated functional changes through receptors or channels[318] and structural changes up to the level dendritic spines[319], it does provide a framework for considering how changes in dendrite structure could oppose increases in intrinsic dendritic excitability in ATXN1[82Q] Purkinje neurons. If this hypothesis were validated, it would imply that targeting dendrite structure without also improving dendrite physiology might actually be detrimental to performance of the neuron within the circuit.

Dissociating the impact of changes in channels vs. changes in dendrite structure on dendrite physiology would require an experimental paradigm where structure could be held constant while channels were perturbed and vice-versa. While the molecular tools for performing such experiments do not yet exist, such a study is ideally suited for a computational modeling approach. Using the NEURON environment[320], experiments could be performed using biologically realistic representations of Purkinje neurons derived from Neurolucida reconstructions (see chapter 3) and ion channel gene expression data from publicly-available RNAseq data on ATXN1[82Q] transcripts at five and twelve weeks of age[239]. As an initial experiment, backpropagating action potentials could be assessed in 1) neurons where channel conductances per unit membrane are progressively changed proportional to the RNAseq data while structure is held consistent, 2) neurons where channels are held consistent while dendrite structure is changed according to the Neurolucida reconstructions. Although it would be important to validate some of the assumptions of this model (i.e. can a proportional relationship be assumed between transcript abundance and conductance per unit membrane surface area for a

specific channel), such an approach would provide proof-of-principle for the possibility that changes in dendrite structure could themselves influence the evolution of dendritic pathology in SCA1.

6.3 Towards a multi-compartment model of Purkinje neurons in ataxia

As discussed in section 1.3, changes in Purkinje neuron spiking and synaptic physiology have been explored in models of many spinocerebellar ataxias, while dendritic physiology has been largely overlooked. This thesis focused specifically on dendritic physiology in SCA1, and revealed significant changes that impacted both motor performance and neurodegeneration. Sitting between the synapse and the spike, the dendrite mediates the influence of synaptic input onto the soma and also has its own influence on somatic spikes. Now that there is a growing literature identifying changes in spiking, synaptic physiology, and (with this thesis) dendritic excitability, an important priority for the field will be integrating our understanding of these three compartments such that a comprehensive picture of SCA1 Purkinje neuron physiology can be developed.

In considering the literature on synaptic physiology in SCA1, it is difficult at this point to identify clearly any influence that the alterations we have described in dendritic physiology may have on synaptic integration. This is in part due to the conflicting data which already exist regarding Purkinje neuron synaptic function in the ATXN1[82Q] mouse. *In vivo* studies using flavoprotein autofluorescence (a very indirect measure of Purkinje neuron synaptic responses) suggest reduced climbing fiber and parallel fiber responsiveness[134], while *in vitro* studies suggest there is no difference parallel or climbing fiber-evoked AMPA current[135] but a significant reduction in parallel fiber-induced mGluR1 current amplitude[135] or slowed mGluR1 current decay[136]. To complicate things further, *in vitro* measurements of synaptic currents in these

studies were performed with cesium chloride in the pipette, such that the properties of the dendrite are necessarily obscured in pursuit of more accurate current measurements. Based on the data outlined in chapter 3, we would predict that synaptic PSPs should spread more readily along ATXN1[82Q] Purkinje neuron dendrites than wild-type dendrites. This should mean a given synaptic PSP will produce a larger effect on somatic spiking (as has been observed during blockade of Kv1 channels in wild-type Purkinje neurons[278]), and would also suggest that PSPs originating from nearby dendritic branches might influence one another more than they might in a wild-type Purkinje neuron. Future studies to assess the impact of altered dendritic excitability on synaptic integration could be done in a rudimentary fashion through multi-site stimulation and somatic recording, but would be done best using confocal microscopy with genetically-encoded voltage sensors[321, 322] to monitor the spread of depolarization throughout the dendritic tree in response to different types of input. Ideally, dendritic integration of synaptic input will be monitored *in vivo*[245], as it is very likely that the properties of the dendrite differ substantially in a slice preparation where much of the synaptic input is severed[323].

It is clear from studies of wild-type Purkinje neurons that the dendrite influences somatic spiking, providing an active contribution linked to the function of dendritic conductances[101, 308] as well as a passive contribution stemming from the significant capacitance of the Purkinje neuron dendrite[324]. This influence extends beyond baseline spiking frequency[325] to produce changes in spike shape, such that elimination of the dendrite's influence by pinching it with pipettes results in increased spike height and a larger AHP[324]. Importantly, changes in somatic spiking have been described in several studies of the ATXN1[82Q] mouse, including changes in the AHP[116], reduced baseline firing frequency[114, 116], and altered spiking in response to somatically-injected current[114, 116, 309]. It is reasonable to consider the possibility that some of

these changes, such as the observed rescue of the BK-mediated fast AHP in aged ATXN1[82Q] Purkinje neurons[116], could arise in part as a result of changes in the dendrite. Future studies could address any contribution that altered dendritic physiology may have on somatic spiking, either through the use of local dendritic sucrose perfusion[325] to eliminate active contributions or the use of dendrite pinching[324] to eliminate active and passive contributions.

It is important to note that while the work of this thesis adds the dendrite as a third compartment for consideration in SCA1 Purkinje neuron physiology, future studies should acknowledge that a three-compartment Purkinje neuron is itself an oversimplification, as the Purkinje neuron is not really three compartments but many. Experiments performed in chapter 3 and 4 to examine intrinsic dendritic excitability only demonstrate that signal propagation is altered in the Purkinje neuron dendrite arbor generally, without much consideration given to dendrites of different orders, dendrites receiving different inputs, or state-dependent characteristics of the dendrite, all of which confer significant complexity to dendritic computation in Purkinje neurons[245] and many other neuronal subtypes[326-329]. Computational modeling can be used to generate hypotheses, but these questions can also be addressed experimentally through imaging of neuronal activity, as imaging provides significantly wider spatial coverage (at a cost of temporal and spatial resolution) than patch clamp electrophysiology. As discussed previously, our lab currently has the capacity for laser-scanning confocal microscopy, allowing for *in vitro* calcium or voltage imaging. There are also other techniques being used that could provide even better information. Multiphoton calcium imaging has been used effectively *in vitro*[330] to perform studies with high temporal resolution and wide spatial coverage across the Purkinje neuron dendrite arbor, revealing complex signal processing rules such as mGluR1-dependent gating of calcium spike spread[150]. Similarly, two-photon

calcium imaging has been used *in vivo* to demonstrate further complexity in Purkinje neuron dendrites, including the observation that individual dendrite segment responses to climbing fiber stimulus are tuned by local interneurons[245] and the observation that dendritic calcium spikes can serve as analogue signals encoding stimulus strength[331]. Although calcium flux may be a poor proxy for membrane potential in ATXN1[82Q] Purkinje neurons due to changes in calcium channel expression, it will be important to assess the extent to which these rules are intact or altered in ATXN1[82Q] Purkinje neurons, and ideally changes will be connected to clinically-meaningful outcomes.

6.4 Understanding the relationship between physiology, structure, and motor impairment in spinocerebellar ataxias

To move beyond a descriptive characterization of dendritic physiology in ATXN1[82Q] Purkinje neurons, this thesis identified specific ion channels mediating those changes and also identified treatment strategies which targeted dendritic physiology to produce relatively rapid improvement of motor performance (within two weeks of initiating treatment) and long-term dendroprotection. These studies move towards establishing increased intrinsic dendritic excitability as an immediate cause of motor impairment and also a driver of neurodegeneration. They also raise a question: in SCA1 and neurodegenerative ataxias more generally, is it the structural change in the network that causes symptoms, the functional changes in the neurons, or both?

It is clear from studies of ion channel mutant mice that changes in Purkinje neuron physiology can produce profound ataxia without any changes in Purkinje neuron structure[104-107]. It has also been demonstrated in a model of Niemann-Pick disease, Type C1 that Purkinje neuron degeneration and ataxia can occur without changes in Purkinje neuron physiology[332],

demonstrating that structural changes in the network are also sufficient to produce motor impairment. In SCA models where both electrophysiologic and structural changes in the network are observed, it is vital to understand in what way each contributes to motor impairment. This is a clinically-meaningful question because it will identify whether normalizing physiology or normalizing structure will have a greater impact on patient symptoms, although it is worth noting that our work suggests that physiology and structure are linked.

I propose that early in disease progression, altered physiology may play a proportionally more significant role in motor impairment, but that in more advanced disease there is a significant contribution from structural changes in the network. This is best supported by a study examining aminopyridine treatment for improving Purkinje neuron physiology in ATXN1[82Q] mice[114]. This study found that chronic aminopyridine treatment *in vivo* could produce neuroprotection and long-term behavioral improvement. Importantly, short-term treatment with aminopyridines could only improve motor behavior in young mice but not old mice, despite the fact that aminopyridines could improve Purkinje neuron spiking in both young and older ATXN1[82Q] Purkinje neurons. These findings are consistent with ongoing studies in our own lab which suggest that treatments which improve spiking are effective if administered short-term in young but not old ATXN1[82Q] mice (data not shown). Taken together, these data suggest that alterations in Purkinje neuron physiology are a consistent feature of disease, but that treatments which target physiology may only be effective for motor symptoms over the short term when the network architecture is relatively intact.

This hypothesis presents several important experiments that can be performed with BK-AAV and baclofen. Future studies will assess whether BK-AAV and baclofen is able to produce motor improvement if viral delivery, treatment, and testing occur at fifteen weeks of age. If no

motor rescue is observed (as we would predict), baclofen treatment can continue until a later time point to assess whether treatment can halt further dendrite degeneration or even allow for dendrite regrowth. Studies where ATXN1[82Q] was knocked down in SCA1 mice using synthetic microRNAs or doxycycline-based conditional knockdown revealed that late-stage knockdown could produce significant (although incomplete) reversal of motor impairment[229, 333] and partial recovery of dendrite structure[333], so if the mechanism of dendrite degeneration continues to depend on changes in dendritic excitability it should be possible to prevent or reverse further dendrite degeneration if treatment is initiated in older animals. Important insights could also be gained through employing these tools or antisense oligonucleotide-based knockdown[334] and comparing the kinetics of rescue in expression of channels of interest (*Itpr1*, *Trpc3*, *Cacna1g*, and *Kcnma1*) to the kinetics of rescue in dendrite structure as far as how closely they coincide with behavioral rescue. Such studies could provide important caveats for clinical pursuit of physiology-based therapies, and therefore represent a meaningful research priority.

6.5 Exploring and expanding the dendroprotective PKC pathway in ataxia

The findings outlined in chapter 5 demonstrate increased PKC activity in SCA1 Purkinje is dendroprotective and opposes increases in dendritic excitability. The findings in chapter 6 demonstrate that increased PKC is also dendroprotective in a model of SCA2 and is observed in post-mortem MSA tissue, suggesting that PKC activity is a critical modifier of neurodegeneration in SCA1, SCA2, and potentially beyond. These findings represent an important first step in characterizing a neuroprotective mechanism in ataxia that has not yet been described. However, important questions remain unanswered that must be addressed to better understand this mechanism and potentially leverage it for clinical application.

One of the most pressing questions relates to why PKC activity is increased in SCA1, SCA2, and MSA. It is possible that the activation of PKC is regulated in a manner that is in some way specifically linked to these disease entities; alternatively, it may be a non-specific protective response induced by Purkinje neurons during neurodegeneration. These possibilities are best addressed by exploring PKC activation in other models of ataxia with robust Purkinje neuron pathology, such as models of SCA6[12] or SCA7[13]. Future studies will perform Western blots to assess PKC substrate phosphorylation at the onset of Purkinje neuron dendrite degeneration in these models. A consistent finding of increased PKC substrate phosphorylation across all models favors the interpretation that it is a non-specific protective pathway, whereas a finding that only some ataxia models show increased PKC substrate phosphorylation would suggest disease-specific regulation.

Regardless of which result is obtained, the question of what triggers the increase in activity remains. The fact that EGTA can eliminate the increased PKC substrate phosphorylation in ATXN1[82Q] and ATXN2[127Q] slice cultures implicates conventional PKC isozymes, and because these isozymes are activated by a combination of DAG and Ca^{2+} ions[268], it suggests that pathways which regulate cytosolic calcium, DAG production, or both might be involved. The presumed role for calcium as a trigger for increased conventional PKC activity is at odds with the hypothesis outlined in section 6.1, which proposes that ATXN1[82Q] Purkinje neurons actually have reduced cytosolic [Ca^{2+}]. There are several possibilities: 1) there is sufficient calcium available under baseline conditions to allow for conventional PKC activation, but the increase in activation occurs through changes in DAG processing, 2) the hypothesis that there is decreased cytosolic [Ca^{2+}] in ATXN1[82Q] Purkinje neurons is incorrect or at least imprecise, or 3) conventional PKC isozymes are being activated by some other mechanism.

The first possibility would involve some mechanism by which DAG in the membrane would be increased. It is intriguing to note that diacylglycerol lipase-α (DAGLα), an enzyme which breaks down DAG to the endocannabinoid 2-Arachidonoyl-glycerol, is highly expressed in Purkinje neuron dendrites[335] and promotes neurite outgrowth[336] but is suppressed at the mRNA transcript level starting at five weeks of age in ATXN1[82Q] cerebella[239]. Future studies to investigate this hypothesis will begin by characterizing expression of DAGLα and other key players in membrane lipid metabolism, as well as determining whether there are in fact changes in DAG levels in the membrane. The second possibility can be confirmed or ruled out based on experiments described in section 6.1. The third possibility is difficult to assess, in part because there are many mechanisms by which PKC activity could be increased, although experiments to investigate the possibility of ectopic expression of PKCβI or PKCβII have been discussed in section 5.4.

Beyond the question of what triggers neuroprotective increases in PKC activity, it is also important to identify mechanisms by which PKC activity exerts its protective effect. As discussed in sections 4.4 and 5.4, this can be most easily investigated using –omics approaches and leveraging the fact that the neuroprotective effect has been observed in both the ATXN1[82Q] model and the ATXN2[127Q] model. PKC targets that consistently correlate with neuroprotection will not only provide mechanistic insight for PKC neuroprotection, but may also represent therapeutic targets in their own right, particularly if increased PKC activity is identified as a protective pathway induced only in some forms of ataxia.

In summary, much remains to be understood regarding the increased PKC activity and neuroprotection identified in this thesis. Events both upstream and downstream of PKC remain unclear, and a more complete understanding of this pathway could yield scientifically or

clinically important insights. These insights may be applied beyond SCA1, SCA2, and MSA to other forms of ataxia, and therefore represent a significant research priority.

6.6 Concluding remarks

Dendrite degeneration is a ubiquitous feature of neurodegenerative diseases, including degenerative cerebellar ataxias. Studies of spinocerebellar ataxias, a disabling and currently untreatable subset of genetic ataxias, have suggested that Purkinje neuron dendrite degeneration contributes meaningfully to motor impairment. Despite this, Purkinje neuron dendrite degeneration in ataxia remains poorly understood. My work in this thesis helps establish that Purkinje neuron dendrite degeneration is regulated by intrinsic dendritic excitability and protein kinase C activity in SCA1, and also demonstrates a role for protein kinase C activity in SCA2 and MSA. Contrary to conceptions of dendrite degeneration as a passive response to toxic insult, these data imply that dendrite degeneration in ataxia may be a regulated process mediated by some of the same systems that regulate dendrite development and maintenance in healthy neurons.

This thesis provides several important contributions to the field. First, it demonstrates that dendritic excitability and protein kinase C activity are capable of regulating adult Purkinje neuron dendrite remodeling, which is itself a novel finding. Second, it identifies both dendritic excitability and PKC activity as being important for disease progression in SCA1 and likely also for SCA2 and MSA, suggesting that these processes may be amenable to therapeutic intervention. Finally, this thesis provides a novel conceptual framework for understanding dendrite degeneration in cerebellar ataxia and potentially other neurodegenerative diseases. Future studies could expand upon the studies presented here to identify channel targets, PKC regulators, and downstream effectors that link both excitability and PKC to dendrite remodeling.

The work of this thesis, as well as the research it motivates, could bring about the development of novel therapies to preserve dendrite structure and function in ataxia and other neurodegenerative diseases.

References

1. Apps R, Garwicz M. Anatomical and physiological foundations of cerebellar information processing. Nature reviews Neuroscience. 2005 Apr;6(4):297-311.

2. Durr A. Autosomal dominant cerebellar ataxias: polyglutamine expansions and beyond. The Lancet Neurology. 2010 Sep;9(9):885-94.

3. Schols L, Bauer P, Schmidt T, Schulte T, Riess O. Autosomal dominant cerebellar ataxias: clinical features, genetics, and pathogenesis. The Lancet Neurology. 2004 May;3(5):291-304.

4. Ferrer I, Genis D, Davalos A, Bernado L, Sant F, Serrano T. The Purkinje cell in olivopontocerebellar atrophy. A Golgi and immunocytochemical study. Neuropathology and applied neurobiology. 1994 Feb;20(1):38-46.

5. Koeppen AH. The pathogenesis of spinocerebellar ataxia. Cerebellum. 2005;4(1):62-73.

6. Sasaki H, Kojima H, Yabe I, et al. Neuropathological and molecular studies of spinocerebellar ataxia type 6 (SCA6). Acta neuropathologica. 1998 Feb;95(2):199-204.

7. Xia G, McFarland KN, Wang K, Sarkar PS, Yachnis AT, Ashizawa T. Purkinje cell loss is the major brain pathology of spinocerebellar ataxia type 10. Journal of neurology, neurosurgery, and psychiatry. 2013 Dec;84(12):1409-11.

8. Palau F, Espinos C. Autosomal recessive cerebellar ataxias. Orphanet journal of rare diseases. 2006 Nov 17;1:47.

9. Clark HB, Burright EN, Yunis WS, et al. Purkinje cell expression of a mutant allele of SCA1 in transgenic mice leads to disparate effects on motor behaviors, followed by a progressive cerebellar dysfunction and histological alterations. The Journal of neuroscience : the official journal of the Society for Neuroscience. 1997 Oct 1;17(19):7385-95.

10. Watase K, Weeber EJ, Xu B, et al. A long CAG repeat in the mouse Sca1 locus replicates SCA1 features and reveals the impact of protein solubility on selective neurodegeneration. Neuron. 2002 Jun 13;34(6):905-19.

11. Hansen ST, Meera P, Otis TS, Pulst SM. Changes in Purkinje cell firing and gene expression precede behavioral pathology in a mouse model of SCA2. Human molecular genetics. 2013 Jan 15;22(2):271-83.

12. Unno T, Wakamori M, Koike M, et al. Development of Purkinje cell degeneration in a knockin mouse model reveals lysosomal involvement in the pathogenesis of SCA6. Proceedings of the National Academy of Sciences of the United States of America. 2012 Oct 23;109(43):17693-8.

13. Furrer SA, Mohanachandran MS, Waldherr SM, et al. Spinocerebellar ataxia type 7 cerebellar disease requires the coordinated action of mutant ataxin-7 in neurons and glia, and displays non-cell-autonomous bergmann glia degeneration. The Journal of neuroscience : the official journal of the Society for Neuroscience. 2011 Nov 9;31(45):16269-78.

14. Mangiarini L, Sathasivam K, Seller M, et al. Exon 1 of the HD gene with an expanded CAG repeat is sufficient to cause a progressive neurological phenotype in transgenic mice. Cell. 1996 Nov 01;87(3):493-506.

15. Hodges A, Hughes G, Brooks S, et al. Brain gene expression correlates with changes in behavior in the R6/1 mouse model of Huntington's disease. Genes, brain, and behavior. 2008 Apr;7(3):288-99.

16. Slow EJ, van Raamsdonk J, Rogers D, et al. Selective striatal neuronal loss in a YAC128 mouse model of Huntington disease. Human molecular genetics. 2003 Jul 01;12(13):1555-67.

17. Gray M, Shirasaki DI, Cepeda C, et al. Full-length human mutant huntingtin with a stable polyglutamine repeat can elicit progressive and selective neuropathogenesis in BACHD mice. The Journal of neuroscience : the official journal of the Society for Neuroscience. 2008 Jun 11;28(24):6182-95.

18. Heng MY, Tallaksen-Greene SJ, Detloff PJ, Albin RL. Longitudinal evaluation of the Hdh(CAG)150 knock-in murine model of Huntington's disease. The Journal of neuroscience : the official journal of the Society for Neuroscience. 2007 Aug 22;27(34):8989-98.

19. Hickey MA, Kosmalska A, Enayati J, et al. Extensive early motor and non-motor behavioral deficits are followed by striatal neuronal loss in knock-in Huntington's disease mice. Neuroscience. 2008 Nov 11;157(1):280-95.

20. Yu ZX, Li SH, Evans J, Pillarisetti A, Li H, Li XJ. Mutant huntingtin causes context-dependent neurodegeneration in mice with Huntington's disease. The Journal of neuroscience : the official journal of the Society for Neuroscience. 2003 Mar 15;23(6):2193-202.

21. Dansithong W, Paul S, Figueroa KP, et al. Ataxin-2 regulates RGS8 translation in a new BAC-SCA2 transgenic mouse model. PLoS genetics. 2015 Apr;11(4):e1005182.

22. Zuo J, De Jager PL, Takahashi KA, Jiang W, Linden DJ, Heintz N. Neurodegeneration in Lurcher mice caused by mutation in delta2 glutamate receptor gene. Nature. 1997 Aug 21;388(6644):769-73.

23. Wetts R, Herrup K. Interaction of granule, Purkinje and inferior olivary neurons in lurcher chimaeric mice. I. Qualitative studies. Journal of embryology and experimental morphology. 1982 Apr;68:87-98.

24. Martin LA, Goldowitz D, Mittleman G. The cerebellum and spatial ability: dissection of motor and cognitive components with a mouse model system. The European journal of neuroscience. 2003 Oct;18(7):2002-10.

25. Woodruff-Pak DS. Stereological estimation of Purkinje neuron number in C57BL/6 mice and its relation to associative learning. Neuroscience. 2006 Aug 11;141(1):233-43.

26. Caddy KW, Herrup K. Studies of the dendritic tree of wild-type cerebellar Purkinje cells in lurcher chimeric mice. The Journal of comparative neurology. 1990 Jul 01;297(1):121-31.

27. Burright EN, Clark HB, Servadio A, et al. SCA1 transgenic mice: a model for neurodegeneration caused by an expanded CAG trinucleotide repeat. Cell. 1995 Sep 22;82(6):937-48.

28. Orr HT. SCA1-phosphorylation, a regulator of Ataxin-1 function and pathogenesis. Progress in neurobiology. 2012 Dec;99(3):179-85.

29. Emamian ES, Kaytor MD, Duvick LA, et al. Serine 776 of ataxin-1 is critical for polyglutamine-induced disease in SCA1 transgenic mice. Neuron. 2003 May 08;38(3):375-87.

30. Orr HT, Chung MY, Banfi S, et al. Expansion of an unstable trinucleotide CAG repeat in spinocerebellar ataxia type 1. Nature genetics. 1993 Jul;4(3):221-6.

31. Girard M, Lariviere R, Parfitt DA, et al. Mitochondrial dysfunction and Purkinje cell loss in autosomal recessive spastic ataxia of Charlevoix-Saguenay (ARSACS). Proceedings of the National Academy of Sciences of the United States of America. 2012 Jan 31;109(5):1661-6.

32. Skinner PJ, Vierra-Green CA, Clark HB, Zoghbi HY, Orr HT. Altered trafficking of membrane proteins in purkinje cells of SCA1 transgenic mice. The American journal of pathology. 2001 Sep;159(3):905-13.

33. Ramani B, Harris GM, Huang R, et al. A knockin mouse model of spinocerebellar ataxia type 3 exhibits prominent aggregate pathology and aberrant splicing of the disease gene transcript. Human molecular genetics. 2015 Mar 01;24(5):1211-24.

34. Emoto K. Dendrite remodeling in development and disease. Development, growth & differentiation. 2011 Apr;53(3):277-86.

35. Lin YC, Koleske AJ. Mechanisms of synapse and dendrite maintenance and their disruption in psychiatric and neurodegenerative disorders. Annual review of neuroscience. 2010;33:349-78.

36. Kulkarni VA, Firestein BL. The dendritic tree and brain disorders. Molecular and cellular neurosciences. 2012 May;50(1):10-20.

37. Maravall M, Koh IY, Lindquist WB, Svoboda K. Experience-dependent changes in basal dendritic branching of layer 2/3 pyramidal neurons during a critical period for developmental plasticity in rat barrel cortex. Cerebral cortex. 2004 Jun;14(6):655-64.

38. Lee LJ, Chen WJ, Chuang YW, Wang YC. Neonatal whisker trimming causes long-lasting changes in structure and function of the somatosensory system. Experimental neurology. 2009 Oct;219(2):524-32.

39. Kossel A, Lowel S, Bolz J. Relationships between dendritic fields and functional architecture in striate cortex of normal and visually deprived cats. The Journal of neuroscience : the official journal of the Society for Neuroscience. 1995 May;15(5 Pt 2):3913-26.

40. Attardo A, Fitzgerald JE, Schnitzer MJ. Impermanence of dendritic spines in live adult CA1 hippocampus. Nature. 2015 Jul 30;523(7562):592-6.

41. Majewska AK, Newton JR, Sur M. Remodeling of synaptic structure in sensory cortical areas in vivo. The Journal of neuroscience : the official journal of the Society for Neuroscience. 2006 Mar 15;26(11):3021-9.

42. Keck T, Mrsic-Flogel TD, Vaz Afonso M, Eysel UT, Bonhoeffer T, Hubener M. Massive restructuring of neuronal circuits during functional reorganization of adult visual cortex. Nature neuroscience. 2008 Oct;11(10):1162-7.

43. Grueber WB, Jan LY, Jan YN. Different levels of the homeodomain protein cut regulate distinct dendrite branching patterns of Drosophila multidendritic neurons. Cell. 2003 Mar 21;112(6):805-18.

44. Li W, Wang F, Menut L, Gao FB. BTB/POZ-zinc finger protein abrupt suppresses dendritic branching in a neuronal subtype-specific and dosage-dependent manner. Neuron. 2004 Sep 16;43(6):823-34.

45. Aizawa H, Hu SC, Bobb K, et al. Dendrite development regulated by CREST, a calcium-regulated transcriptional activator. Science. 2004 Jan 09;303(5655):197-202.

46. Redmond L, Kashani AH, Ghosh A. Calcium regulation of dendritic growth via CaM kinase IV and CREB-mediated transcription. Neuron. 2002 Jun 13;34(6):999-1010.

47. Le R, Esquenazi S. Astrocytes mediate cerebral cortical neuronal axon and dendrite growth, in part, by release of fibroblast growth factor. Neurological research. 2002 Jan;24(1):81-92.

48. McAllister AK, Lo DC, Katz LC. Neurotrophins regulate dendritic growth in developing visual cortex. Neuron. 1995 Oct;15(4):791-803.

49. Tan ZJ, Peng Y, Song HL, Zheng JJ, Yu X. N-cadherin-dependent neuron-neuron interaction is required for the maintenance of activity-induced dendrite growth. Proceedings of the National Academy of Sciences of the United States of America. 2010 May 25;107(21):9873-8.

50. Lohmann C, Myhr KL, Wong RO. Transmitter-evoked local calcium release stabilizes developing dendrites. Nature. 2002 Jul 11;418(6894):177-81.

51. Rajan I, Witte S, Cline HT. NMDA receptor activity stabilizes presynaptic retinotectal axons and postsynaptic optic tectal cell dendrites in vivo. Journal of neurobiology. 1999 Feb 15;38(3):357-68.

52. Wang Y, Rubel EW. In vivo reversible regulation of dendritic patterning by afferent input in bipolar auditory neurons. The Journal of neuroscience : the official journal of the Society for Neuroscience. 2012 Aug 15;32(33):11495-504.

53. Sin WC, Haas K, Ruthazer ES, Cline HT. Dendrite growth increased by visual activity requires NMDA receptor and Rho GTPases. Nature. 2002 Oct 03;419(6906):475-80.

54. Duch C, Vonhoff F, Ryglewski S. Dendrite elongation and dendritic branching are affected separately by different forms of intrinsic motoneuron excitability. Journal of neurophysiology. 2008 Nov;100(5):2525-36.

55. Sim S, Antolin S, Lin CW, Lin Y, Lois C. Increased cell-intrinsic excitability induces synaptic changes in new neurons in the adult dentate gyrus that require Npas4. The Journal of neuroscience : the official journal of the Society for Neuroscience. 2013 May 01;33(18):7928-40.

56. Luo L, Hensch TK, Ackerman L, Barbel S, Jan LY, Jan YN. Differential effects of the Rac GTPase on Purkinje cell axons and dendritic trunks and spines. Nature. 1996 Feb 29;379(6568):837-40.

57. Buttery P, Beg AA, Chih B, Broder A, Mason CA, Scheiffele P. The diacylglycerol-binding protein alpha1-chimaerin regulates dendritic morphology. Proceedings of the National Academy of Sciences of the United States of America. 2006 Feb 07;103(6):1924-9.

58. Rui Y, Myers KR, Yu K, et al. Activity-dependent regulation of dendritic growth and maintenance by glycogen synthase kinase 3beta. Nature communications. 2013;4:2628.

59. Trachtenberg JT, Chen BE, Knott GW, et al. Long-term in vivo imaging of experience-dependent synaptic plasticity in adult cortex. Nature. 2002 Dec 19-26;420(6917):788-94.

60. Mizrahi A, Katz LC. Dendritic stability in the adult olfactory bulb. Nature neuroscience. 2003 Nov;6(11):1201-7.

61. Matter C, Pribadi M, Liu X, Trachtenberg JT. Delta-catenin is required for the maintenance of neural structure and function in mature cortex in vivo. Neuron. 2009 Nov 12;64(3):320-7.

62. Lee WC, Huang H, Feng G, et al. Dynamic remodeling of dendritic arbors in GABAergic interneurons of adult visual cortex. PLoS biology. 2006 Feb;4(2):e29.

63. Espinosa JS, Wheeler DG, Tsien RW, Luo L. Uncoupling dendrite growth and patterning: single-cell knockout analysis of NMDA receptor 2B. Neuron. 2009 Apr 30;62(2):205-17.

64. Greenough WT, Larson JR, Withers GS. Effects of unilateral and bilateral training in a reaching task on dendritic branching of neurons in the rat motor-sensory forelimb cortex. Behavioral and neural biology. 1985 Sep;44(2):301-14.

65. Withers GS, Greenough WT. Reach training selectively alters dendritic branching in subpopulations of layer II-III pyramids in rat motor-somatosensory forelimb cortex. Neuropsychologia. 1989;27(1):61-9.

66. Robinson TE, Kolb B. Alterations in the morphology of dendrites and dendritic spines in the nucleus accumbens and prefrontal cortex following repeated treatment with amphetamine or cocaine. The European journal of neuroscience. 1999 May;11(5):1598-604.

67. Robinson TE, Gorny G, Mitton E, Kolb B. Cocaine self-administration alters the morphology of dendrites and dendritic spines in the nucleus accumbens and neocortex. Synapse. 2001 Mar 01;39(3):257-66.

68. Li Y, Acerbo MJ, Robinson TE. The induction of behavioural sensitization is associated with cocaine-induced structural plasticity in the core (but not shell) of the nucleus accumbens. The European journal of neuroscience. 2004 Sep;20(6):1647-54.

69. Zhang J, Zhang L, Jiao H, et al. c-Fos facilitates the acquisition and extinction of cocaine-induced persistent changes. The Journal of neuroscience : the official journal of the Society for Neuroscience. 2006 Dec 20;26(51):13287-96.

70. Armengol JA, Sotelo C. Early dendritic development of Purkinje cells in the rat cerebellum. A light and electron microscopic study using axonal tracing in 'in vitro' slices. Brain research Developmental brain research. 1991 Dec 17;64(1-2):95-114.

71. Crepel F, Delhaye-Bouchaud N, Dupont JL, Sotelo C. Dendritic and axonic fields of Purkinje cells in developing and x-irradiated rat cerebellum. A comparative study using intracellular staining with horseradish peroxidase. Neuroscience. 1980;5(2):333-47.

72. Weiss GM, Pysh JJ. Evidence for loss of Purkinje cell dendrites during late development: a morphometric Golgi analysis in the mouse. Brain research. 1978 Oct 13;154(2):219-30.

73. Boukhtouche F, Janmaat S, Vodjdani G, et al. Retinoid-related orphan receptor alpha controls the early steps of Purkinje cell dendritic differentiation. The Journal of neuroscience : the official journal of the Society for Neuroscience. 2006 Feb 01;26(5):1531-8.

74. Poulain FE, Chauvin S, Wehrle R, et al. SCLIP is crucial for the formation and development of the Purkinje cell dendritic arbor. The Journal of neuroscience : the official journal of the Society for Neuroscience. 2008 Jul 16;28(29):7387-98.

75. Kim J, Kwon N, Chang S, et al. Altered branching patterns of Purkinje cells in mouse model for cortical development disorder. Scientific reports. 2011;1:122.

76. Koibuchi N. The role of thyroid hormone on cerebellar development. Cerebellum. 2008;7(4):530-3.

77. Haraguchi S, Sasahara K, Shikimi H, Honda S, Harada N, Tsutsui K. Estradiol promotes purkinje dendritic growth, spinogenesis, and synaptogenesis during neonatal life by inducing the expression of BDNF. Cerebellum. 2012 Jun;11(2):416-7.

78. Gibson DA, Tymanskyj S, Yuan RC, et al. Dendrite self-avoidance requires cell-autonomous slit/robo signaling in cerebellar purkinje cells. Neuron. 2014 Mar 05;81(5):1040-56.

79. Shima Y, Kengaku M, Hirano T, Takeichi M, Uemura T. Regulation of dendritic maintenance and growth by a mammalian 7-pass transmembrane cadherin. Developmental cell. 2004 Aug;7(2):205-16.

80. Lefebvre JL, Kostadinov D, Chen WV, Maniatis T, Sanes JR. Protocadherins mediate dendritic self-avoidance in the mammalian nervous system. Nature. 2012 Aug 23;488(7412):517-21.

81. Lanoue V, Usardi A, Sigoillot SM, et al. The adhesion-GPCR BAI3, a gene linked to psychiatric disorders, regulates dendrite morphogenesis in neurons. Molecular psychiatry. 2013 Aug;18(8):943-50.

82. Berry M, Bradley P. The growth of the dendritic trees of Purkinje cells in irradiated agranular cerebellar cortex. Brain research. 1976 Nov 12;116(3):361-87.

83. Baptista CA, Hatten ME, Blazeski R, Mason CA. Cell-cell interactions influence survival and differentiation of purified Purkinje cells in vitro. Neuron. 1994 Feb;12(2):243-60.

84. Hirai H, Launey T. The regulatory connection between the activity of granule cell NMDA receptors and dendritic differentiation of cerebellar Purkinje cells. The Journal of neuroscience : the official journal of the Society for Neuroscience. 2000 Jul 15;20(14):5217-24.

85. Schilling K, Dickinson MH, Connor JA, Morgan JI. Electrical activity in cerebellar cultures determines Purkinje cell dendritic growth patterns. Neuron. 1991 Dec;7(6):891-902.

86. Soha JM, Herrup K. Stunted morphologies of cerebellar Purkinje cells in lurcher and staggerer mice are cell-intrinsic effects of the mutant genes. The Journal of comparative neurology. 1995 Jun 19;357(1):65-75.

87. Becker EB, Oliver PL, Glitsch MD, et al. A point mutation in TRPC3 causes abnormal Purkinje cell development and cerebellar ataxia in moonwalker mice. Proceedings of the National Academy of Sciences of the United States of America. 2009 Apr 21;106(16):6706-11.

88. Sekerkova G, Kim JA, Nigro MJ, et al. Early onset of ataxia in moonwalker mice is accompanied by complete ablation of type II unipolar brush cells and Purkinje cell dysfunction. The Journal of neuroscience : the official journal of the Society for Neuroscience. 2013 Dec 11;33(50):19689-94.

89. Thach WT. Discharge of Purkinje and cerebellar nuclear neurons during rapidly alternating arm movements in the monkey. Journal of neurophysiology. 1968 Sep;31(5):785-97.

90. Loewenstein Y, Mahon S, Chadderton P, et al. Bistability of cerebellar Purkinje cells modulated by sensory stimulation. Nature neuroscience. 2005 Feb;8(2):202-11.

91. Schonewille M, Khosrovani S, Winkelman BH, et al. Purkinje cells in awake behaving animals operate at the upstate membrane potential. Nature neuroscience. 2006 Apr;9(4):459-61; author reply 61.

92. Walter JT, Khodakhah K. The advantages of linear information processing for cerebellar computation. Proceedings of the National Academy of Sciences of the United States of America. 2009 Mar 17;106(11):4471-6.

93. Person AL, Raman IM. Purkinje neuron synchrony elicits time-locked spiking in the cerebellar nuclei. Nature. 2011 Dec 25;481(7382):502-5.

94. Bean BP. The action potential in mammalian central neurons. Nature reviews Neuroscience. 2007 Jun;8(6):451-65.

95. Stuart G, Hausser M. Initiation and spread of sodium action potentials in cerebellar Purkinje cells. Neuron. 1994 Sep;13(3):703-12.

96. Raman IM, Bean BP. Ionic currents underlying spontaneous action potentials in isolated cerebellar Purkinje neurons. The Journal of neuroscience : the official journal of the Society for Neuroscience. 1999 Mar 01;19(5):1663-74.

97. Raman IM, Sprunger LK, Meisler MH, Bean BP. Altered subthreshold sodium currents and disrupted firing patterns in Purkinje neurons of Scn8a mutant mice. Neuron. 1997 Oct;19(4):881-91.

98. Kalume F, Yu FH, Westenbroek RE, Scheuer T, Catterall WA. Reduced sodium current in Purkinje neurons from Nav1.1 mutant mice: implications for ataxia in severe myoclonic epilepsy in infancy. The Journal of neuroscience : the official journal of the Society for Neuroscience. 2007 Oct 10;27(41):11065-74.

99. Martina M, Metz AE, Bean BP. Voltage-dependent potassium currents during fast spikes of rat cerebellar Purkinje neurons: inhibition by BDS-I toxin. Journal of neurophysiology. 2007 Jan;97(1):563-71.

100. Womack MD, Khodakhah K. Characterization of large conductance Ca2+-activated K+ channels in cerebellar Purkinje neurons. The European journal of neuroscience. 2002 Oct;16(7):1214-22.

101. Womack MD, Khodakhah K. Somatic and dendritic small-conductance calcium-activated potassium channels regulate the output of cerebellar Purkinje neurons. The Journal of neuroscience : the official journal of the Society for Neuroscience. 2003 Apr 01;23(7):2600-7.

102. Sailer CA, Kaufmann WA, Marksteiner J, Knaus HG. Comparative immunohistochemical distribution of three small-conductance Ca2+-activated potassium channel subunits, SK1, SK2, and SK3 in mouse brain. Molecular and cellular neurosciences. 2004 Jul;26(3):458-69.

103. Womack MD, Chevez C, Khodakhah K. Calcium-activated potassium channels are selectively coupled to P/Q-type calcium channels in cerebellar Purkinje neurons. The Journal of neuroscience : the official journal of the Society for Neuroscience. 2004 Oct 06;24(40):8818-22.

104. Chen X, Kovalchuk Y, Adelsberger H, et al. Disruption of the olivo-cerebellar circuit by Purkinje neuron-specific ablation of BK channels. Proceedings of the National Academy of Sciences of the United States of America. 2010 Jul 06;107(27):12323-8.

105. Walter JT, Alvina K, Womack MD, Chevez C, Khodakhah K. Decreases in the precision of Purkinje cell pacemaking cause cerebellar dysfunction and ataxia. Nature neuroscience. 2006 Mar;9(3):389-97.

106. Levin SI, Khaliq ZM, Aman TK, et al. Impaired motor function in mice with cell-specific knockout of sodium channel Scn8a (NaV1.6) in cerebellar purkinje neurons and granule cells. Journal of neurophysiology. 2006 Aug;96(2):785-93.

107. Hurlock EC, McMahon A, Joho RH. Purkinje-cell-restricted restoration of Kv3.3 function restores complex spikes and rescues motor coordination in Kcnc3 mutants. The Journal of neuroscience : the official journal of the Society for Neuroscience. 2008 Apr 30;28(18):4640-8.

108. Waters MF, Minassian NA, Stevanin G, et al. Mutations in voltage-gated potassium channel KCNC3 cause degenerative and developmental central nervous system phenotypes. Nature genetics. 2006 Apr;38(4):447-51.

109. Lee YC, Durr A, Majczenko K, et al. Mutations in KCND3 cause spinocerebellar ataxia type 22. Annals of neurology. 2012 Dec;72(6):859-69.

110. Duarri A, Jezierska J, Fokkens M, et al. Mutations in potassium channel kcnd3 cause spinocerebellar ataxia type 19. Annals of neurology. 2012 Dec;72(6):870-80.

111. Browne DL, Gancher ST, Nutt JG, et al. Episodic ataxia/myokymia syndrome is associated with point mutations in the human potassium channel gene, KCNA1. Nature genetics. 1994 Oct;8(2):136-40.

112. Ophoff RA, Terwindt GM, Vergouwe MN, et al. Familial hemiplegic migraine and episodic ataxia type-2 are caused by mutations in the Ca2+ channel gene CACNL1A4. Cell. 1996 Nov 01;87(3):543-52.

113. Catarino CB, Liu JY, Liagkouras I, et al. Dravet syndrome as epileptic encephalopathy: evidence from long-term course and neuropathology. Brain : a journal of neurology. 2011 Oct;134(Pt 10):2982-3010.

114. Hourez R, Servais L, Orduz D, et al. Aminopyridines correct early dysfunction and delay neurodegeneration in a mouse model of spinocerebellar ataxia type 1. The Journal of neuroscience : the official journal of the Society for Neuroscience. 2011 Aug 17;31(33):11795-807.

115. Kasumu AW, Hougaard C, Rode F, et al. Selective positive modulator of calcium-activated potassium channels exerts beneficial effects in a mouse model of spinocerebellar ataxia type 2. Chemistry & biology. 2012 Oct 26;19(10):1340-53.

116. Dell'Orco JM, Wasserman AH, Chopra R, et al. Neuronal Atrophy Early in Degenerative Ataxia Is a Compensatory Mechanism to Regulate Membrane Excitability. The Journal of neuroscience : the official journal of the Society for Neuroscience. 2015 Aug 12;35(32):11292-307.

117. Perkins EM, Clarkson YL, Sabatier N, et al. Loss of beta-III spectrin leads to Purkinje cell dysfunction recapitulating the behavior and neuropathology of spinocerebellar ataxia type 5 in humans. The Journal of neuroscience : the official journal of the Society for Neuroscience. 2010 Apr 07;30(14):4857-67.

118. Shakkottai VG, do Carmo Costa M, Dell'Orco JM, Sankaranarayanan A, Wulff H, Paulson HL. Early changes in cerebellar physiology accompany motor dysfunction in the polyglutamine disease spinocerebellar ataxia type 3. The Journal of neuroscience : the official journal of the Society for Neuroscience. 2011 Sep 07;31(36):13002-14.

119. Jayabal S, Chang HH, Cullen KE, Watt AJ. 4-aminopyridine reverses ataxia and cerebellar firing deficiency in a mouse model of spinocerebellar ataxia type 6. Scientific reports. 2016 Jul 06;6:29489.

120. Shakkottai VG, Xiao M, Xu L, et al. FGF14 regulates the intrinsic excitability of cerebellar Purkinje neurons. Neurobiology of disease. 2009 Jan;33(1):81-8.

121. Duarri A, Lin MC, Fokkens MR, et al. Spinocerebellar ataxia type 19/22 mutations alter heterocomplex Kv4.3 channel function and gating in a dominant manner. Cellular and molecular life sciences : CMLS. 2015 Sep;72(17):3387-99.

122. Zhang Y, Kaczmarek LK. Kv3.3 potassium channels and spinocerebellar ataxia. The Journal of physiology. 2016 Aug 15;594(16):4677-84.

123. Norris AJ, Nerbonne JM. Molecular dissection of I(A) in cortical pyramidal neurons reveals three distinct components encoded by Kv4.2, Kv4.3, and Kv1.4 alpha-subunits. The Journal of neuroscience : the official journal of the Society for Neuroscience. 2010 Apr 07;30(14):5092-101.

124. Lam YC, Bowman AB, Jafar-Nejad P, et al. ATAXIN-1 interacts with the repressor Capicua in its native complex to cause SCA1 neuropathology. Cell. 2006 Dec 29;127(7):1335-47.

125. Lai S, O'Callaghan B, Zoghbi HY, Orr HT. 14-3-3 Binding to ataxin-1(ATXN1) regulates its dephosphorylation at Ser-776 and transport to the nucleus. The Journal of biological chemistry. 2011 Oct 07;286(40):34606-16.

126. Napper RM, Harvey RJ. Number of parallel fiber synapses on an individual Purkinje cell in the cerebellum of the rat. The Journal of comparative neurology. 1988 Aug 08;274(2):168-77.

127. Jorntell H, Bengtsson F, Schonewille M, De Zeeuw CI. Cerebellar molecular layer interneurons - computational properties and roles in learning. Trends in neurosciences. 2010 Nov;33(11):524-32.

128. De Zeeuw CI, Hoogland TM. Reappraisal of Bergmann glial cells as modulators of cerebellar circuit function. Frontiers in cellular neuroscience. 2015;9:246.

129. Walter JT, Khodakhah K. The linear computational algorithm of cerebellar Purkinje cells. The Journal of neuroscience : the official journal of the Society for Neuroscience. 2006 Dec 13;26(50):12861-72.

130. Ichikawa R, Miyazaki T, Kano M, et al. Distal extension of climbing fiber territory and multiple innervation caused by aberrant wiring to adjacent spiny branchlets in cerebellar Purkinje cells lacking glutamate receptor delta 2. The Journal of neuroscience : the official journal of the Society for Neuroscience. 2002 Oct 01;22(19):8487-503.

131. Eccles JC, Llinas R, Sasaki K. The excitatory synaptic action of climbing fibres on the Purkinje cells of the cerebellum. The Journal of physiology. 1966 Jan;182(2):268-96.

132. Hansel C, Linden DJ, D'Angelo E. Beyond parallel fiber LTD: the diversity of synaptic and non-synaptic plasticity in the cerebellum. Nature neuroscience. 2001 May;4(5):467-75.

133. Barmack NH, Yakhnitsa V. Cerebellar climbing fibers modulate simple spikes in Purkinje cells. The Journal of neuroscience : the official journal of the Society for Neuroscience. 2003 Aug 27;23(21):7904-16.

134. Barnes JA, Ebner BA, Duvick LA, et al. Abnormalities in the climbing fiber-Purkinje cell circuitry contribute to neuronal dysfunction in ATXN1[82Q] mice. The Journal of neuroscience : the official journal of the Society for Neuroscience. 2011 Sep 07;31(36):12778-89.

135. Shuvaev AN, Hosoi N, Sato Y, Yanagihara D, Hirai H. Progressive impairment of cerebellar mGluR signalling and its therapeutic potential for cerebellar ataxia in spinocerebellar ataxia type 1 model mice. The Journal of physiology. 2016 Jul 21.

136. Power EM, Morales A, Empson RM. Prolonged Type 1 Metabotropic Glutamate Receptor Dependent Synaptic Signaling Contributes to Spino-Cerebellar Ataxia Type 1. The Journal of neuroscience : the official journal of the Society for Neuroscience. 2016 May 4;36(18):4910-6.

137. Custer SK, Garden GA, Gill N, et al. Bergmann glia expression of polyglutamine-expanded ataxin-7 produces neurodegeneration by impairing glutamate transport. Nature neuroscience. 2006 Oct;9(10):1302-11.

138. Perkins EM, Suminaite D, Clarkson YL, et al. Posterior cerebellar Purkinje cells in an SCA5/SPARCA1 mouse model are especially vulnerable to the synergistic effect of loss of beta-III spectrin and GLAST. Human molecular genetics. 2016 Aug 15.

139. Sjostrom PJ, Rancz EA, Roth A, Hausser M. Dendritic excitability and synaptic plasticity. Physiological reviews. 2008 Apr;88(2):769-840.

140. Shah MM, Hammond RS, Hoffman DA. Dendritic ion channel trafficking and plasticity. Trends in neurosciences. 2010 Jul;33(7):307-16.

141. Tonnesen J, Katona G, Rozsa B, Nagerl UV. Spine neck plasticity regulates compartmentalization of synapses. Nature neuroscience. 2014 May;17(5):678-85.

142. Waters J, Larkum M, Sakmann B, Helmchen F. Supralinear Ca2+ influx into dendritic tufts of layer 2/3 neocortical pyramidal neurons in vitro and in vivo. The Journal of neuroscience : the official journal of the Society for Neuroscience. 2003 Sep 17;23(24):8558-67.

143. Golding NL, Staff NP, Spruston N. Dendritic spikes as a mechanism for cooperative long-term potentiation. Nature. 2002 Jul 18;418(6895):326-31.

144. Callaway JC, Ross WN. Spatial distribution of synaptically activated sodium concentration changes in cerebellar Purkinje neurons. Journal of neurophysiology. 1997 Jan;77(1):145-52.

145. Jaeger D, De Schutter E, Bower JM. The role of synaptic and voltage-gated currents in the control of Purkinje cell spiking: a modeling study. The Journal of neuroscience : the official journal of the Society for Neuroscience. 1997 Jan 01;17(1):91-106.

146. Jelitai M, Puggioni P, Ishikawa T, Rinaldi A, Duguid I. Dendritic excitation-inhibition balance shapes cerebellar output during motor behaviour. Nature communications. 2016 Dec 15;7:13722.

147. Llinas R, Hess R. Tetrodotoxin-resistant dendritic spikes in avian Purkinje cells. Proceedings of the National Academy of Sciences of the United States of America. 1976 Jul;73(7):2520-3.

148. Davie JT, Clark BA, Hausser M. The origin of the complex spike in cerebellar Purkinje cells. The Journal of neuroscience : the official journal of the Society for Neuroscience. 2008 Jul 23;28(30):7599-609.

149. Rancz EA, Hausser M. Dendritic calcium spikes are tunable triggers of cannabinoid release and short-term synaptic plasticity in cerebellar Purkinje neurons. The Journal of neuroscience : the official journal of the Society for Neuroscience. 2006 May 17;26(20):5428-37.

150. Otsu Y, Marcaggi P, Feltz A, et al. Activity-dependent gating of calcium spikes by A-type K+ channels controls climbing fiber signaling in Purkinje cell dendrites. Neuron. 2014 Oct 01;84(1):137-51.

151. Martina M, Yao GL, Bean BP. Properties and functional role of voltage-dependent potassium channels in dendrites of rat cerebellar Purkinje neurons. The Journal of neuroscience : the official journal of the Society for Neuroscience. 2003 Jul 02;23(13):5698-707.

152. Zagha E, Manita S, Ross WN, Rudy B. Dendritic Kv3.3 potassium channels in cerebellar purkinje cells regulate generation and spatial dynamics of dendritic Ca2+ spikes. Journal of neurophysiology. 2010 Jun;103(6):3516-25.

153. Hosy E, Piochon C, Teuling E, Rinaldo L, Hansel C. SK2 channel expression and function in cerebellar Purkinje cells. The Journal of physiology. 2011 Jul 15;589(Pt 14):3433-40.

154. Rancz EA, Hausser M. Dendritic spikes mediate negative synaptic gain control in cerebellar Purkinje cells. Proceedings of the National Academy of Sciences of the United States of America. 2010 Dec 21;107(51):22284-9.

155. Fernandez-Alacid L, Aguado C, Ciruela F, et al. Subcellular compartment-specific molecular diversity of pre- and post-synaptic GABA-activated GIRK channels in Purkinje cells. Journal of neurochemistry. 2009 Aug;110(4):1363-76.

156. Kanjhan R, Anselme AM, Noakes PG, Bellingham MC. Postnatal changes in TASK-1 and TREK-1 expression in rat brain stem and cerebellum. Neuroreport. 2004 Jun 07;15(8):1321-4.

157. Kanamori T, Kanai MI, Dairyo Y, Yasunaga K, Morikawa RK, Emoto K. Compartmentalized calcium transients trigger dendrite pruning in Drosophila sensory neurons. Science. 2013 Jun 21;340(6139):1475-8.

158. Alvina K, Khodakhah K. KCa channels as therapeutic targets in episodic ataxia type-2. The Journal of neuroscience : the official journal of the Society for Neuroscience. 2010 May 26;30(21):7249-57.

159. Hall AM, Throesch BT, Buckingham SC, et al. Tau-dependent Kv4.2 depletion and dendritic hyperexcitability in a mouse model of Alzheimer's disease. The Journal of neuroscience : the official journal of the Society for Neuroscience. 2015 Apr 15;35(15):6221-30.

160. Siskova Z, Justus D, Kaneko H, et al. Dendritic structural degeneration is functionally linked to cellular hyperexcitability in a mouse model of Alzheimer's disease. Neuron. 2014 Dec 3;84(5):1023-33.

161. LaHoste GJ, Yu J, Marshall JF. Striatal Fos expression is indicative of dopamine D1/D2 synergism and receptor supersensitivity. Proceedings of the National Academy of Sciences of the United States of America. 1993 Aug 15;90(16):7451-5.

162. Day M, Wang Z, Ding J, et al. Selective elimination of glutamatergic synapses on striatopallidal neurons in Parkinson disease models. Nature neuroscience. 2006 Feb;9(2):251-9.

163. Day M, Wokosin D, Plotkin JL, Tian X, Surmeier DJ. Differential excitability and modulation of striatal medium spiny neuron dendrites. The Journal of neuroscience : the official journal of the Society for Neuroscience. 2008 Nov 05;28(45):11603-14.

164. Dryanovski DI, Guzman JN, Xie Z, et al. Calcium entry and alpha-synuclein inclusions elevate dendritic mitochondrial oxidant stress in dopaminergic neurons. The Journal of neuroscience : the official journal of the Society for Neuroscience. 2013 Jun 12;33(24):10154-64.

165. Goldberg JA, Guzman JN, Estep CM, et al. Calcium entry induces mitochondrial oxidant stress in vagal neurons at risk in Parkinson's disease. Nature neuroscience. 2012 Oct;15(10):1414-21.

166. Sanchez-Padilla J, Guzman JN, Ilijic E, et al. Mitochondrial oxidant stress in locus coeruleus is regulated by activity and nitric oxide synthase. Nature neuroscience. 2014 Jun;17(6):832-40.

167. Surmeier DJ, Guzman JN, Sanchez-Padilla J, Goldberg JA. The origins of oxidant stress in Parkinson's disease and therapeutic strategies. Antioxidants & redox signaling. 2011 Apr 01;14(7):1289-301.

168. Gaudilliere B, Konishi Y, de la Iglesia N, Yao G, Bonni A. A CaMKII-NeuroD signaling pathway specifies dendritic morphogenesis. Neuron. 2004 Jan 22;41(2):229-41.

169. Wu JI, Lessard J, Olave IA, et al. Regulation of dendritic development by neuron-specific chromatin remodeling complexes. Neuron. 2007 Oct 04;56(1):94-108.

170. Koleske AJ. Molecular mechanisms of dendrite stability. Nature reviews Neuroscience. 2013 Aug;14(8):536-50.

171. Korobova F, Svitkina T. Molecular architecture of synaptic actin cytoskeleton in hippocampal neurons reveals a mechanism of dendritic spine morphogenesis. Molecular biology of the cell. 2010 Jan 01;21(1):165-76.

172. Sternberger LA, Sternberger NH. Monoclonal antibodies distinguish phosphorylated and nonphosphorylated forms of neurofilaments in situ. Proceedings of the National Academy of Sciences of the United States of America. 1983 Oct;80(19):6126-30.

173. Rochlin MW, Dailey ME, Bridgman PC. Polymerizing microtubules activate site-directed F-actin assembly in nerve growth cones. Molecular biology of the cell. 1999 Jul;10(7):2309-27.

174. Lafont F, Rouget M, Rousselet A, Valenza C, Prochiantz A. Specific responses of axons and dendrites to cytoskeleton perturbations: an in vitro study. Journal of cell science. 1993 Feb;104 (Pt 2):433-43.

175. Ikegaya Y, Kim JA, Baba M, Iwatsubo T, Nishiyama N, Matsuki N. Rapid and reversible changes in dendrite morphology and synaptic efficacy following NMDA receptor activation: implication for a cellular defense against excitotoxicity. Journal of cell science. 2001 Nov;114(Pt 22):4083-93.

176. Kong J, Tung VW, Aghajanian J, Xu Z. Antagonistic roles of neurofilament subunits NF-H and NF-M against NF-L in shaping dendritic arborization in spinal motor neurons. The Journal of cell biology. 1998 Mar 09;140(5):1167-76.

177. Georges PC, Hadzimichalis NM, Sweet ES, Firestein BL. The yin-yang of dendrite morphology: unity of actin and microtubules. Molecular neurobiology. 2008 Dec;38(3):270-84.

178. Albertinazzi C, Gilardelli D, Paris S, Longhi R, de Curtis I. Overexpression of a neural-specific rho family GTPase, cRac1B, selectively induces enhanced neuritogenesis and neurite branching in primary neurons. The Journal of cell biology. 1998 Aug 10;142(3):815-25.

179. O'Kane EM, Stone TW, Morris BJ. Distribution of Rho family GTPases in the adult rat hippocampus and cerebellum. Brain research Molecular brain research. 2003 May 26;114(1):1-8.

180. Donald S, Humby T, Fyfe I, et al. P-Rex2 regulates Purkinje cell dendrite morphology and motor coordination. Proceedings of the National Academy of Sciences of the United States of America. 2008 Mar 18;105(11):4483-8.

181. Ohkawa N, Fujitani K, Tokunaga E, Furuya S, Inokuchi K. The microtubule destabilizer stathmin mediates the development of dendritic arbors in neuronal cells. Journal of cell science. 2007 Apr 15;120(Pt 8):1447-56.

182. Metzger F, Kapfhammer JP. Protein kinase C activity modulates dendritic differentiation of rat Purkinje cells in cerebellar slice cultures. The European journal of neuroscience. 2000 Jun;12(6):1993-2005.

183. Gugger OS, Hartmann J, Birnbaumer L, Kapfhammer JP. P/Q-type and T-type calcium channels, but not type 3 transient receptor potential cation channels, are involved in inhibition of dendritic growth after chronic metabotropic glutamate receptor type 1 and protein kinase C activation in cerebellar Purkinje cells. The European journal of neuroscience. 2012 Jan;35(1):20-33.

184. Calabrese B, Halpain S. Essential role for the PKC target MARCKS in maintaining dendritic spine morphology. Neuron. 2005 Oct 06;48(1):77-90.

185. Adachi N, Kobayashi T, Takahashi H, et al. Enzymological analysis of mutant protein kinase Cgamma causing spinocerebellar ataxia type 14 and dysfunction in Ca2+ homeostasis. The Journal of biological chemistry. 2008 Jul 11;283(28):19854-63.

186. Chen DH, Raskind WH, Bird TD. Spinocerebellar ataxia type 14. Handbook of clinical neurology. 2012;103:555-9.

187. Hubener J, Weber JJ, Richter C, et al. Calpain-mediated ataxin-3 cleavage in the molecular pathogenesis of spinocerebellar ataxia type 3 (SCA3). Human molecular genetics. 2013 Feb 01;22(3):508-18.

188. Koch P, Breuer P, Peitz M, et al. Excitation-induced ataxin-3 aggregation in neurons from patients with Machado-Joseph disease. Nature. 2011 Nov 23;480(7378):543-6.

189. Stankewich MC, Gwynn B, Ardito T, et al. Targeted deletion of betaIII spectrin impairs synaptogenesis and generates ataxic and seizure phenotypes. Proceedings of the National Academy of Sciences of the United States of America. 2010 Mar 30;107(13):6022-7.

190. Watase K, Gatchel JR, Sun Y, et al. Lithium therapy improves neurological function and hippocampal dendritic arborization in a spinocerebellar ataxia type 1 mouse model. PLoS medicine. 2007 May;4(5):e182.

191. Tolias KF, Duman JG, Um K. Control of synapse development and plasticity by Rho GTPase regulatory proteins. Progress in neurobiology. 2011 Jul;94(2):133-48.

192. Ishikawa Y, Katoh H, Negishi M. Small GTPase Rnd1 is involved in neuronal activity-dependent dendritic development in hippocampal neurons. Neuroscience letters. 2006 Jun 12;400(3):218-23.

193. Valdez CM, Murphy GG, Beg AA. The Rac-GAP alpha2-chimaerin regulates hippocampal dendrite and spine morphogenesis. Molecular and cellular neurosciences. 2016 Sep;75:14-26.

194. Iyer SC, Wang D, Iyer EP, et al. The RhoGEF trio functions in sculpting class specific dendrite morphogenesis in Drosophila sensory neurons. PloS one. 2012;7(3):e33634.

195. Rosario M, Schuster S, Juttner R, Parthasarathy S, Tarabykin V, Birchmeier W. Neocortical dendritic complexity is controlled during development by NOMA-GAP-dependent inhibition of Cdc42 and activation of cofilin. Genes & development. 2012 Aug 01;26(15):1743-57.

196. Hayashi K, Ohshima T, Mikoshiba K. Pak1 is involved in dendrite initiation as a downstream effector of Rac1 in cortical neurons. Molecular and cellular neurosciences. 2002 Aug;20(4):579-94.

197. You JJ, Lin-Chao S. Gas7 functions with N-WASP to regulate the neurite outgrowth of hippocampal neurons. The Journal of biological chemistry. 2010 Apr 09;285(15):11652-66.

198. Pilpel Y, Segal M. Activation of PKC induces rapid morphological plasticity in dendrites of hippocampal neurons via Rac and Rho-dependent mechanisms. The European journal of neuroscience. 2004 Jun;19(12):3151-64.

199. Matsuoka Y, Li X, Bennett V. Adducin is an in vivo substrate for protein kinase C: phosphorylation in the MARCKS-related domain inhibits activity in promoting spectrin-actin complexes and occurs in many cells, including dendritic spines of neurons. The Journal of cell biology. 1998 Jul 27;142(2):485-97.

200. Rocca DL, Martin S, Jenkins EL, Hanley JG. Inhibition of Arp2/3-mediated actin polymerization by PICK1 regulates neuronal morphology and AMPA receptor endocytosis. Nature cell biology. 2008 Mar;10(3):259-71.

201. Ahuja R, Pinyol R, Reichenbach N, et al. Cordon-bleu is an actin nucleation factor and controls neuronal morphology. Cell. 2007 Oct 19;131(2):337-50.

202. Hou W, Izadi M, Nemitz S, Haag N, Kessels MM, Qualmann B. The Actin Nucleator Cobl Is Controlled by Calcium and Calmodulin. PLoS biology. 2015;13(9):e1002233.

203. Li Z, Jo J, Jia JM, et al. Caspase-3 activation via mitochondria is required for long-term depression and AMPA receptor internalization. Cell. 2010 May 28;141(5):859-71.

204. Erturk A, Wang Y, Sheng M. Local pruning of dendrites and spines by caspase-3-dependent and proteasome-limited mechanisms. The Journal of neuroscience : the official journal of the Society for Neuroscience. 2014 Jan 29;34(5):1672-88.

205. Amini M, Ma CL, Farazifard R, et al. Conditional disruption of calpain in the CNS alters dendrite morphology, impairs LTP, and promotes neuronal survival following injury. The Journal of neuroscience : the official journal of the Society for Neuroscience. 2013 Mar 27;33(13):5773-84.

206. Faddis BT, Hasbani MJ, Goldberg MP. Calpain activation contributes to dendritic remodeling after brief excitotoxic injury in vitro. The Journal of neuroscience : the official journal of the Society for Neuroscience. 1997 Feb 01;17(3):951-9.

207. Wilson MT, Kisaalita WS, Keith CH. Glutamate-induced changes in the pattern of hippocampal dendrite outgrowth: a role for calcium-dependent pathways and the microtubule cytoskeleton. Journal of neurobiology. 2000 May;43(2):159-72.

208. Tan M, Ma S, Huang Q, Hu K, Song B, Li M. GSK-3alpha/beta-mediated phosphorylation of CRMP-2 regulates activity-dependent dendritic growth. Journal of neurochemistry. 2013 Jun;125(5):685-97.

209. Szebenyi G, Bollati F, Bisbal M, et al. Activity-driven dendritic remodeling requires microtubule-associated protein 1A. Current biology : CB. 2005 Oct 25;15(20):1820-6.

210. Harada A, Teng J, Takei Y, Oguchi K, Hirokawa N. MAP2 is required for dendrite elongation, PKA anchoring in dendrites, and proper PKA signal transduction. The Journal of cell biology. 2002 Aug 05;158(3):541-9.

211. Farnsworth CL, Freshney NW, Rosen LB, Ghosh A, Greenberg ME, Feig LA. Calcium activation of Ras mediated by neuronal exchange factor Ras-GRF. Nature. 1995 Aug 10;376(6540):524-7.

212. Zhou Y, Wong CO, Cho KJ, et al. SIGNAL TRANSDUCTION. Membrane potential modulates plasma membrane phospholipid dynamics and K-Ras signaling. Science. 2015 Aug 21;349(6250):873-6.

213. Wu GY, Deisseroth K, Tsien RW. Spaced stimuli stabilize MAPK pathway activation and its effects on dendritic morphology. Nature neuroscience. 2001 Feb;4(2):151-8.

214. Komulainen E, Zdrojewska J, Freemantle E, et al. JNK1 controls dendritic field size in L2/3 and L5 of the motor cortex, constrains soma size, and influences fine motor coordination. Frontiers in cellular neuroscience. 2014;8:272.

215. Akum BF, Chen M, Gunderson SI, Riefler GM, Scerri-Hansen MM, Firestein BL. Cypin regulates dendrite patterning in hippocampal neurons by promoting microtubule assembly. Nature neuroscience. 2004 Feb;7(2):145-52.

216. Kim AH, Puram SV, Bilimoria PM, et al. A centrosomal Cdc20-APC pathway controls dendrite morphogenesis in postmitotic neurons. Cell. 2009 Jan 23;136(2):322-36.

217. Puram SV, Kim AH, Ikeuchi Y, et al. A CaMKIIbeta signaling pathway at the centrosome regulates dendrite patterning in the brain. Nature neuroscience. 2011 Jul 03;14(8):973-83.

218. Puram SV, Riccio A, Koirala S, et al. A TRPC5-regulated calcium signaling pathway controls dendrite patterning in the mammalian brain. Genes & development. 2011 Dec 15;25(24):2659-73.

219. Wayman GA, Impey S, Marks D, et al. Activity-dependent dendritic arborization mediated by CaM-kinase I activation and enhanced CREB-dependent transcription of Wnt-2. Neuron. 2006 Jun 15;50(6):897-909.

220. Ghiretti AE, Kenny K, Marr MT, 2nd, Paradis S. CaMKII-dependent phosphorylation of the GTPase Rem2 is required to restrict dendritic complexity. The Journal of neuroscience : the official journal of the Society for Neuroscience. 2013 Apr 10;33(15):6504-15.

221. Halpain S, Greengard P. Activation of NMDA receptors induces rapid dephosphorylation of the cytoskeletal protein MAP2. Neuron. 1990 Sep;5(3):237-46.

222. Quinlan EM, Halpain S. Emergence of activity-dependent, bidirectional control of microtubule-associated protein MAP2 phosphorylation during postnatal development. The Journal of neuroscience : the official journal of the Society for Neuroscience. 1996 Dec 01;16(23):7627-37.

223. Penzes P, Cahill ME, Jones KA, Srivastava DP. Convergent CaMK and RacGEF signals control dendritic structure and function. Trends in cell biology. 2008 Sep;18(9):405-13.

224. De Zeeuw CI, Hansel C, Bian F, et al. Expression of a protein kinase C inhibitor in Purkinje cells blocks cerebellar LTD and adaptation of the vestibulo-ocular reflex. Neuron. 1998 Mar;20(3):495-508.

225. Llano I, Marty A, Armstrong CM, Konnerth A. Synaptic- and agonist-induced excitatory currents of Purkinje cells in rat cerebellar slices. The Journal of physiology. 1991 Mar;434:183-213.

226. Althaus AL, Sagher O, Parent JM, Murphy GG. Intrinsic neurophysiological properties of hilar ectopic and normotopic dentate granule cells in human temporal lobe epilepsy and a rat model. Journal of neurophysiology. 2015 Feb 15;113(4):1184-94.

227. Sholl DA. Dendritic organization in the neurons of the visual and motor cortices of the cat. Journal of anatomy. 1953 Oct;87(4):387-406.

228. Livak KJ, Schmittgen TD. Analysis of relative gene expression data using real-time quantitative PCR and the 2(-Delta Delta C(T)) Method. Methods. 2001 Dec;25(4):402-8.

229. Keiser MS, Monteys AM, Corbau R, Gonzalez-Alegre P, Davidson BL. RNAi prevents and reverses phenotypes induced by mutant human ataxin-1. Annals of neurology. 2016 Sep 30.

230. Zhang Z, Larner SF, Liu MC, Zheng W, Hayes RL, Wang KK. Multiple alphaII-spectrin breakdown products distinguish calpain and caspase dominated necrotic and apoptotic cell death

pathways. Apoptosis : an international journal on programmed cell death. 2009 Nov;14(11):1289-98.

231. Zoghbi HY, Orr HT. Pathogenic mechanisms of a polyglutamine-mediated neurodegenerative disease, spinocerebellar ataxia type 1. The Journal of biological chemistry. 2009 Mar 20;284(12):7425-9.

232. Chung MY, Ranum LP, Duvick LA, Servadio A, Zoghbi HY, Orr HT. Evidence for a mechanism predisposing to intergenerational CAG repeat instability in spinocerebellar ataxia type I. Nature genetics. 1993 Nov;5(3):254-8.

233. Ranum LP, Chung MY, Banfi S, et al. Molecular and clinical correlations in spinocerebellar ataxia type I: evidence for familial effects on the age at onset. American journal of human genetics. 1994 Aug;55(2):244-52.

234. Rub U, Burk K, Timmann D, et al. Spinocerebellar ataxia type 1 (SCA1): new pathoanatomical and clinico-pathological insights. Neuropathology and applied neurobiology. 2012 Dec;38(7):665-80.

235. Servadio A, Koshy B, Armstrong D, Antalffy B, Orr HT, Zoghbi HY. Expression analysis of the ataxin-1 protein in tissues from normal and spinocerebellar ataxia type 1 individuals. Nature genetics. 1995 May;10(1):94-8.

236. Serra HG, Duvick L, Zu T, et al. RORalpha-mediated Purkinje cell development determines disease severity in adult SCA1 mice. Cell. 2006 Nov 17;127(4):697-708.

237. Ohtsuki G, Piochon C, Adelman JP, Hansel C. SK2 channel modulation contributes to compartment-specific dendritic plasticity in cerebellar Purkinje cells. Neuron. 2012 Jul 12;75(1):108-20.

238. Crespo-Barreto J, Fryer JD, Shaw CA, Orr HT, Zoghbi HY. Partial loss of ataxin-1 function contributes to transcriptional dysregulation in spinocerebellar ataxia type 1 pathogenesis. PLoS genetics. 2010 Jul 08;6(7):e1001021.

239. Ingram M, Wozniak EA, Duvick L, et al. Cerebellar Transcriptome Profiles of ATXN1 Transgenic Mice Reveal SCA1 Disease Progression and Protection Pathways. Neuron. 2016 Mar 16;89(6):1194-207.

240. Klement IA, Skinner PJ, Kaytor MD, et al. Ataxin-1 nuclear localization and aggregation: role in polyglutamine-induced disease in SCA1 transgenic mice. Cell. 1998 Oct 02;95(1):41-53.

241. Engbers JD, Anderson D, Asmara H, et al. Intermediate conductance calcium-activated potassium channels modulate summation of parallel fiber input in cerebellar Purkinje cells. Proceedings of the National Academy of Sciences of the United States of America. 2012 Feb 14;109(7):2601-6.

242. Indriati DW, Kamasawa N, Matsui K, Meredith AL, Watanabe M, Shigemoto R. Quantitative localization of Cav2.1 (P/Q-type) voltage-dependent calcium channels in Purkinje cells: somatodendritic gradient and distinct somatic coclustering with calcium-activated potassium channels. The Journal of neuroscience : the official journal of the Society for Neuroscience. 2013 Feb 20;33(8):3668-78.

243. Fierro L, Llano I. High endogenous calcium buffering in Purkinje cells from rat cerebellar slices. The Journal of physiology. 1996 Nov 01;496 (Pt 3):617-25.

244. Lev-Ram V, Miyakawa H, Lasser-Ross N, Ross WN. Calcium transients in cerebellar Purkinje neurons evoked by intracellular stimulation. Journal of neurophysiology. 1992 Oct;68(4):1167-77.

245. Kitamura K, Hausser M. Dendritic calcium signaling triggered by spontaneous and sensory-evoked climbing fiber input to cerebellar Purkinje cells in vivo. The Journal of neuroscience : the official journal of the Society for Neuroscience. 2011 Jul 27;31(30):10847-58.

246. Miyakawa H, Lev-Ram V, Lasser-Ross N, Ross WN. Calcium transients evoked by climbing fiber and parallel fiber synaptic inputs in guinea pig cerebellar Purkinje neurons. Journal of neurophysiology. 1992 Oct;68(4):1178-89.

247. Hartmann J, Dragicevic E, Adelsberger H, et al. TRPC3 channels are required for synaptic transmission and motor coordination. Neuron. 2008 Aug 14;59(3):392-8.

248. Hartmann J, Henning HA, Konnerth A. mGluR1/TRPC3-mediated Synaptic Transmission and Calcium Signaling in Mammalian Central Neurons. Cold Spring Harbor perspectives in biology. 2011 Apr 01;3(4).

249. Dzubay JA, Otis TS. Climbing fiber activation of metabotropic glutamate receptors on cerebellar purkinje neurons. Neuron. 2002 Dec 19;36(6):1159-67.

250. Tempia F, Kano M, Schneggenburger R, et al. Fractional calcium current through neuronal AMPA-receptor channels with a low calcium permeability. The Journal of neuroscience : the official journal of the Society for Neuroscience. 1996 Jan 15;16(2):456-66.

251. Masu M, Tanabe Y, Tsuchida K, Shigemoto R, Nakanishi S. Sequence and expression of a metabotropic glutamate receptor. Nature. 1991 Feb 28;349(6312):760-5.

252. Takechi H, Eilers J, Konnerth A. A new class of synaptic response involving calcium release in dendritic spines. Nature. 1998 Dec 24-31;396(6713):757-60.

253. Henning HA. Synaptic signaling by mGluR1 and TRPC3 in spiny dendrites of cerebellar Purkinje cells. 71: Technical University Munich, Munich, Germany; 2011.

254. Canepari M, Ogden D. Evidence for protein tyrosine phosphatase, tyrosine kinase, and G-protein regulation of the parallel fiber metabotropic slow EPSC of rat cerebellar Purkinje neurons. The Journal of neuroscience : the official journal of the Society for Neuroscience. 2003 May 15;23(10):4066-71.

255. Weaver AK, Olsen ML, McFerrin MB, Sontheimer H. BK channels are linked to inositol 1,4,5-triphosphate receptors via lipid rafts: a novel mechanism for coupling [Ca(2+)](i) to ion channel activation. The Journal of biological chemistry. 2007 Oct 26;282(43):31558-68.

256. Senadheera S, Kim Y, Grayson TH, et al. Transient receptor potential canonical type 3 channels facilitate endothelium-derived hyperpolarization-mediated resistance artery vasodilator activity. Cardiovascular research. 2012 Sep 01;95(4):439-47.

257. Sharp AH, Nucifora FC, Jr., Blondel O, et al. Differential cellular expression of isoforms of inositol 1,4,5-triphosphate receptors in neurons and glia in brain. The Journal of comparative neurology. 1999 Apr 05;406(2):207-20.

258. Lin X, Antalffy B, Kang D, Orr HT, Zoghbi HY. Polyglutamine expansion down-regulates specific neuronal genes before pathologic changes in SCA1. Nature neuroscience. 2000 Feb;3(2):157-63.

259. Takigawa T, Alzheimer C. G protein-activated inwardly rectifying K+ (GIRK) currents in dendrites of rat neocortical pyramidal cells. The Journal of physiology. 1999 Jun 1;517 (Pt 2):385-90.

260. Tabata T, Haruki S, Nakayama H, Kano M. GABAergic activation of an inwardly rectifying K+ current in mouse cerebellar Purkinje cells. The Journal of physiology. 2005 Mar 1;563(Pt 2):443-57.

261. Tabata T, Kano M. GABA(B) receptor-mediated modulation of glutamate signaling in cerebellar Purkinje cells. Cerebellum. 2006;5(2):127-33.

262. Lai HC, Jan LY. The distribution and targeting of neuronal voltage-gated ion channels. Nature reviews Neuroscience. 2006 Jul;7(7):548-62.

263. Kim J, Jung SC, Clemens AM, Petralia RS, Hoffman DA. Regulation of dendritic excitability by activity-dependent trafficking of the A-type K+ channel subunit Kv4.2 in hippocampal neurons. Neuron. 2007 Jun 21;54(6):933-47.

264. Shen W, Tian X, Day M, et al. Cholinergic modulation of Kir2 channels selectively elevates dendritic excitability in striatopallidal neurons. Nature neuroscience. 2007 Nov;10(11):1458-66.

265. Shuvaev AN, Horiuchi H, Seki T, et al. Mutant PKCgamma in spinocerebellar ataxia type 14 disrupts synapse elimination and long-term depression in Purkinje cells in vivo. The Journal of neuroscience : the official journal of the Society for Neuroscience. 2011 Oct 5;31(40):14324-34.

266. Price LS, Langeslag M, ten Klooster JP, Hordijk PL, Jalink K, Collard JG. Calcium signaling regulates translocation and activation of Rac. The Journal of biological chemistry. 2003 Oct 10;278(41):39413-21.

267. Rossner S, Mehlhorn G, Schliebs R, Bigl V. Increased neuronal and glial expression of protein kinase C isoforms in neocortex of transgenic Tg2576 mice with amyloid pathology. European Journal of Neuroscience. 2001 Jan;13(2):269-78.

268. Rosse C, Linch M, Kermorgant S, Cameron AJ, Boeckeler K, Parker PJ. PKC and the control of localized signal dynamics. Nature reviews Molecular cell biology. 2010 Feb;11(2):103-12.

269. Barmack NH, Qian Z, Yoshimura J. Regional and cellular distribution of protein kinase C in rat cerebellar Purkinje cells. The Journal of comparative neurology. 2000 Nov 13;427(2):235-54.

270. Goto MM, Romero GG, Balaban CD. Transient changes in flocculonodular lobe protein kinase C expression during vestibular compensation. The Journal of neuroscience : the official journal of the Society for Neuroscience. 1997 Jun 1;17(11):4367-81.

271. Hoebeek FE, Stahl JS, van Alphen AM, et al. Increased noise level of purkinje cell activities minimizes impact of their modulation during sensorimotor control. Neuron. 2005 Mar 24;45(6):953-65.

272. Desai R, Kronengold J, Mei J, Forman SA, Kaczmarek LK. Protein kinase C modulates inactivation of Kv3.3 channels. The Journal of biological chemistry. 2008 Aug 8;283(32):22283-94.

273. Mao J, Wang X, Chen F, et al. Molecular basis for the inhibition of G protein-coupled inward rectifier K(+) channels by protein kinase C. Proceedings of the National Academy of Sciences of the United States of America. 2004 Jan 27;101(4):1087-92.

274. Williams AD, Jung S, Poolos NP. Protein kinase C bidirectionally modulates Ih and hyperpolarization-activated cyclic nucleotide-gated (HCN) channel surface expression in hippocampal pyramidal neurons. The Journal of physiology. 2015 Jul 1;593(13):2779-92.

275. Trebak M, Hempel N, Wedel BJ, Smyth JT, Bird GS, Putney JW, Jr. Negative regulation of TRPC3 channels by protein kinase C-mediated phosphorylation of serine 712. Molecular pharmacology. 2005 Feb;67(2):558-63.

276. Gao Z, Todorov B, Barrett CF, et al. Cerebellar ataxia by enhanced Ca(V)2.1 currents is alleviated by Ca2+-dependent K+-channel activators in Cacna1a(S218L) mutant mice. The

Journal of neuroscience : the official journal of the Society for Neuroscience. 2012 Oct 31;32(44):15533-46.

277. Park JY, Kang HW, Moon HJ, et al. Activation of protein kinase C augments T-type Ca2+ channel activity without changing channel surface density. The Journal of physiology. 2006 Dec 01;577(Pt 2):513-23.

278. Khavandgar S, Walter JT, Sageser K, Khodakhah K. Kv1 channels selectively prevent dendritic hyperexcitability in rat Purkinje cells. The Journal of physiology. 2005 Dec 1;569(Pt 2):545-57.

279. Caino MC, von Burstin VA, Lopez-Haber C, Kazanietz MG. Differential regulation of gene expression by protein kinase C isozymes as determined by genome-wide expression analysis. The Journal of biological chemistry. 2011 Apr 01;286(13):11254-64.

280. Santi CM, Ferreira G, Yang B, et al. Opposite regulation of Slick and Slack K+ channels by neuromodulators. The Journal of neuroscience : the official journal of the Society for Neuroscience. 2006 May 10;26(19):5059-68.

281. Barcia G, Fleming MR, Deligniere A, et al. De novo gain-of-function KCNT1 channel mutations cause malignant migrating partial seizures of infancy. Nature genetics. 2012 Nov;44(11):1255-9.

282. Leitges M, Kovac J, Plomann M, Linden DJ. A unique PDZ ligand in PKCalpha confers induction of cerebellar long-term synaptic depression. Neuron. 2004 Nov 18;44(4):585-94.

283. Kano M, Hashimoto K, Tabata T. Type-1 metabotropic glutamate receptor in cerebellar Purkinje cells: a key molecule responsible for long-term depression, endocannabinoid signalling and synapse elimination. Philosophical transactions of the Royal Society of London Series B, Biological sciences. 2008 Jun 27;363(1500):2173-86.

284. Kunkel MT, Newton AC. Calcium transduces plasma membrane receptor signals to produce diacylglycerol at Golgi membranes. The Journal of biological chemistry. 2010 Jul 23;285(30):22748-52.

285. Nishikawa K, Toker A, Johannes FJ, Songyang Z, Cantley LC. Determination of the specific substrate sequence motifs of protein kinase C isozymes. The Journal of biological chemistry. 1997 Jan 10;272(2):952-60.

286. Gundlfinger A, Kapfhammer JP, Kruse F, Leitges M, Metzger F. Different regulation of Purkinje cell dendritic development in cerebellar slice cultures by protein kinase Calpha and -beta. Journal of neurobiology. 2003 Oct;57(1):95-109.

287. Klockgether T. Sporadic ataxia with adult onset: classification and diagnostic criteria. The Lancet Neurology. 2010 Jan;9(1):94-104.

288. Kemp KC, Cook AJ, Redondo J, Kurian KM, Scolding NJ, Wilkins A. Purkinje cell injury, structural plasticity and fusion in patients with Friedreich's ataxia. Acta neuropathologica communications. 2016 May 23;4(1):53.

289. Lim J, Hao T, Shaw C, et al. A protein-protein interaction network for human inherited ataxias and disorders of Purkinje cell degeneration. Cell. 2006 May 19;125(4):801-14.

290. Bettencourt C, Ryten M, Forabosco P, et al. Insights from cerebellar transcriptomic analysis into the pathogenesis of ataxia. JAMA neurology. 2014 Jul 01;71(7):831-9.

291. Pulst SM, Nechiporuk A, Nechiporuk T, et al. Moderate expansion of a normally biallelic trinucleotide repeat in spinocerebellar ataxia type 2. Nature genetics. 1996 Nov;14(3):269-76.

292. Geschwind DH, Perlman S, Figueroa CP, Treiman LJ, Pulst SM. The prevalence and wide clinical spectrum of the spinocerebellar ataxia type 2 trinucleotide repeat in patients with

autosomal dominant cerebellar ataxia. American journal of human genetics. 1997 Apr;60(4):842-50.

293. Al-Ramahi I, Perez AM, Lim J, et al. dAtaxin-2 mediates expanded Ataxin-1-induced neurodegeneration in a Drosophila model of SCA1. PLoS genetics. 2007 Dec 28;3(12):e234.

294. Fanciulli A, Wenning GK. Multiple-system atrophy. The New England journal of medicine. 2015 Apr 02;372(14):1375-6.

295. Wenning GK, Stefanova N, Jellinger KA, Poewe W, Schlossmacher MG. Multiple system atrophy: a primary oligodendrogliopathy. Annals of neurology. 2008 Sep;64(3):239-46.

296. Yoshida M. Multiple system atrophy: alpha-synuclein and neuronal degeneration. Neuropathology : official journal of the Japanese Society of Neuropathology. 2007 Oct;27(5):484-93.

297. Papp MI, Kahn JE, Lantos PL. Glial cytoplasmic inclusions in the CNS of patients with multiple system atrophy (striatonigral degeneration, olivopontocerebellar atrophy and Shy-Drager syndrome). Journal of the neurological sciences. 1989 Dec;94(1-3):79-100.

298. Andersen K, Andersen BB, Pakkenberg B. Stereological quantification of the cerebellum in patients with Alzheimer's disease. Neurobiology of aging. 2012 Jan;33(1):197 e11-20.

299. Thal DR, Rub U, Orantes M, Braak H. Phases of A beta-deposition in the human brain and its relevance for the development of AD. Neurology. 2002 Jun 25;58(12):1791-800.

300. Brini M, Cali T, Ottolini D, Carafoli E. Neuronal calcium signaling: function and dysfunction. Cellular and molecular life sciences : CMLS. 2014 Aug;71(15):2787-814.

301. Wong RO, Ghosh A. Activity-dependent regulation of dendritic growth and patterning. Nature reviews Neuroscience. 2002 Oct;3(10):803-12.

302. Zhivotovsky B, Orrenius S. Calcium and cell death mechanisms: a perspective from the cell death community. Cell calcium. 2011 Sep;50(3):211-21.

303. LaFerla FM. Calcium dyshomeostasis and intracellular signalling in Alzheimer's disease. Nature reviews Neuroscience. 2002 Nov;3(11):862-72.

304. Mattson MP. Calcium and neurodegeneration. Aging cell. 2007 Jun;6(3):337-50.

305. Bezprozvanny IB. Calcium signaling and neurodegeneration. Acta naturae. 2010 Apr;2(1):72-82.

306. Cepeda C, Ariano MA, Calvert CR, et al. NMDA receptor function in mouse models of Huntington disease. Journal of neuroscience research. 2001 Nov 15;66(4):525-39.

307. Dong XX, Wang Y, Qin ZH. Molecular mechanisms of excitotoxicity and their relevance to pathogenesis of neurodegenerative diseases. Acta pharmacologica Sinica. 2009 Apr;30(4):379-87.

308. Womack MD, Hoang C, Khodakhah K. Large conductance calcium-activated potassium channels affect both spontaneous firing and intracellular calcium concentration in cerebellar Purkinje neurons. Neuroscience. 2009 Sep 15;162(4):989-1000.

309. Inoue T, Lin X, Kohlmeier KA, Orr HT, Zoghbi HY, Ross WN. Calcium dynamics and electrophysiological properties of cerebellar Purkinje cells in SCA1 transgenic mice. Journal of neurophysiology. 2001 Apr;85(4):1750-60.

310. Habela CW, Olsen ML, Sontheimer H. ClC3 is a critical regulator of the cell cycle in normal and malignant glial cells. The Journal of neuroscience : the official journal of the Society for Neuroscience. 2008 Sep 10;28(37):9205-17.

311. Kong BY, Bernhardt ML, Kim AM, O'Halloran TV, Woodruff TK. Zinc maintains prophase I arrest in mouse oocytes through regulation of the MOS-MAPK pathway. Biology of reproduction. 2012 Jul;87(1):11, 1-2.

312. Petrilli V, Papin S, Dostert C, Mayor A, Martinon F, Tschopp J. Activation of the NALP3 inflammasome is triggered by low intracellular potassium concentration. Cell death and differentiation. 2007 Sep;14(9):1583-9.

313. Kong BY, Duncan FE, Que EL, et al. The inorganic anatomy of the mammalian preimplantation embryo and the requirement of zinc during the first mitotic divisions. Developmental dynamics : an official publication of the American Association of Anatomists. 2015 Aug;244(8):935-47.

314. Dodani SC, Firl A, Chan J, et al. Copper is an endogenous modulator of neural circuit spontaneous activity. Proceedings of the National Academy of Sciences of the United States of America. 2014 Nov 18;111(46):16280-5.

315. Blackiston DJ, McLaughlin KA, Levin M. Bioelectric controls of cell proliferation: ion channels, membrane voltage and the cell cycle. Cell cycle. 2009 Nov 01;8(21):3527-36.

316. Pardo LA, Stuhmer W. The roles of K(+) channels in cancer. Nature reviews Cancer. 2014 Jan;14(1):39-48.

317. Chang CJ. Searching for harmony in transition-metal signaling. Nature chemical biology. 2015 Oct;11(10):744-7.

318. Turrigiano GG, Nelson SB. Homeostatic plasticity in the developing nervous system. Nature reviews Neuroscience. 2004 Feb;5(2):97-107.

319. Wefelmeyer W, Puhl CJ, Burrone J. Homeostatic Plasticity of Subcellular Neuronal Structures: From Inputs to Outputs. Trends in neurosciences. 2016 Oct;39(10):656-67.

320. Carnevale NT, Hines ML. The NEURON book. Cambridge, UK ; New York: Cambridge University Press; 2006.

321. Kralj JM, Douglass AD, Hochbaum DR, Maclaurin D, Cohen AE. Optical recording of action potentials in mammalian neurons using a microbial rhodopsin. Nature methods. 2011 Nov 27;9(1):90-5.

322. Gong Y, Huang C, Li JZ, et al. High-speed recording of neural spikes in awake mice and flies with a fluorescent voltage sensor. Science. 2015 Dec 11;350(6266):1361-6.

323. Rapp M, Yarom Y, Segev I. The Impact of Parallel Fiber Background Activity on the Cable Properties of Cerebellar Purkinje-Cells. Neural Comput. 1992 Jul;4(4):518-33.

324. Bekkers JM, Hausser M. Targeted dendrotomy reveals active and passive contributions of the dendritic tree to synaptic integration and neuronal output. Proceedings of the National Academy of Sciences of the United States of America. 2007 Jul 03;104(27):11447-52.

325. Womack M, Khodakhah K. Active contribution of dendrites to the tonic and trimodal patterns of activity in cerebellar Purkinje neurons. The Journal of neuroscience : the official journal of the Society for Neuroscience. 2002 Dec 15;22(24):10603-12.

326. Smith SL, Smith IT, Branco T, Hausser M. Dendritic spikes enhance stimulus selectivity in cortical neurons in vivo. Nature. 2013 Nov 07;503(7474):115-20.

327. Kim Y, Hsu CL, Cembrowski MS, Mensh BD, Spruston N. Dendritic sodium spikes are required for long-term potentiation at distal synapses on hippocampal pyramidal neurons. eLife. 2015 Aug 06;4.

328. Lovett-Barron M, Kaifosh P, Kheirbek MA, et al. Dendritic inhibition in the hippocampus supports fear learning. Science. 2014 Feb 21;343(6173):857-63.

329. Murayama M, Perez-Garci E, Nevian T, Bock T, Senn W, Larkum ME. Dendritic encoding of sensory stimuli controlled by deep cortical interneurons. Nature. 2009 Feb 26;457(7233):1137-41.

330. Otsu Y, Bormuth V, Wong J, et al. Optical monitoring of neuronal activity at high frame rate with a digital random-access multiphoton (RAMP) microscope. Journal of neuroscience methods. 2008 Aug 30;173(2):259-70.

331. Najafi F, Giovannucci A, Wang SS, Medina JF. Coding of stimulus strength via analog calcium signals in Purkinje cell dendrites of awake mice. eLife. 2014 Sep 09;3:e03663.

332. Elrick MJ, Pacheco CD, Yu T, et al. Conditional Niemann-Pick C mice demonstrate cell autonomous Purkinje cell neurodegeneration. Human molecular genetics. 2010 Mar 01;19(5):837-47.

333. Zu T, Duvick LA, Kaytor MD, et al. Recovery from polyglutamine-induced neurodegeneration in conditional SCA1 transgenic mice. The Journal of neuroscience : the official journal of the Society for Neuroscience. 2004 Oct 06;24(40):8853-61.

334. Kordasiewicz HB, Stanek LM, Wancewicz EV, et al. Sustained therapeutic reversal of Huntington's disease by transient repression of huntingtin synthesis. Neuron. 2012 Jun 21;74(6):1031-44.

335. Yoshida T, Fukaya M, Uchigashima M, et al. Localization of diacylglycerol lipase-alpha around postsynaptic spine suggests close proximity between production site of an endocannabinoid, 2-arachidonoyl-glycerol, and presynaptic cannabinoid CB1 receptor. The Journal of neuroscience : the official journal of the Society for Neuroscience. 2006 May 03;26(18):4740-51.

336. Jung KM, Astarita G, Thongkham D, Piomelli D. Diacylglycerol lipase-alpha and -beta control neurite outgrowth in neuro-2a cells through distinct molecular mechanisms. Molecular pharmacology. 2011 Jul;80(1):60-7.